LINEAR LONG CHAIN HYDROCARBONS FROM DEOXYGENATION OF PALMITIC ACID OVER METAL OXIDES

SUPPAWAT TAWEESIN

A THESIS SUBMITTED IN PARTIAL FULFILLMENT

OF THE REQUIREMENT FOR THE DEGREE OF

MASTER OF SCIENCE IN PETROCHEMICALS AND HYDROCARBON CHEMISTRY

FACULTY OF SCIENCE

KING MONGKUT'S INSTITUTE OF TECHNOLOGY LADKRABANG

2010

KMITL-2010-SC-M-015-010

หัวข้อวิทยานิพนธ์	ไฮโดรคาร์บอนสายยาวจากปฏิกิริยาดีออกซีจีเนชันของกรดปาล์มมิติก โดยใช้โลหะออกไซด์เป็นตัวเร่งปฏิกิริยา
นักศึกษา	นายศุภวัฒน์ ทวีสิน
รหัสประจำตัว	49068002
ปริญญา	วิทยาศาสตรมหาบัณฑิต
สาขาวิชา	ปิโตรเคมีและเคมีของไฮโดรคาร์บอน
อาจารย์ที่ปรึกษาวิทยานิพนธ์	รศ. ดร.ตะวัน สุขน้อย

บทคัดย่อ

ไฮโดรคาร์บอนสายโซ่ยาวสามารถผลิตได้จากกรดปาล์มมิติก ซึ่งเป็นกรดไขมันหลักในน้ำมันปาล์ม นำมาทำปฏิกิริยาในกระบวนการแบบกะ โดยใช้ตัวเร่งปฏิกิริยาโลหะออกไซด์ในกลุ่มแอลคาไลน์เอิร์ทและกลุ่มแลนทาไนด์ ได้แก่ แมกนีเซียมออกไซด์ แคลเซียมออกไซด์ แบเรียมออกไซด์ สตรอนเทียมออกไซด์ และซีเรียมออกไซด์ ประสิทธิภาพของตัวเร่งปฏิกิริยาหาได้จากปริมาณสารไฮโดรคาร์บอนและอุณหภูมิในการเผาตัวเร่งปฏิกิริยาเพื่อนำกลับมาใช้ใหม่ โดยทั้งโลหะออกไซด์ในกลุ่มแอลคาไลน์เอิร์ทและกลุ่มแลนทาไนด์จะได้ผลิตภัณฑ์หลักที่ประกอบด้วยแอลฟาโอเลฟินสายยาวและไฮโดรคาร์บอนสายยาว ส่วนแก๊สที่ได้จากปฏิกิริยาดีออกซีจีเนชันจะประกอบด้วย แก๊สคาร์บอนมอนอกไซด์ แก๊สไฮโดรเจนและไฮโดรคาร์บอนโมเลกุลต่ำ อย่างไรก็ตามเมื่อปริมาณของตัวเร่งปฏิกิริยามากกว่า 1 โมล ทำให้ได้สารไฮโดรคาร์บอนลดลง เนื่องจากเกิดปฏิกิริยาคีโตไนเซชันได้สารประกอบอะลิฟาติกคีโตนน้ำหนักโมเลกุลสูง สภาวะที่เหมาะสมสำหรับปฏิกิริยาดีออกซีจีเนชันของทั้งในกลุ่มแอลคาไลน์เอิร์ทและกลุ่มแลนทาไนด์คือ อุณหภูมิในการทำปฏิกิริยา 460 องศาเซลเซียส ด้วยอัตราส่วน 1 ต่อ 1 โดยโมลของกรดปาล์มมิติกต่อตัวเร่งปฏิกิริยาภายใต้แก๊สไนโตรเจน ที่เวลา 6 ชั่วโมง การทำปฏิกิริยาดีออกซีจีเนชันด้วยโลหะออกไซด์ในกลุ่มแอลคาไลน์เอิร์ทพบว่า ตัวเร่งปฏิกิริยาแคลเซียมออกไซด์จะทำปฏิกิริยาดีออกซีจีเนชันกับกรดปาล์มมิติก ได้สารไฮโดรคาร์บอนร้อยละ 84 ทั้งนี้เพราะแคลเซียมออกไซด์มีความเป็นเบสสูง ซึ่งหลังจากเกิดปฏิกิริยาดีออกซีจีเนชันแล้วแคลเซียมออกไซด์จะเปลี่ยนเป็นแคลเซียมคาร์บอเนต และสามารถเผากลับมาเป็นแคลเซียมออกไซด์อีกครั้งได้ที่อุณหภูมิ 685 องศาเซลเซียส แต่การเผาเพื่อนำกลับมาใช้ทำให้พื้นที่ผิวของแคลเซียมออกไซด์ลดลง ซึ่งได้สารไฮโดรคาร์บอนเพียงร้อยละ 76 สำหรับซีเรียมออกไซด์เมื่อถูกรีดิวซ์ที่ 300 องศาเซลเซียส จะให้ผลิตภัณฑ์สูงที่สุดคือร้อยละ 76 เนื่องจากเมื่อซีเรียมออกไซด์เมื่อถูกรีดิวซ์แล้วจะเกิดการสูญหายของออกซิเจน ซึ่งว่องไวต่อการเกิดปฏิกิริยาดีออกซีจีเนชันกับกรดปาล์มมิติก แต่เมื่อซีเรียมออกไซด์ถูก

รีดิวซ์ที่ 460 องศาเซลเซียส จะเกิดการสูญหายของออกซิเจนมากเกินไป ทำให้เกิดผลิตภัณฑ์จากการแตกสลายพันธะมากกว่าผลิตภัณฑ์จากปฏิกิริยาดีออกซีจีเนชัน ซึ่งได้สารไฮโดรคาร์บอนสายยาวลดลง เมื่อนำซีเรียมออกไซด์หลังจากปฏิกิริยามารีดิวซ์อีกครั้งจะให้ผลิตภัณฑ์ของไฮโดรคาร์บอนร้อยละ 51 ทั้งนี้เพราะการรีดิวซ์อีกครั้งไม่สามารถทำให้อนุภาคคาร์บอนที่เกาะอยู่บนตำแหน่งกัมมันต์ของซีเรียมออกไซด์หลังจากทำปฏิกิริยาครั้งแรกนั้นสลายตัวได้หมด ซึ่งอนุภาคคาร์บอนที่อยู่บนพื้นผิวตัวเร่งปฏิกิริยาจะบดบังตำแหน่งกัมมันต์สำหรับปฏิกิริยาดีออกซีจีเนชัน นอกจากนี้ซีเรียมออกไซด์ยังให้แก๊สคาร์บอนไดออกไซด์ ซึ่งเกิดจากซีเรียมออกไซด์ไม่ทำปฏิกิริยาเป็นซีเรียมคาร์บอเนตเหมือนกับในกลุ่มแอลคาไลน์เอิร์ทออกไซด์

Thesis Title	Linear long chain hydrocarbons from deoxygenation of palmitic acid over metal oxides
Student	Mr. Suppawat Taweesin
Student ID.	49068002
Degree	Master of Science
Program	Petrochemicals and Hydrocarbon Chemistry
Thesis Adviser	Assoc. Prof. Dr. Tawan Sooknoi

ABSTRACT

Linear long chain hydrocarbons can be produced from renewable vegetable oil derivatives. In this work the deoxygenation of palmitic acid, a major fatty acid in palm oil, was carried out in a batch reactor using alkaline earth metal oxides and lanthanide metal oxide as catalysts (MgO, CaO, SrO, BaO and CeO_2). The catalytic performance of metal oxides was determined by the extent of hydrocarbon produced and with a minimum regeneration temperature. Major products were linear long chain α-olefins (C_{14} and C_{15}) and linear paraffinic hydrocarbons (C_{14} and C_{15}). Gas products from the reaction were consisted hydrogen, carbon monoxide and light hydrocarbons (C_3 and C_4). Increase in amount of catalyst give a higher liquid yield except for the reaction with ratio metal oxide/ palmitic acid >1 where lower liquild hydrocarbon was obtain due to formation of high molecular weight hydrocarbon by coupling reaction. The appropriate reaction condition of deoxygenation of palmitic acid was as follows; reaction time 6 hr; reaction temperature 460 °C; 1/1 mol ratio of catalyst/palmitic acid. The alkaline earth metal oxides are basic catalysts, and can form metal carbonate from after deoxygenation. Calcium oxide shows the best result for deoxygenation of palmitic acid yielding 84% of liquid hydrocarbons, and requires a lower regenerating temperature (685 °C) for decomposing calcium carbonate to calcium oxide. However, the regenerated catalyst shows a lower activity (76%) for liquid hydrocarbons due to decrease surface area. For lanthanide metal oxide group, the yield of liquid hydrocarbons is increased when the cerium oxide is reduced with H_2 at high temperature (200-460 °C). The cerium oxide reduced at 300 °C, gives 76 % of almost long chain hydrocarbons, while the catalyst reduced at 460 °C give predominantly cracked products. This is believed that oxygen vacancy of cerium oxide can be readily generated on cerium oxide surface after reduction and become active site for deoxygenation. After reaction

cerium carbonate were not detected and carbon dioxide is released as co-product from deoxygenation. Cerium oxide regenerated with hydrogen at 300 °C provides up to 51 % of liquid hydrocarbons, this is because coke deposit may remain on surface of cerium oxide causing a lower activity. Unlike alkaline earth metal oxide, it was shown that, carbon dioxide is produced from the deoxygenation over cerium oxide catalyst.

ACKNOWLEDGEMENT

The author would like to express my profound gratitude to my advisor, Assoc. Prof. Dr. Tawan Sooknoi for helpful suggestions and encouragements thoughout this thesis. I am also grateful to Asst. Prof. Dr. Vanchat Chuenchom, Dr. Pesak Rungrojchaipon and Asst. Prof. Dr. Kandis Sudsakorn for serving as the chairperson and the committee, and their valuable comments.

The special thanks are also to PTT public company limited for financial support. I also appreciate the supports from the Department of Chemistry, Faculty of Science, King Mongkut's Institute of Technology Ladkrabang for the equipments, chemicals and facilities.

The author would like to extend this sincere appreciation to all of my friends and my research group for their advice, support and encouragement.

Finally, the author dedicates this thesis to my parents and my family for the constant love and encouragement.

Suppawat Taweesin

TABLE OF CONTENTS

	Page
Thai Abstract	I
English Abstract	III
Acknowledgement	V
List of Contents	VI
List of Tables	IX
List of Figures	X
CHAPTER 1 INTRODUCTION	1
1.1 Motivation	1
1.2 Objectives	3
1.3 Scope of Study	3
1.4 Expected Results	3
CHAPTER 2 LITERATURE REVIEW AND THEORY	4
2.1 Fatty acid	4
2.1.1 Reaction of fatty acid	4
2.1.1.1 Esterification	4
2.1.1.2 Hydrogenation	5
2.1.1.3 Decarboxylation	6
2.2 Metal oxides and base catalysts	7
2.2.1 Solid bases	7
2.2.1.1 Deffinition of acids and bases	7
2.2.1.2 Solid base and basic Sites	7
2.2.2 Basic strength of basic sites	8
2.2.3 Solid base materials	9
2.2.3.1 Alkaline earth oxides	9
2.2.4 Oxygen vacancies catalyst	11

TABLE OF CONTENTS (Continued)

2.3 Fuels..... 12

2.3.1 Kerosene..... 12

2.3.2 Diesel..... 14

2.4 Linear alpha olefins..... 15

2.4.1 Synthesis..... 16

2.4.1.1 Ineos (Ethyl) Process..... 16

2.4.1.2 CP Chemicals (Gulf) Process..... 16

2.4.2 Application..... 17

2.5 Literature reviews..... 18

CHAPTER 3 EXPERIMENTAL DETAILS..... 21

3.1 Reagents..... 21

3.2 Apparatus..... 21

3.3 Experimental procedure..... 22

3.3.1 Preparation of catalyst 21

3.3.2 Characterization of metal oxides..... 22

3.3.2.1 Determination of crystal morphology of metal oxides using scanning electron microscope (SEM)..... 22

3.3.2.2 Investigation of the metal oxides structure using X-rays powder diffractometer..... 23

3.3.2.3 Determination of specific surface area using gas adsorption analyzer..... 23

3.3.2.4 Carbon dioxide adsorption on the metal oxides using gas adsorption analyzer 23

3.3.2.5 Thermal decomposition of metal oxides, fatty acids and fatty acids salt using thermal gravimetric analyzer (TGA)..... 24

3.3.3 Reduction oxide of lanthanide metal..... 24

3.3.4 Reaction testing..... 24

3.3.5 Analysis of products..... 25

TABLE OF CONTENTS (Continued)

CHAPTER 4 RESULTS AND DISCUSSION 26

4.1 Characterization of palmitic acid 26

4.2 Catalyst characterization 26

4.2.1 Morphology of Metal oxide 26

4.2.2 X-ray diffraction (XRD) 28

4.2.3 Gas adsorption analysis 29

4.2.4 Decomposition of metal oxides 30

4.3 Decomposition of palmitic acid over metal oxides 31

4.4 Deoxygenation of palmitic acid over alkaline earth metal oxide 33

4.4.1 Study on metal oxide-carbonate interconversion 38

4.5 Deoxygenation of palmitic acid over cerium oxide 41

4.6 Catalytic deoxygenation of different fatty acids 46

4.7 Effect of catalyst/ fatty acid ratio 50

4.8 Regeneration of catalyst 54

4.8.1 Regeneration temperature of reused CaO 54

4.8.2 Regeneration of CeO_2 56

CHAPTER 5 CONCLUSION AND SUGGESTIONS 57

5.1 Conclusion 57

5.2 Suggestions 58

REFERENCES 59

APPENDICES 64

APPENDIX A Calculation 64

APPENDIX B Reaction data 66

APPENDIX C Gas chromatogram 71

APPENDIX D Characterization data 78

AUTHOR BIOGRAPHY 89

LIST OF TABLES

Table		Page
2.1	Boiling range of petroleum products.....	14
2.2	Application of Linear alpha olefins.....	17
4.1	Show phases of metal oxide catalysts from XRD pattern	28
4.1	Show X-ray diffraction crystallite size of metal oxide calculate using scherrer equation...	27
4.2	Show surface area (m^2/g) and CO_2 adsorption (cc/g) of metal oxide.....	29
4.3	Show thermal decomposition of catalysts with thermal gravimetric analysis.....	30
4.4	Show stability of catalyst with thermal gravimetric analysis.....	31
4.5	Liquid products from reaction of palmitic acid over alkaline earth metal oxides.....	33
4.6	TGA of residue from deoxygenation over alkaline earth metal oxide at 6 hour.....	40
4.7	Liquid products from reaction of palmitic acid over cerium oxide.....	41
4.8	DTG/TGA of residue from deoxygenation of linoleic acid with CaO.....	48
4.9	Yield of liquid hydrocarbons from various amount of catalysts	50
4.10	Surface area of calcium oxide regenerated.....	55

LIST OF FIGURES

Figure		Page
1.1	Catalytic cycle deoxygenation of palmitic acid over alkaline earth metal oxide.....	1
1.2	Catalytic cycle deoxygenation of palmitic acid over cerium oxide.....	2
2.1	Variations of activity of MgO for different types of reactions as a function of pre-treatment temperature: (○), 1-butene isomerization at 303 K; (▲), CH4–D2 exchange at 673 K; (Δ), amination of 1,3-butadiene with dimethylamine at 273 K, (□), 1,3-butadiene hydrogenation 273 K.....	10
2.2	Ions in low coordination on the surface of MgO.....	10
2.3	Reactive defect in a ceria surface.....	11
3.1	The catalytic test rig.....	25
4.1	Thermogravimetric Analyzer of Palmitic acid.....	26
4.2	SEM of metal oxide (CaO, MgO, SrO, BaO, CeO_2).....	27
4.3	XRD pattern of metal oxide catalyst.....	28
4.4	DTG of interaction between palmitic acid with metal oxide.....	32
4.5	% Yield of liquid hydrocarbon form deoxygenation (palmitic acid/catalyst =1/0.5 by mol)..	34
4.6	% Yield of liquid hydrocarbon form deoxygenation (palmitic acid/catalyst =1/1 by mol)....	34
4.7	Deacetylation of alkaline earth palmitate a) C14 unsaturated hydrocarbon; b) C14 saturated hydrocarbon.....	35
4.8	Chromatogram of gas product from deoxygenation of palmitic acid and CaO.....	35
4.9	Ketonisation of alkaline earth palmitate with methoxy group	36

LIST OF FIGURES (Continued)

Figure		Page
4.10	Decarboxylation of alkaline earth palmitate a) C15 saturated hydrocarbon; b) C15 Unsaturated hydrocarbon	36
4.11	Product from cracking reaction of C14 radical; a) C10 unsaturated hydrocarbon and C4 radical; b) C7 unsaturated hydrocarbon and C7 radical c); C10 unsaturated hydrocarbon and C4 radical	37
4.12	XRD pattern of residue from deoxygenation over CaO	38
4.13	DTG of residue from deoxygenation over alkaline earth metal oxide at 6 hour	39
4.14	Hydrogen temperature programmed reduction of CeO_2 catalyst	42
4.15	% Yield of liquid hydrocarbon form deoxygenation (palmitic acid/CeO_2 =1/1 by mol)	42
4.16	XRD pattern of cerium oxide after deoxygenation with palmitic acid	43
4.17	Decarboxylation of reduced cerium oxide a) C15 saturated hydrocarbon; b) C15 unsaturated hydrocarbon	44
4.18	Deacetylation of reduced cerium oxide a) C14 unsaturated hydrocarbon; b) C14 Saturated hydrocarbon	44
4.19	Chromatogram of gas product from deoxygenation of palmitic acid over CeO_2 reduced 300°C	45
4.20	Liquid hydrocarbon yield form reaction of fatty acids with CaO at various reaction times; palmitic acid,(b) linoleic acid, (c) oleic acid	46
4.21	Crosslink reaction of unsaturated fatty acid	47

LIST OF FIGURES (Continued)

Figure		Page
4.22	FT-IR spectra of product from ketonization; (1) CaO/palmitc acid (2:1mol), (2) CeO_2 redu 300 °C /palmitc acid (2:1mol)	51
4.23	H-NMR of product from ketonization; (a) CaO/palmitc acid (2:1mol), (b) CeO_2 reduced 300 /palmitc acid (2:1mol)	52
4.24	DTG of residue form palmitic acid over catalyst; (a) CaO:palmitic acid (2:1mol), CeO_2:palmitic acid (2:1mol)	52
4.25	Liquid hydrocarbon from deoxygenation of CaO regenerate	54
4.26	XRD pattern of CaO regenerated at various temperature	55
4.27	Liquid hydrocarbon from deoxygenation of CeO_2 regenerated	56

CHAPTER 1

INTRODUCTION

1.1 Motivation

In the recent years, the increasing fuel consumption has led to a rapid decrease in petroleum feed stock. Hence, research on renewable raw materials for fuel production, particularly the diesel components, is increasingly important because the global diesel fuel consumption is expected to exponentially increase [1]. In addition, the renewable source can be used as raw materials for petrochemicals, particularly the olefins. As they are main used for the production of the various polymers. In line with this view, animal fats and vegetable oils can be alternative source for the production of long chain hydrocarbons. They have lower limit of availability and give suitable product properties such as negligible sulfur, nitrogen, and metal content [2-3]. Hence, derivatives from animal fats and vegetable oils may partially replace petroleum products in a near future.

Hydrolysis of animal fats and vegetable oils can readily give various types of fatty acids. These fatty acids can interact with metal oxides forming metal-carboxylic acid on the catalyst surface. Upon heating, the adsorbed metal-carboxylic acid can undergo deoxygenation bearing long chain hydrocarbons as parafins [i] and olefins [ii]. The paraffins are raw material for the production of diesel while olefins are source of related petrochemicals. For alkaline earth metal oxide, it can absorbs and reacts with fatty acid to form metal palmitate, that can be deoxygenated to hydrocarbons and metal carbonate with acid-base neutralization. The metal carbonate can be further decomposed to carbon dioxide recovering active metal oxide catalyst [4]. With such catalyst, a catalytic cycle for fatty acid deoxygenation can be obtained as shown in Figure 1.1.

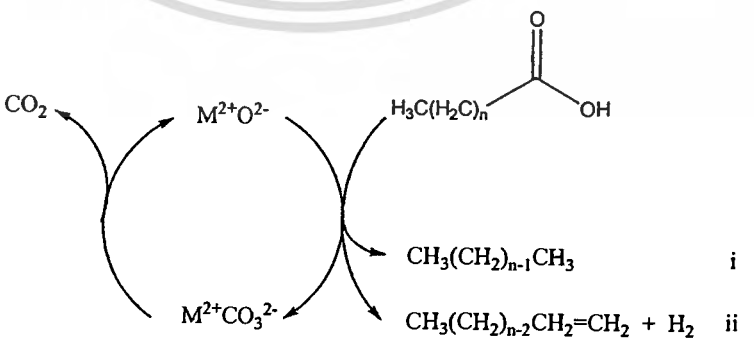

Figure 1.1 Catalytic cycle deoxygenation of palmitic acid over alkaline earth metal oxide

For lanthanide oxide, it can be reduced with hydrogen gas at higher temperature, exposing the oxygen defect site, namely oxygen vacancies on the surface. The mechanism of the deoxygenation of fatty acid occurs on oxygen vacancies at the surface of the reduced lanthanide oxide [5-6]. Attractive interaction is expected for fatty acid and oxygen vacancies of the reduced lanthanide oxide, forming intermediate and filled oxygen vacancies at the surface of the lanthanide oxide. Afterward, such intermediate could decompose to give long chain hydrocarbon and CO_2 as shown in Figure 1.2.

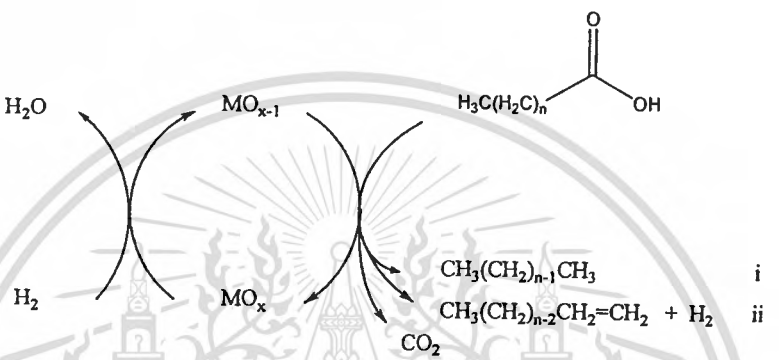

Figure 1.2 Catalytic cycle deoxygenation of palmitic acid over cerium oxide

In this thesis, deoxygenation of fatty acid to produce long chain hydrocarbons will be investigated over various alkaline earth metal oxides and cerium oxide to obtain appropriate condition, decomposition and regeneration of catalyst. An appropriate catalyst should provide the certain range of reaction temperature for both decomposition of metal-carboxylic acid or metal palmitate and metal oxide regeneration. Palmitic acid will be used as model compound since it is a major component found in triglyceride from palm oil. Alkaline earth metal oxide (MgO, CaO, SrO and BaO) and cerium oxide will be used as catalysts, as they showed strong interaction with carboxylic acids. Effect of type of fatty acid, catalyst content and effect of reduction temperature of cerium oxide will also be highlighted.

1.2 Objectives

1.2.1 To obtain a mixture of long chain hydrocarbons from deoxygenation of palmitic acid

1.2.2 To understand the role of catalyst in deoxygenation activity and selectivity.

1.2.3 To obtain appropriate reaction conditions for deoxygenation with reasonable catalyst stability.

1.3 Scopes of study

The scopes of this thesis are as follows:

1.3.1 Catalyst preparation by precipitating and calcining alkaline earth metal oxides and oxide of lanthanide metal.

1.3.2 Characterization of metal oxide by X-ray Diffraction (XRD), Scanning Electron Microscope (SEM), Gas adsorption analysis (Autosorb-1) and Thermogravimetric analysis (TGA).

1.3.3 Study on thermal degradation of palmitic acid and metal palmitate will be studied by Thermogravimetric analysis (TGA).

1.3.4 Study on decarboxylation of palmitic acid with various metal oxides in a batch reactor.

1.3.5 Study catalytic deoxygenation of different fatty acids, effect of the types of catalyst, effect of amount of catalyst/palmitic acid, metal oxide-carbonate interconversion and regeneration of catalyst.

1.3.6 Analysis and quantification of liquid products by Gas chromatography with flame ionization detecter (GC-FID) and analysis of gas products by online Gas chromatography with a thermal conductivity detector (GC-TCD).

1.3.7 Analysis of residue using Thermogravimetric analysis (TGA) and X-ray Diffraction (XRD).

1.4 Expected results

It is expected that a new technology for production of long chain hydrocarbon from palmitic acid will be obtained. This technology could potentially be developed into a process for long chain hydrocarbons production from the renewable sources within the country.

CHAPTER 2

THEORY AND LITERATURE REVIEWS

2.1 Fatty acids

Fatty acids are aliphatic monocarboxylic acids, present mainly as triglycerides from animal fats (e.g., butter, lard, beef) or vegetable oil (e.g., jatropha oil, coconut oil, soybean oil, palm oil) or wax. Natural fatty acids commonly have a chain of 16 to 22 carbons (usually unbranched and even numbered), which may be saturated or unsaturated [7-10]. Fatty acids can be produced by the hydrolysis of triglycerides in fat or biological oil with the removal of glycerol.

Saturated fatty acids do not contain any double bonds or other functional groups along the chain. The term "saturated" refers to hydrogen, in that all carbons (apart from the carboxylic acid [-COOH] group) contain as many hydrogens as possible.

Unsaturated fatty acids are long chain alkenyl group contain the carboxylic functional group. In most naturally-occurring unsaturated fatty acid are cis double bonds. Most fatty acids in the *trans* configuration (trans fats) are not found in nature and are the result of human processing (e.g., hydrogenation).

The world production of fatty acids from the hydrolysis of natural fats and oils totaled about 4 million metric tons per year. Fatty acids are ultimately consumed in a wide variety of end-use industries (rubber, plastics, detergents...). Fatty acids make up the greatest proportion of the current consumption of raw material in the chemical industry. The extent of the chemical reactions which are used to transform these renewable materials has been summarized.

2.1.1 Reaction of fatty acid

2.1.1.1 Esterification

Fatty acids react just like any other carboxylic acid, which means they can undergo esterification and acid-base reactions. Esterification is chemical reaction of alcohol and carboxylic acid forming an ester as the reaction product. Esters are common in organic chemistry and biological materials, and can be alternative fuel [11-12].

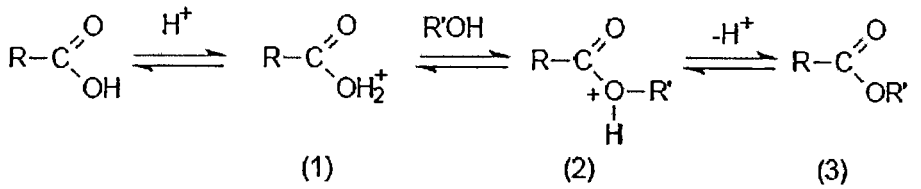

(1) (2) (3)

The initial step is protonation of the acid to give an oxonium ion (**1**), which can undergo an exchange reaction with an alcohol to give an intermediate (**2**), and this in turn can lose a proton to become an ester (**3**). Each step in the process is reversible but in the presence of a large excess of the alcohol, the equilibrium point of the reaction is displaced so that esterification proceeds virtually to completion [13].

2.1.1.2 Hydrogenation

Hydrogenation is the chemical reaction that results in addition of hydrogen (H_2). The process is usually employed to produce saturate organic compounds. The process typically constitutes the addition of pairs of hydrogen atoms to a molecule. Catalysts are required for the reaction to be usable; non-catalytic hydrogenation takes place only at very high pressure [14].

For example, titania-supported monometallic ruthenium catalyst prepared by the impregnation method is more active and selective for the hydrogenation of oleic acid to the saturated stearic acid and saturated stearyl alcohol [15].

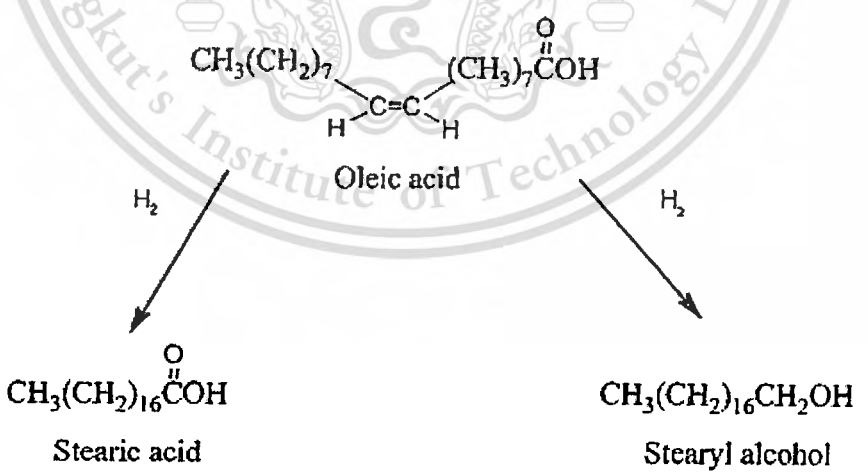

However, carboxylic acid can be hydrogenated with hydrogen atom, the addition of hydrogen such as maleic acid can be hydrogenation at double bond to form succinic acid [16].

2.1.1.3 Decarboxylation

Decarboxylation is a chemical reaction in which a carboxyl group (-COOH) is split off from a compound as carbon dioxide (CO_2). Chemical decarboxylations often require extensive heating in high-boiling solvents.

Catalytic liquid-phase decarboxylation of fatty acids and esters over Pd/C catalysts for the production of linear hydrocarbons has been investigated in a semibatch reactor [17].

Stearic acid n- heptadecane

The initial reaction in the decarboxylation of stearic acid over catalyst at 300°C under helium with a total pressure of 6 bar in dodecane was increased with an increasing initial concentration of stearic acid. The selectivity to the desired products, *n*-heptadecane was very high under conditions, being above 98%. Other products formed were unsaturated isomers containing 17 carbon atoms (3%) [17].

In another case, catalytic decarboxylation of lauric acid was studied over Pd/C catalyst in a continuous process at 255–300°C. Very high selectivity, >95%, to the desired products, namely C11 hydrocarbons can be achieved [18].

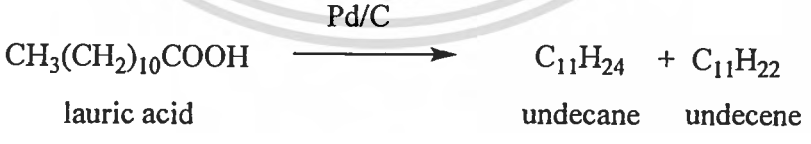

lauric acid undecane undecene

The conversion of lauric acid declined substantially to a steady state level within 10–20 min of time-on-stream. The initial concentration of lauric acid was decisive for the catalyst deactivation, the higher was the initial concentration of fatty acid, the more extensive catalyst deactivation occurred.

2.2 Metal oxides and base catalysts

2.2.1 Solid bases

2.2.1.1 Definition of acids and bases.

There are two main definitions of acids and bases, the definition by Brønsted and that by Lewis. According to Brønsted, acids are substances that donate a proton to another molecule or ion. In the following reaction, AH is an acid and B^-, is a base. In the reverse reaction, BH is an acids and A^- is a base. The reaction between AH and A^- is called conjugated. Thus, AH is a conjugated acid of A^-, and A^- a conjugated base of AH. Similarly, B^- is a conjugated base of BH and BH is a conjugated acid of B^-. AH and BH are called Brønsted acids (or protonic acids), while B^- and A^- are called Brønsted bases.

$$AH + B^- \longrightarrow A^- + BH$$

According to Lewis, acids are substances that accept an electron pair to form a covalent bond, while bases are substances that donate an electron pair to another molecule or ion. In the following reaction, NH_3 is a Lewis base and BF_3 is a Lewis acid.

$$BF_3 + :NH_3 \longrightarrow F_3B\text{--}NH_3$$

2.2.1.2 Solid base and basic sites.

Solid bases are defined as solids that serve as base by either the definition of Brønsted or that of Lewis. According to their functions, they are classified into Brønsted bases and Lewis bases. On the surface of solid bases, there are specific sites or centers that function as base. The sites are called basic sites. For example, isomerization of alkenes proceeds via allylic carbanions that are formed by abstraction of a proton from the reactant molecules.

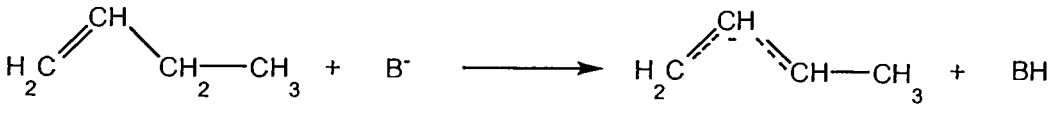

Here, the basic site B^- on the solid surface acts as a Brønsted base. In the reactions of ketones or aldehydes, the reactants are often activated by bases without proton transfer [19].

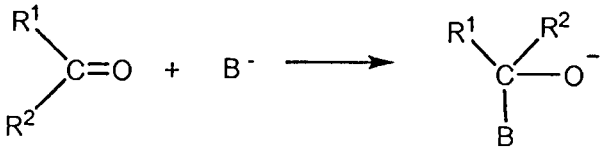

Here, the basic site B^- acts as a Lewis base. It should be noted that the same surface sites could serve as the Brønsted base as well as Lewis base, depending on the nature of the adsorbate. The classification has to be made only after the mode of interaction with an adsorbate is clarified.

2.2.2 Basic strength of basic sites

The H_ acidity function is defined as a measure of the ability of the basic solution to abstract a proton from an acidic neutral solute.

$$H_- = pK_a - \log([AH]/[A^-])$$

To determine the H_ value of the solution, the concentrations of AH and A^- have to measured accurately. When one half of a solute AH is deprotonated in the solution, i.e., $[A^-] = [AH]$, the H_ value of the solution is equal to the pK_a value of AH.

It was proposed that the H_ scale can be used as the measure of the strength of solid bases [20]. The basic strength of solid bases is expressed by means of the H_ value, equated to the highest among the pK_a values of the adsorbates from which the basic site is able to abstract a proton.

Two important points should be noted. *(1)* In the discussion of solid based, the H_ scale is treated as a parameter to describe the nature of individual basic sites. It is often assumed that there are a certain number of basic sites on the solid surfaces, and each of the basic sites has its own basic strength. In the original definition, the H_ scale is used to describe basic (or acidic) property of solution, not that of individual basic molecules (or ions) in the solution. *(2)* In the principle, the idea of the H_0 scale is only applicable to Brønsted bases. It can not be, at least directly, related to the capability of the sites as Lewis bases.

Apart from the appropriateness of applying the concept of the H_ scale to basic sites on the surfaces, the pK_a values of the adsorbates (or reactants) is a good measure of the ability of the basic sites to abstract a proton from an adsorbate (or reactant).

2.2.3 Solid base materials

2.2.3.1 Alkaline earth oxides

Alkaline earth oxides (MgO, CaO, SrO, BaO) are strong solid bases. The order of activity among alkaline earth oxide catalysts is BaO > SrO > CaO > MgO [21-23]. They are active for a variety of reactions including isomerization of alkenes and hydrogenation of 1,3-butadiene. To obtain high activity, it is essential to remove adsorbed molecules such as carbon dioxide and water. The catalytic activities of these oxides depend on the pretreatment temperature [24-25]. Figure 2.1 shows the change in the catalytic activities of MgO for various reactions with calcining temperature. When pretreatment temperature is low (below 700 K), MgO shows no activity. The activity for 1-butene isomerization develops at a pretreatment temperature of 800 K and declines at higher pretreatment temperature. The maximum activities for H-D exchange between CH_4 and D_2 appears at 923 K, while the activities for hydrogenations develop at higher pretreatment temperature of 1200-1300 K. This depend of the catalytic activities on pretreatment temperature indicates the there are at least three types of basic sites on the surface of MgO [26-29]. A model of MgO surface is shown in Figure 2.2 [25]. There are several types of oxygen anions with a different coordination number on the surface. It is plausible that each type of oxygen anion manifests its own basic strength and changes its amount with pretreatment conditions. Oxygen anions at low coordination numbers exist at corners, edges, and high Miller index surfaces. As increase in pretreatment temperature occurs, desorption of adsorbed molecules such as carbon dioxide occurs and oxygen anions on the surface become available for the reactant. Desorption of adsorbed molecules starts from the basic sites. At the same time, pretreatment at higher temperature cause the rearrangement of the surface structure. These two factors induce complex dependence of the catalytic activities with pretreatment temperature. In general, the catalytic activities of metal oxides are very sensitive to the pretreatment conditions.

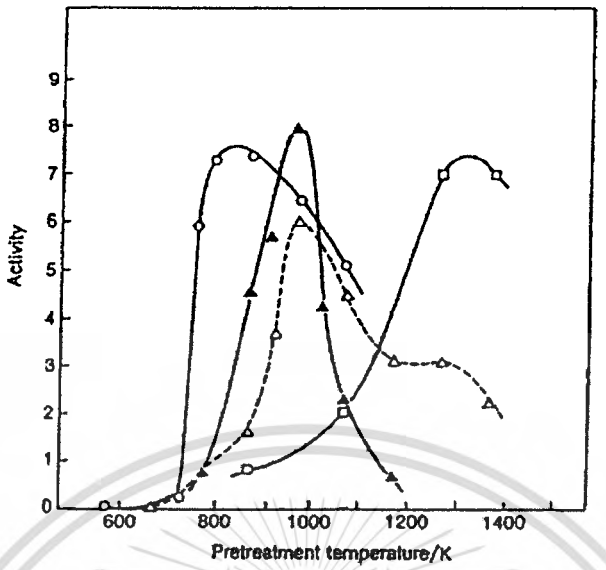

Figure 2.1 Variations of activity of MgO for different types of reactions as a function of pre-treatment temperature: (○), 1-butene isomerization at 303 K; (▲), CH_4–D_2 exchange at 673 K; (Δ), amination of 1,3-butadiene with dimethylamine at 273 K, (□), 1,3-butadiene hydrogenation at 273 K **[Error! Bookmark not defined.]**.

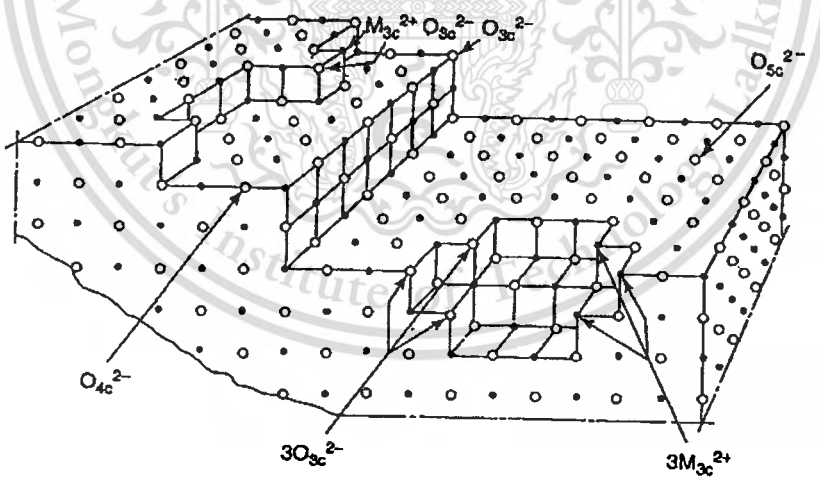

Figure 2.2 Ions in low coordination on the surface of MgO [25].

In the alkaline-earth metal oxide, it was considered that strength of the basic site was related to electronegativity of the conjugated metal cation. Since the large electronegativity intensifies the electron attractive force for the conjugated metal cation, the basic characteristics of the oxygen anion was deteriorated [30].

2.2.4 Oxygen vacancies catalyst

The oxygen vacancies catalysts are substituted by oxygen on surface catalyst. It is suggested that a diatomic species of peroxide (O_2^{2-}) ion is also an active species on catalyst surface. The oxygen vacancies catalysts are one of the most interesting oxides industrially because oxygen vacancy defects can be rapidly formed and eliminated, giving it a high "oxygen storage capacity." The metal oxide catalysts have been oxygen vacancies that transition metal oxide such as CeO_2, ZrO_2, and MoO_3. They are useful in a wide variety of applications involving oxidation or partial oxidation of hydrocarbons.

The CeO_2 is a basic oxide having excellent redox properties owing to the very fast reduction of Ce^{4+} to Ce^{3+} associated with the formation of oxygen vacancies at the surface and in the solid. The catalyst surface with a high basicity lead to the adsorption and activation of carbon dioxide to produce oxygen active species [31]. Relative to other oxide supports, ceria also enhances the performance of transition metal catalysts in a variety of other reactions including water-gas shift, steam reforming of oxygenates, and PROX (preferential oxidation of CO)

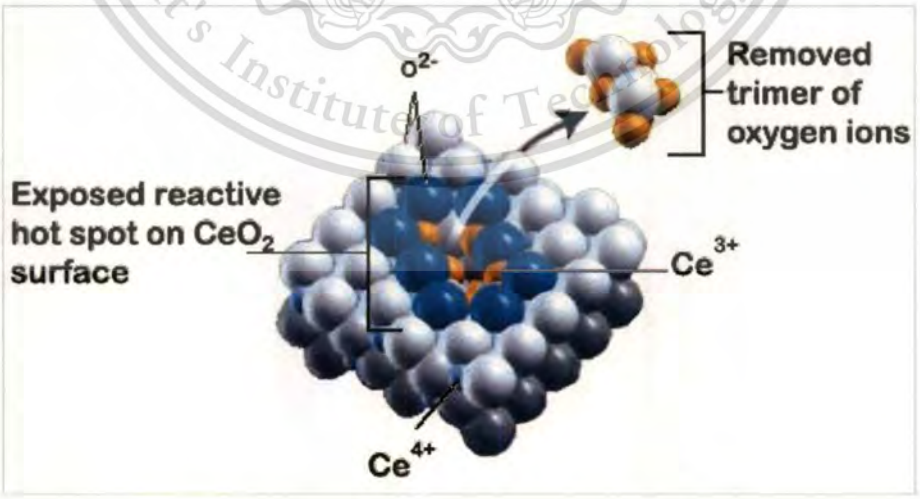

Figure 2.3 Reactive defect in a ceria surface [31]

To gain new insight into CeO_2 surfaces, Esch and co-workers [32] elegantly combine beautiful, atomic-resolution imaging using scanning tunneling microscopy (STM) on a ceria surface with state-of-the-art quantum mechanical calculations using density functional theory (DFT). They show that surface oxygen vacancies on $CeO_2(111)$ are immobile at room temperature, but linear clusters of these vacancies form at higher temperatures. These vacancy clusters expose exclusively Ce^{3+} ions to gas phase reactants. Thus, exposed Ce^{3+} ions are grouped into large ensembles, whereas the sites immediately adjacent to these vacancy clusters remain as pure Ce^{4+} ions.

Surface oxygen vacancies are proposed to participate in many chemical reactions catalyzed by metal oxides. For example, when an adsorbate is oxidized at the surface, the oxidant is often surface lattice oxygen atom, thus creating a surface oxygen vacancy. Vacancies also bind adsorbates more strongly than normal oxide sites and assist in their dissociation [33].

2.3 Fuels

The fuel products that are derived from petroleum supply more than half of the world's total supply of energy [34]. Gasoline, kerosene, and diesel oil provide fuel for automobiles, tractors, trucks, aircraft, and ships. Fuel oil and natural gas are used to heat homes and commercial buildings, as well as to generate electricity. The constant demand for products, such as liquid fuels, is the main driving force behind the petroleum industry. Other products, such as lubricating oils, waxes, and asphalt, have also added to the popularity of petroleum s a national resource. However, for the main part, the petroleum industry was inspired by the development of the automobile and the continued demand for gasoline, and other fuels. Such a demand has been accompanied by the demand for other products: diesel fuel for engines, lubricants for engine and machinery parts, fuel oil to provide power for the industrial complex, and asphalt for roadways.

2.3.1 Kerosene

Kerosene, also called paraffin or paraffin oil, is a flammable pale-yellow or colorless oily liquid with a characteristic odor. It is obtained from petroleum and used for burning in lamps and domestic heaters or furnaces, as a fuel or fuel component for jet engines, and as a solvent for greases and insecticides. Kerosene is also defined as a refined petroleum distillate that has a flash point of about 25°C (77°F) and is suitable for use as an illuminant when burned in a wide lamp. The term kerosene

is also too often incorrectly applied to various fuel oils, but a fuel oil is actually any liquid or liquid petroleum product that produces heat when burned in a suitable container or that produces power when burned in an engine. Kerosene originated as a straight-run petroleum fraction that boiled between approximately 205 and 260°C (400-500°F). Chemically, kerosene is usually consists of about 10 different hydrocarbons, each containing from 10 to 16 carbon atoms per molecule; the constituents include *n*-dodecane (*n*-$C_{12}H_{26}$), alkyl benzenes, and naphthalene and its derivatives [35-36]. Kerosene, because of its use as burning oil, must be free of aromatic and unsaturated hydrocarbons, as well as free of the more obnoxious sulfur compounds. It is a stable product, and additives are not required to improve the quality. Apart from the removal of excessive quantities of aromatics by the Edeleanu process, kerosene fractions may need only a lye wash or a doctor treatment if hydrogen sulfide is present to remove mercaptans. The essential properties of kerosene are flash point, fire point, distillation range, burning sulfur content, color, and cloud point. In the case of the flash point, the minimum flash temperature is generally placed above the prevailing ambient temperature; fire point determines the fire hazard associated with its handling and use. The boiling range is of less importance for kerosene than for gasoline, but it can be taken as an indication of the viscosity of the product. The ability of kerosene to burn steadily and cleanly over an extended period is an important property and gives some indication of the purity or composition of the product. The significance of the total sulfur content of a fuel oil varies greatly with the type of oil and the use to which it is put. Sulfur content is of great importance when the oil to be burned produces sulfur oxides that contaminate the surroundings. The color of kerosene is of little significance, but a product darker than usual may have resulted from contamination or aging, and in fact a color dark than specified may be considered by some users as unsatisfactory. Finally, the cloud point of kerosene gives indication of the temperature at which the wick may become coated with wax particles, thus lowering the burning qualities of the oil.

2.3.2 Diesel

Diesel fuel oil is also a distillate fuel oil. In general, it is a blend of straight-run gas oil and cracked gas oil to produce a product boiling in the 175-345°C (350-650°F) range. Diesel fuel oil is essentially the same as furnace fuel oil, but the proportion of cracked gas oil is usually less since the high aromatic content of the cracked gas oil reduces the cetane value of the diesel fuel [37]. Cetane number is a measure of the tendency of a diesel fuel to knock in a diesel engine. The scale is based upon the ignition characteristics of two hydrocarbons n-hexadecane (cetane) and 2, 3, 4, 5, 6, 7, 8-heptamethylnonane. Cetane has a short delay period during ignition and is assigned a cetane number of 100; heptamethylnonane has a long delay period and has been assigned a cetane number of 15. Just as the octane number is meaningful for automobile fuels, the cetane number is a means of determining the ignition quality of diesel fuels and is equivalent to the percentage by volume of cetane in the blend with heptamethylnonane, which matches the ignition quality of the test fuel. The boiling range, carbon atom and phase of petroleum products are shown in Table 2.1.

Table 2.1 Boiling range of petroleum products

Product	Boiling range, °C	Phase	Carbon atoms
Gas petroleum	< 10	Gas	1-4
Gasoline	30-185	Liquid	4-13
Kerosene	170-250	Liquid	10-14
Diesel	175-350	Liquid	14-19
Lubricant	350-500	Liquid	19-35
Wax	350-500	Solid	19-35
Fuel oil	> 500	Liquid	> 35
Bitumen	> 500	Solid	> 35

2.4 Linear alpha olefins

The term 'olefins', also known as alkenes, refers to a large number of compounds that contain carbon and hydrogen and have at least one double bond in their structure. Short-chain olefins, like ethylene, are cracked from naphtha or natural gas. Ethylene is then oligomerised into longer chain linear alpha olefins, ranging from 6 to 30 carbons in length. Alpha olefins are characterized by their high purity, high degree of linearity, and a double bond uniformly positioned between the first and second carbon. For drilling fluid applications, alpha olefins in the C14 to C18 range are used because they have the right mix of physical properties like viscosity, pour point and flash point. Internal olefins are then produced from linear alpha olefins by catalytically moving the double bond to different locations in the molecule. As a result, the pour point of the fluid decreases significantly, thus enabling these materials to be used successfully in deep-water applications. Internal olefins used as base fluids for drilling muds typically have carbon chain lengths in the C15 to C18 range [38].

Linear Alpha Olefins (LAO) or Normal Alpha Olefins (NAO) are olefins or alkenes with a chemical formula C_xH_{2x}, distinguished from other mono-olefins with a similar molecular formula by linearity of the hydrocarbon chain and the position of the double bond at the primary or alpha position.

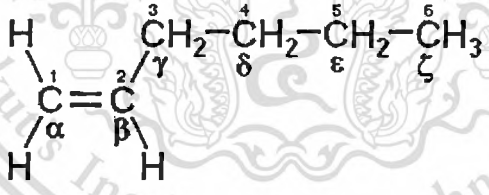

1-hexene, a typical linear alpha-olefin

Linear alpha olefins are a range of industrially important alpha-olefins, including 1-butene, 1-hexene, 1-octene, 1-decene, 1-dodecene, 1-tetradecene, 1-hexadecene, 1-octadecene and higher blends of C_{20}-C_{24}, C_{24}-C_{30}, and C_{20}-C_{30} ranges.

2.4.1 Synthesis

Industrially, linear alpha olefins are commonly manufactured by two main routes: oligomerization of ethylene and by Fischer-Tropsch synthesis followed by purification. Another route to linear alpha olefins which has been used commercially on small scale is dehydration of alcohols. Prior to about 1970's linear alpha olefins were also manufactured by thermal cracking of waxes, whereas linear internal olefins were also manufactured by chlorination/dehydrochlorination of linear paraffins. There are six commercial processes which oligomerize ethylene to linear alpha olefins. Four of these processes produce wide distributions of linear alpha olefins. These are the Ethyl Corporation (Ineos) process, Gulf (Chevron Phillips Chemical Company) process.

2.4.1.1 Ineos (Ethyl) Process

Ethyl linear alpha olefin process is commonly called stoichiometric Ziegler process. It is a two-step process. In the first step, a stoichiometric quantity of triethyl aluminium in olefin diluent is reacted with excess ethylene at high pressure (above 1000 psig) and relatively low temperature (below 400°F). On the average, nine moles of ethylene are added per mole of triethyl aluminium, resulting in, on average, a tri-octyl aluminium. The distribution of alkyl chains on the aluminium is determined by statistical bell curve distribution except for some smearing to the light side due to the kinetic phenomena and some smearing to the heavy side due to some incorporation of heavier olefins into the chain. Excess ethylene and olefin diluent are flashed off. The heavy aluminium tri-alkyls are reacted with ethylene again in a displacement or a tranalkylation reaction, but at high temperature (over 400°F) and at low pressure (less than 1000 psig) to recover triethyl aluminium and a statistical distribution of linear alpha olefins, which serve as the olefin diluent in the chain-growth step. [39]

2.4.1.2 CP Chemicals (Gulf) Process

The Gulf linear alpha olefin process is commonly called a catalytic Ziegler process. Triethyl aluminium is used as a catalyst, but in catalytic amounts and the process is a single-step process. Tri-ethyl aluminium and excess ethylene are fed to a plug flow-reactor. The reaction is conducted at high pressure and high temperature. Excess ethylene is flashed off. The tri-ethyl aluminium catalyst is washed out of the product with caustic and the linear alpha olefins are separated. The product distribution is a Schultz-Flory distribution of typical catalytic processes.

2.4.2 Applications

There is a wide range of applications for linear alpha olefins. The lower carbon numbers, 1-butene, 1-hexene and 1-octene are overwhelmingly used as comonomers in production of polyethylene. High Density PolyEthylene (HDPE) and Linear Low Density PolyEthylene (LLDPE) use approximately 2-4% and 8-10% of comonomers, respectively.

Another significant use of C_4-C_8 linear alpha olefins is for production of linear aldehyde via oxo synthesis (hydroformylation) for later production of short-chain fatty acid, a carboxylic acid, by oxidation of an intermediate aldehyde, or linear alcohols for plasticizer application by hydrogenation of the aldehyde. The predominant application of 1-decene is in making polyalphaolefin synthetic lubricant basestock (PAO) and to make surfactants in a blend with higher linear alpha olefins.

The high molecular weight of linear alpha olefins are primary raw material in the chemical industry [40-41] shown in table 2.10.

Table 2.2 Application of Linear alpha olefins

Linear alpha olefins	**Application**
1-Decene ($C_{10}H_{20}$)	Detergent alcohols, polyalphaolefins, alkyl aromatics, plasticizer alcohols, epoxides, di-/poly- halides, personal care, flavors and fragrances
1-Dodecene ($C_{12}H_{24}$)	Detergents, plasticizer alcohols, polyalphaolefins, alkyl aromatics, ADMA, ASA, epoxides, mercaptans, di-/poly- halides, alkyl silanes, personal care, flavors and fragrances
1-Tetradecene ($C_{14}H_{28}$)	Maleic anhydride copolymers, AOS, alkyl aromatics, ADMA, detergent alcohols, ASA, epoxides, metal working fluids, di-/poly- halides, alkyl silanes, personal care, flavors and fragrances
1-Hexadecene ($C_{16}H_{32}$)	Maleic anhydride copolymers, AOS, alkyl aromatics, ADMA, ASA, lube oil additives, epoxides, metal working fluids, di-/poly- halides, alkyl silanes, personal care, flavors and fragrances

Table 2.2 Application of Linear alpha olefins (continued)

Linear alpha olefins	Application
1-Octadecene ($C_{18}H_{36}$)	Maleic anhydride copolymers, AOS, alkyl aromatics, ADMA, ASA, lube oil additives, epoxides, metal working fluids, di-/poly-halides, alkyl silanes, personal care, flavors and fragrances
Alpha Olefin C_{20-24}	Lube oil additives, personal care, epoxides, alkyl aromatics, drilling fluids, maleic anhydride copolymers, pour point depressants
Alpha Olefin C_{24-28}	Epoxides, di-/poly- halides, candles, pour point depressants, personal care

2.5 Literature reviews

Catalytic decarboxylation is a well-established chemical reaction in organic processes that has been widely applied in organic synthesis. It has been studied in a broad reaction condition and over various types of catalysts, but works on fatty acid over metal oxide as catalyst are rather limited.

Recently decarboxylation of organic acid has been extensively investigated over metal oxide as catalyst. MgO-based catalysts can promote the catalytic decarboxylation of naphthenic acid from crude oil. Reactions were typically carried out in the temperature range of 150-300°C for 4 hour. Direct application of MgO to crude oil results in a significant removal of naphthenic acid and a lower total acidity of the crude oil [4]. Various studies were carried out under a high pressure condition [3-4,18,42-44]. While reaction temperature was used in range of 300–400°C [3-4,17-18,42-46].

Additionally, there are reports in 2006, that ZrO_2, Y_2O_3 and CeO_2 can decompose stearic acid (C_{18}-acid) in supercritical water at 673 K, 25–40 MPa in a batch reactor. The catalyst was stable in the reaction using supercritical water and the main product was C_{16} alkene and CO_2. An addition of alkali hydroxide (NaOH and KOH) in the supercritical water reaction enhanced the decarboxylation of stearic acid with the main products being C_{17} alkane and CO_2 [44].

Kubickova *et al* (2005) use fatty acid and derivatives (stearic acid, ethyl stearate and tristearine) as reactants for production of diesel fuel via decarboxylation over palladium supported on activated carbon at 300-360°C, 17-40 bar. The reaction of all three reactants resulted in n-heptadecane as the

main product with high selectivity. The side products consisted of positional isomers of heptadecenes and constitutional isomers of undecylbenzenes. Gas phase products from this reaction contained carbon dioxide, carbon monoxide, ethane and ethylene originating from the decomposition of ethyl stearate [3].

Heterogeneous catalyst such as Ni, Mo, Pd, Pt, Ir, Ru, Rh on Al_2O_3, Cr_2O_3, MgO and SiO_2 were also use as catalysts in deoxygenation of stearic acid for production of biodiesel as reported Maki-Avera *et al* in 2006. The deoxygenation reaction is carried out in a semibatch reactor under constant temperature and pressure, 300°C and 6 bar, respectively. The catalysts were characterized by N_2-physisorption, CO-chemisorption, and temperature-programmed desorption of hydrogen. A highly active and selective in the deoxygenation reaction of stearic acid, carbon supported palladium catalyst converted stearic acid completely with >98% selectivity toward deoxygenated C17 products [17].

Hereafter, Maki-Avera *et al* studied decarboxylation/decarbonylation of fatty acids and their esters over Pd supported on activated carbons in a semibatch reactor. The main studied parameters were catalyst acidity, type of feed, effect of solvent, and atmosphere gas. High yields of desired product, *n*-heptadecane, was achieved from the decarboxylation of stearic acid at 300°C,6-17.5 bar under helium [42]. While deoxygenation of lauric acid (C12) were studied in a continuous fixed bed reactor over Pd/C by using decane as a solvent (in 2008). The conversion of lauric acid declined substantially to a steady state level within 10–20 min of time-on-stream. The selectivity to the desired products, undecane and undecene was very high under all conditions, being above 95% [18].

In 2008, Snare *et al* studied method for production of diesel-like hydrocarbons via catalytic deoxygenation of stearic acid. The palladium supported carbon can completely converted stearic acid completely with 98% selectivity toward deoxygenated C_{17} products. The deoxygenation reaction is carried out in a semibatch reactor at 300°C-360°C, 15-27 bar [43].

In 2009, Catalytic deoxygenation of palmitic and stearic acids mixture was studied over 1 wt.% Pd/C catalysts supported on synthetic mesoporous carbon (Sibunit) in a semibatch reactor and dodecane as a solvent at 260–300°C under overall pressure of 17.5 bar of 5 vol% of hydrogen in helium. The main liquid phase products were n-heptadecane and n-pentadecane, which were formed in parallel [47].

Vegetable oils and animal fats were raw material in catalytic transformation over H-ZSM5 using two-stage riser fluid catalytic cracking (TSRFCC) unit by Hua *et al* . The results show that oils and fats can be singly used as fluid catalytic cracking (FCC) feed or co-feeding with vacuum gas oil (VGO). For palm oil cracking solely, the conversion of feed reach 97%, with, 45% LPG, 23% propylene, and 77.6% total liquid [48].

Some workers attempted to reduce the reaction temperature by utilization of oxidizing catalyst [49]. Catalytic wet air oxidation of stearic acid over noble metals supported on cerium oxide was carried out at 160-230°C, 0.1-2 MPa. The 5% wt Pt/CeO_2 catalyst gives the highest initial rate of mineralization and allows converting in 3 hour more than 95% of stearic acid into CO_2 at 200°C.

It can be seen that the previous works are usually carried out at high pressure over expensive noble metal catalyst. The alkaline earth metal oxide and lanthanide metal oxide can be use as decarboxylation, they are cost effective and can be easily handle. Therefore, the decarboxylation conditions under atmosphere of palmitic acid over alkaline earth metal oxide and lanthanide metal oxide were generally investigated in this work.

CHAPTER 3

EXPERIMENTAL DETAILS

3.1 Reagents

1. Acetone (Merck), AR-grade
2. Barium oxide powder (Riedel-de Haen)), $\geq$ 95%
3. Calcium oxide powder (Merck)
4. Cerium oxide powder (Riedel-de Haen)), $\geq$ 99%
5. Hexane (Merck), AR-grade
6. Hydrogen gas (TIG)
7. Linoleic acid (Fluka), $\geq$ 60-74%
8. Liquid nitrogen (TIG)
9. Liquefied petroleum gas (PTT)
10. Magnesium oxide powder (Fluka), $\geq$ 98%
11. Nitrogen gas (TIG)
12. Oleic acid (Panreac)
13. Palmitic acid (Fluka), $\geq$ 97%
14. Sodium hydroxide (Merck), $\geq$ 99%
15. Standard hydrocarbon (PTT)
16. Strontium nitrate powder (Carlo Erba), $\geq$ 99%

3.2 Apparatus

1. Catalytic testing rig
2. Clamp
3. Dewar
4. Furnace
5. Gas adsorption analyzer (Autosorb-1C, Quantrachrome)
6. Gas chromatography (Model 910, Buck scientific)
7. Heating Tape

8. Hot plate

9. Laboratory glassware

10. Oven

11. Reactor

12. Trap condenser

13. Vial

14. Wash bottle

15. Water bath

16. Scanning Electron Microscope (LEO 1455VP, LEO Electron Microscopy, Scientific Service Centre, KMITL)

17. X-ray Powder Diffractometer (D8 Advance, Bruker AG, Scientific Instrument Service Centre, KMITL)

18. Thermal Gravimetric Analyzer (Perkin-Elmer, Scientific Instrument Service Centre, KMITL)

19. Fourier transform infrared spectroscopy (FT-IR Spectrum GX, Perkin Elmer)

3.3 Experimental procedure

3.3.1. Preparation of catalyst

Magnesium oxide, calcium oxide and barium oxide were calcined for 5 hour at 700°C, 700°C and 400°C respectively. Strontium oxide was prepared by precipitating of 0.1 M strontium nitrate solution with 0.2 M NaOH solution. After stirring for 3 hour, the solid precipitate was dried overnight in an oven at 80°C, and then calcined at 400°C for 5 hour.

3.3.2 Characterization of metal oxides

3.3.2.1 Determination of crystal morphology of metal oxides using scanning electron microscope (SEM)

The crystal morphology and crystal size of the catalysts can be determined by scanning electron microscope (LEO 1455VP, LEO Electron Microscopy, Scientific Instruments Service Centre, KMITL). The sample can be prepared by thoroughly placing catalyst onto the sample holder. It is

then coated with gold by ion sputtering. The sample is placed in the sample chamber of scanning electron microscope and evacuated from ambient pressure to 10^{-1} mbar.

3.3.2.2 Investigation of the metal oxides structure using X-rays powder diffractometer (XRD)

The structure of catalyst can be determined by X-ray diffractometer (D8 Advance, Bruker, Scientific Instruments Service Centre, KMITL). The sample is prepared by packing the catalyst in the sample holder. CuK∝ X-ray beam is used for analysis at 30 kV, 30 mA. The sample is scanned from 2θ angle 5° to 60° with 1 second/step time and 0.04 2θ/step increment. X-ray diffraction pattern of the sample can be compared with the X-ray diffraction pattern of standard catalyst for structure determination.

3.3.2.3 Determination of specific surface area using gas adsorption analyzer

Surface area of the catalysts can be determined by gas adsorption analysis (Autosorb-1, Quantachrome). Approximate 0.02-0.04 grams of sample can be loaded into a cleaned and dried sample cell. The sample is degassed at out-gas station at 350°C for 24 hours. Then, nitrogen is filled and the sample cell is moved to the analysis station. The adsorption isotherm is measured in a pressure range of 0.05-0.30 P/P_0 at 77 K.

3.3.2.4 Carbon dioxide adsorption on the metal oxides using gas adsorption analyzer

Carbon dioxide adsorption is the technique using for determination of the basicity and basic strength of the catalyst. This technique was done according to the following procedure: the metal oxide sample was weighed accurately about 40 mg and transferred to a cleaned, dried empty sample cell. This sample cell was attached to the outgassing station. Then, a heating mantle was installed with the sample cell and the temperature was raised to 350°C. After the residual adsorbate was removed by temperature and reduced pressure, the carbon dioxide adsorbate was filled by open the gas inlet valve. The sample cell was attached to the sample station. In the initiate adsorption, a ice bath of ice was placed around the sample cell and the measurement of carbon dioxide adsorption was set with 3 minutes equilibration time. When adsorption was complete, the sample cell was removed from the sample station, dried thoroughly, and reweight.

3.3.2.5 Thermal decomposition of metal oxides, fatty acids and fatty acids salt using thermal gravimetric analyzer (TGA)

The thermal decomposition of metal oxides, fatty acids and fatty acids salt was investigated by Thermogravimetric Analyzer. Approximately 10 mg of sample was placed in a platinum pan hanging from a microbalance and nitrogen was introduced as a carrier gas. The sample was then heated under oxygen (50 ml/min) for %weight loss from 50°C to 800°C at a heating rate of 10°C/min.

3.3.3 Reduction oxide of lanthanide metal

For lanthanide metal oxide the sample will be reduced with hydrogen gas in flow bed reactor. Cerium oxide was packed in glass tube reactor filled with glass bead. The reactor was installed onto the catalytic test rig. Hydrogen gas was used as carried gas with a flow rate of 60 milliliters per minute (ml/min), at various temperatures at 200°C, 300°C and 460°C for 4 hour before using as catalyst [50-51].

3.3.4 Reaction testing

The catalytic activity is carried out at atmospheric pressure in a batch reactor. The reactor is made with borosilicate glass tube (3.5 cm i.d, length 7 cm). The schematic diagram of the experimental setup is shown in Figure 3.1. The metal oxides (1 mole) and fatty acid (1 mole) mixed in a reactor at 70°C. The reactor is installed onto the catalytic test rig which was located inside a temperature-regulated furnace (1). After that it was heated to the reaction temperature under stream of nitrogen at a flowrate of 27 ml/min (2). The product mixture is carried from the reactor to a series of trap condenser. The heavy product will be condensed to liquid an ice trap condenser (0 °C) (3). The light hydrocarbon will be condensed in the cryogenic of liquid nitrogen trap (-77 °C) (4). In order to prevent condensation of products before trapping, the line after reactor is heated at 250°C.

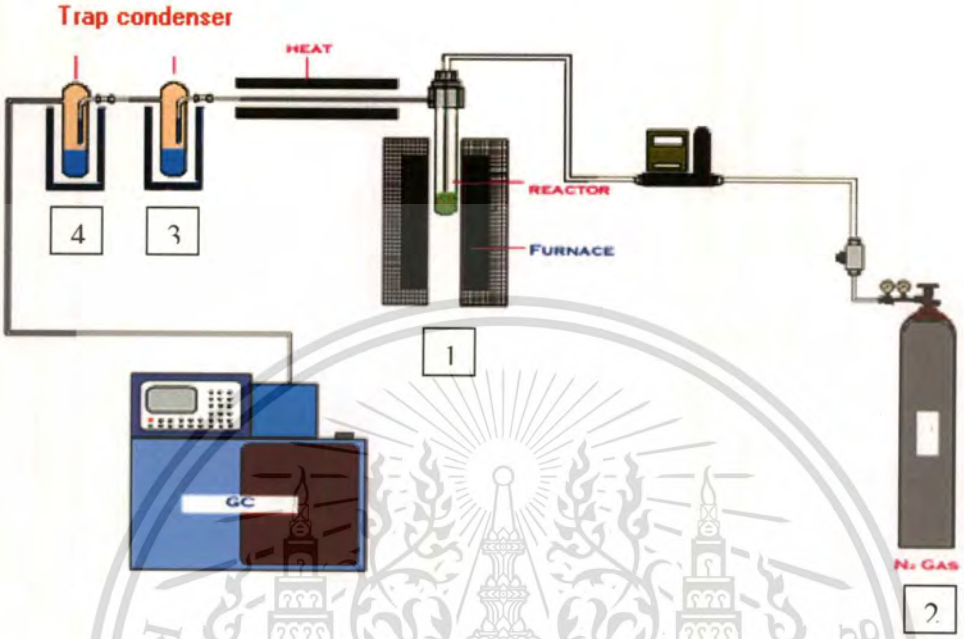

Figure 3.1 The catalytic test rig

3.3.4 Analysis of products

The liquid products were analyzed by a gas chromatograph (HP 6890) equipped with flame ionization detecter (GC-FID) and a capillary column DB-5 (length, 30 m; internal diameter, 0.25 mm;film thickness, 0.25 um). The following temperature program was used for the analysis of liquid hydroarbon: 40°C hold for 10 min, then ramp at 15°C/min to 280°C and hold at this temperature for 60 min by use nitrogen as carrier gas. The structures of products were confirmed by gas chromatography-mass spectrometry (GC-MS). The non-condensable hydrocarbon gases were analyzed online by a gas chromatograph (HP 5890) equipped with a thermal conductivity detector (GC-TCD) and a packed column (Porapak Q, 80/100 75CC). The injection port, the column oven, and TCD detector were set to 200°C, 40°C and 180°C respectively.

CHAPTER 4

RESULTS AND DISCUSSION

4.1 Characterization of palmitic acid

The palmitic acid was characterized with TGA/DTG. Decomposition temperature and the weight loss of palmitic acid were determined after the palmitic acid was decomposed in nitrogen gas.

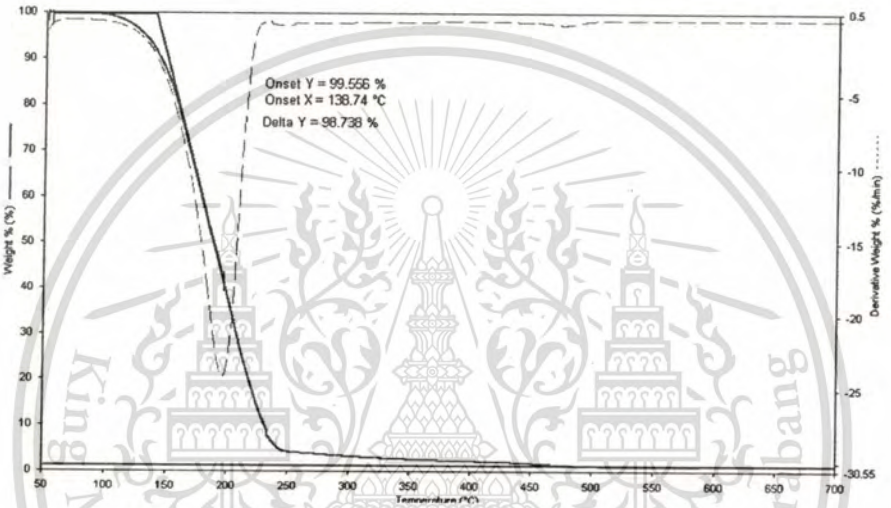

Figure 4.1 Thermogravimetric Analyzer of Palmitic acid

The decomposition temperature and the weight loss of palmitic acid are shown in Figure 4.1. It can be seen that palmitic acid is evaporated at 200°C. Since palmitic acid contain long chain alkyl group with 16 carbon atoms, evaporation of palmitic acid was relative slow. This can be seen from the range of evaporate temperature (100-250°C).

4.2 Catalyst characterization

4.2.1 Morphology of metal oxide

The morphology and the particle size of metal oxide were obtained from Scanning Electron Microscope (LEO 1455VP). The morphology and the particle size of catalysts used in this work were shown in Figure 4.2.

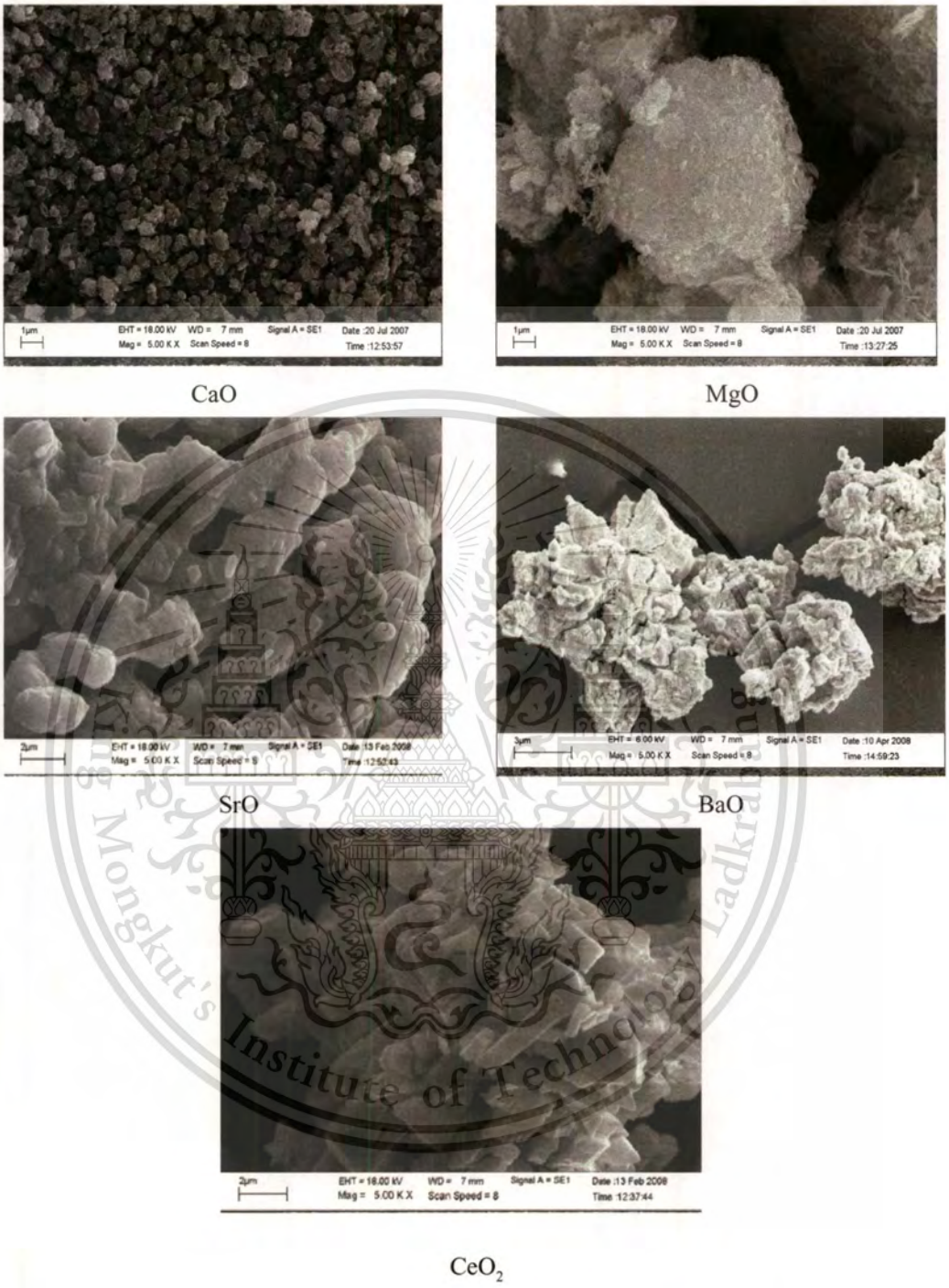

Figure 4.2 SEM of metal oxides (CaO, MgO, SrO, BaO, CeO_2)

From SEM, it can be seen that all metal oxides were crystalline materials with small particle size in a range of 1-7 μm. Magnesium oxide shows agglomerates of small particles, while the particles

size of calcium oxide were very small and evenly dispersed. Cerium oxide shows agglomeration of large crystalline particle.

4.2.2 X-ray diffraction (XRD)

Structure and composition in crystalline phases of catalyst were characterized and identify by XRD pattern as shown in figure 4.3.

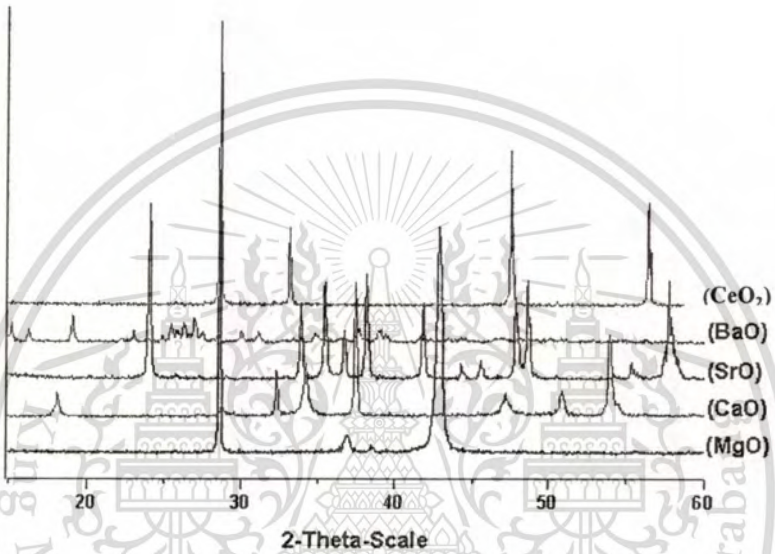

Figure 4.3 XRD pattern of metal oxide catalysts

Table 4.1 Phases of metal oxide catalysts from XRD pattern (2θ)

Metal oxide	Pattern oxide phase (2θ)	Pattern hydroxide phase (2θ)
MgO	37, 43, 63, 75, 79	-
CaO	33, 37, 54, 64 ,67	34, 46, 51, 64
SrO	-	14, 19, 24, 26, 28, 31, 39, 42
BaO	19, 23, 26, 29, 31, 34	14,15, 16, 25, 26, 27
CeO_2	29, 33, 47, 56	-

From XRD, magnesium oxide and cerium oxide exhibit high crystallinity of oxide phases, as shown in figure 4.3 and Table 4.1. Calcium oxide and barium oxide samples consist of both oxide and

hydroxide phases. However, strontium oxide shows only hydroxide phase. This is presumably because strontium oxide is highly hygroscopic and can readily adsorb water in the atmosphere.

4.2.3 Gas absorption analysis

The specific surface area and CO_2 adsorption of metal oxide were determined by BET measurements using Gas Adsorption Analyzer. Nitrogen gas was used to determine surface area. While carbon dioxide gas was also used as the adsorbate for evaluating the acid-base interaction on the catalyst surface as shown in Table 4.2.

Table 4.2 Show specific surface area (m^2/g) and CO_2 adsorption (cc/g) of metal oxide

Metal oxide	Surface Area (m^2/g)	CO_2 adsorption (cc/g)	CO_2/BET (cc/m^2)
Calcium oxide	14	16.0	1.14
Magnesium oxide	91	13.0	0.14
Strontium oxide	19	2.4	0.13
Cerium oxide	5	0.3	0.06
Cerium oxide reduce H_2 200°C	6	1.3	0.22
Cerium oxide reduce H_2 300°C	10	1.8	0.18
Cerium oxide reduce H_2 460°C	13	2.0	0.15

Specific surface area (BET) and CO_2 adsorption of the catalysts were shown in Table 4.2. Magnesium oxide possessed high surface areas since the particle size was relatively small as compared to other metal oxides. Calcium oxide and strontium oxide showed low surface area. In consistent with the large particle size, lowest surface area was obtained from cerium oxide samples. However, after reduction of cerium oxide in hydrogen at elevated temperature, the surface area of reduced cerium oxide was slightly increased. This can be explained that an oxygen vacancy was generated on the surface during hydrogen treatment. Hence, more defect of the lattice can be expected and this would provide higher active surface area for the reduced cerium oxide. Surface area and

carbon dioxide absorption of barium oxide cannot be determined because barium oxide was converted to corrosive barium peroxide when the sample was pretreated in air prior to gas adsorption analysis.

Calcium oxide can adsorb higher carbon dioxide as compared to that of magnesium oxide, strontium oxide and cerium oxide. It can be considered that calcium oxide possesses strong inter action with carbon dioxide. This is in accordance to the observed high basic site density, that is increased in the order of CaO>MgO>SrO>BaO [52]. Again, CO_2 adsorption of cerium oxide was increased, when the catalyst was reduced at elevated temperature. This is because the oxygen vacancies sites of cerium oxide can enhance the CO_2 absorption. The CO_2 adsorption /surface area ratio of cerium oxide was increased when reduced at 200°C. However, CO_2 adsorption /surface area of the reduced cerium oxide was decreased when the reduction temperature was increased. It is suggested that the interaction between CO_2 with the surface of reduced CeO_2 become weaker when more oxygen vacancies was generated. This is because an increase in oxygen vacancies would lead to the formation of Lewis acid site on the surface. Accordingly the interaction with acidic gas, CO_2 would be readily reduced.

4.2.4 Decomposition of metal oxides

Decomposition temperature of metal oxide catalysts were determined using thermogravimetric technique, total the percent weight loss up to 500°C (water, carbon dioxide and contamination) of each catalyst are shown in Table 4.3

Table 4.3 Show thermal decomposition of catalysts with thermal gravimetric analysis

Metal oxide	TGA of catalyst	
	% weight loss	Maximum temperature of decomposition
Magnesium oxide	7	236°C
Calcium oxide	23	385°C
Strontium oxide	7	100°C
Barium oxide	17	110°C
Cerium oxide	0.1	-

From Table 4.3 the cerium oxide show lower percent weight loss as compared to other catalyst. No signal for the decomposition of hydroxide phase and contaminate on surface can be observed. It was suggested that cerium oxide has high stability. Alkaline earth metal oxide shows weight loss most likely due to water. The calcium oxide shows high decomposition of water on surface (385°C). This is because calcium oxide was small particle. Hence, it can easily adsorb water in air.

4.3 Decomposition of palmitic acid over metal oxide

Decomposition of palmitic acids over metal oxides were tested by TGA and the percent weight loss of products on surface catalyst were shown in Table 4.3 and Figure 4.4. The catalysts initially react with palmitic acid to form metal-carboxylic acids intermediates that could decompose to long chain hydrocarbon at high temperature [4].

Table 4.4 Show stability of catalyst with thermal gravimetric analysis

Metal oxide	TGA of Catalyst/palmitate	
	% weight loss at 500 °C	Maximum temperature of decomposition
Magnesium oxide	86	320°C
Calcium oxide	76	425°C
Strontium oxide	62	440°C
Barium oxide	60	460°C
Cerium oxide	60	248°C

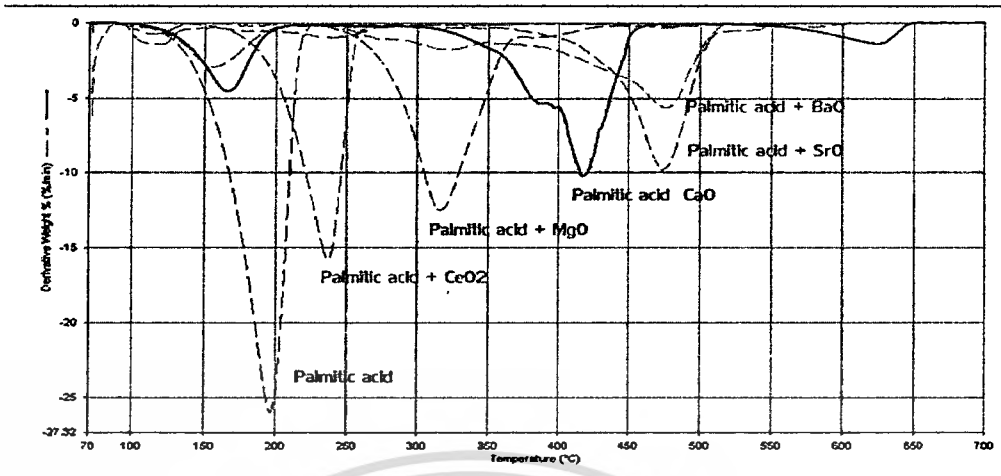

Figure 4.4 DTG of interaction between palmitic acid with metal oxide

The palmitate salt was decomposed at evaluated temperature as compared to the palmitic acid (~200 at 99% weight loss). This interaction of catalyst with palmitic acid depends on basic strength of catalyst. It can be seen that decomposition temperature of alkaline earth metal oxide with palmitic acid increased in the order of MgO < CaO < SrO < BaO, which correspond to basic strength of alkaline earth metal oxide [29, 52]. It was suggested that strong base catalyst would interact with palmitic acid through acid-base neutralization [4]. Hence, the decomposition temperature of alkaline earth palmitate follows the basic strength of the parent alkaline earth metal oxide as observed. However, decomposition temperatures of all metal-carboxylic acids were decomposing below 460°C. Hence, temperature at 460°C was appropriate temperature for deoxygenation of palmitic acid over alkaline earth metal oxide and cerium oxide.

Decomposition temperature of palmitic acid/CeO_2 was relatively low, as compared to the alkaline earth metal oxide. It was believed that CeO_2 does not possess adequate basic strength to form a palmitate salt. The interaction of CeO_2 with palmitic acid presumably arises from interaction only at the surface. Since, CeO_2 was reduced at 200, 300 and 460°C; an oxygen vacancy could be generated. This active site was most likely to interact with the carboxylic group resulting in much lower decomposition temperature of palmitic acid/CeO_2 system, as compared to the alkaline earth metal oxide system.

4.4 Deoxygenation of palmitic acid over alkaline earth metal oxide

The deoxygenation of palmitic acid over alkaline earth metal oxide catalyst is studied using semi-batch reactor. The reaction is investigated using 1/1or 0.5/1 by mol of catalysts/palmitic acid at appropriate temperature 460 °C (from TGA of metal-carboxylic acid), 6 hours using 27 ml/min of nitrogen gas as carrier gas. The product distribution of the reaction obtained over alkaline earth metal oxide is shown in Table 4.5 and Figure 4.5-4.6.

Table 4.5 Liquid products from reaction of palmitic acid over alkaline earth metal oxides

Liquid products	Catalyst: Palmitic acid (mol:mol)									
	BaO (0.5:1)		SrO (0.5:1)		CaO (0.5:1)		CaO (1:1)		MgO (1:1)	
% Yield	82.8		73.9		78.9		83.2		72.9	
Product distribution	Sat.	Uns.	Sat.	Uns.	Sat.	Uns.	Sat.	Uns.	Sat.	Uns.
C15	8.1	5.4	8.4	5.9	12.9	7.8	10.4	6.4	9.3	5.7
C14	4.8	12.8	3.8	14.1	4.1	14.7	3.4	11.7	3.1	10.4
C13	8.1	5.6	6.2	4.5	7.3	4.9	5.9	4.1	5.3	3.7
C12	4.1	3.6	2.6	2.7	3.5	2.8	3	2.3	2.7	2.1
C11	3.1	3.6	1.8	2.2	2.6	2.9	2.3	2.3	2.1	2.1
C10	3.1	2.9	1.6	1.7	2.5	2.3	2.3	2	2	1.8
C9	2.4	2.1	1.1	1.1	1.8	1.9	2	1.4	1.8	1.5
C8	0	0.8	0	0	1.9	0	0.1	9.9	0	8.8
C7	5.2	0.1	9.4	1.7	3.7	0	9.6	0.1	8.6	0
C6	0.1	0	0	0	0	0	0.1	0	0	0
C5	6.8	0	1.8	0	1.4	0	3.8	0	1.4	0
2-heptadecanone	0		4.56		0		0		0.73	

From Table 4.4 yield was defined as the amount of liquid hydrocarbons obtained from palmitic acid after 6 hours resident time. Alkaline earth metal oxides showed high activity (>70% yield) for deoxygenation of palmitic acid. It was believed that when alkaline earth metal oxides were preheated

with palmitic acid, the alkaline earth metal oxides would interact with palmitic acid to form alkaline earth palmitates as shown;

$$CH_3(CH_2)_{14}COOH + M^{+}O^{2-} \longrightarrow M(CH_3(CH_2)_{14}COO)_2$$

As the metal palmitates were heated to temperature higher than 350°C; they could decompose to hydrocarbon products [53]. The liquid products included both saturated and unsaturated hydrocarbons, as confirmed by GC-MS.

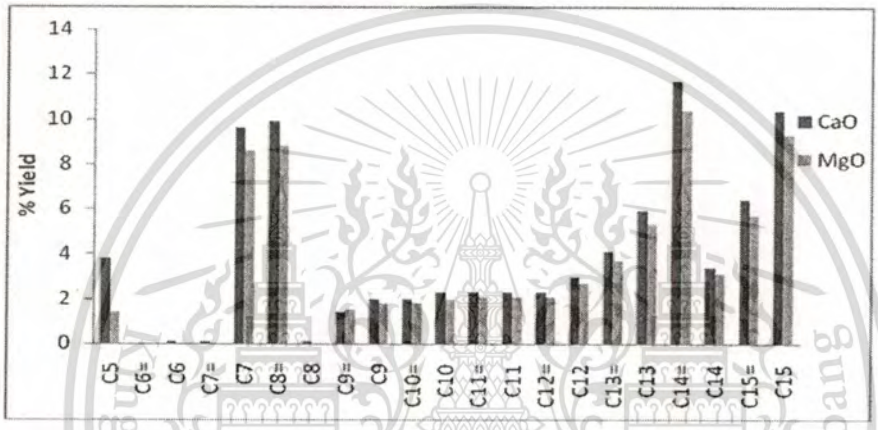

Figure 4.5 % Yield of liquid hydrocarbon from deoxygenation (palmitic acid/catalyst =1/0.5 by mol)

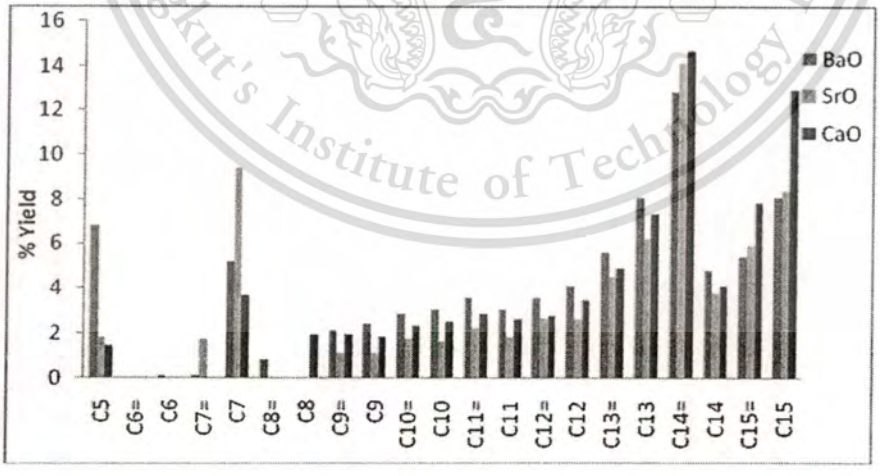

Figure 4.6 % Yield of liquid hydrocarbon from deoxygenation (palmitic acid/catalyst =1/1 by mol)

From Figure 4.5 and 4.6, the main product was C14 hydrocarbons (~15% yield), with mainly C14 unsaturated compound (>10%). While yield of C14 saturated hydrocarbon was relatively lower (3%yield). It was proposed that the metal palmitate undergoes deacetylation by cleavage of β carbon-carbon bond in palmitate species to form C14 unsaturated hydrocarbon (Figure 4.7, a) [54]. Besides, C14 unsaturated hydrocarbon can abstract hydrogen atom on surface of catalyst to form C14 saturated hydrocarbon as shown in Figure 4.7, b.

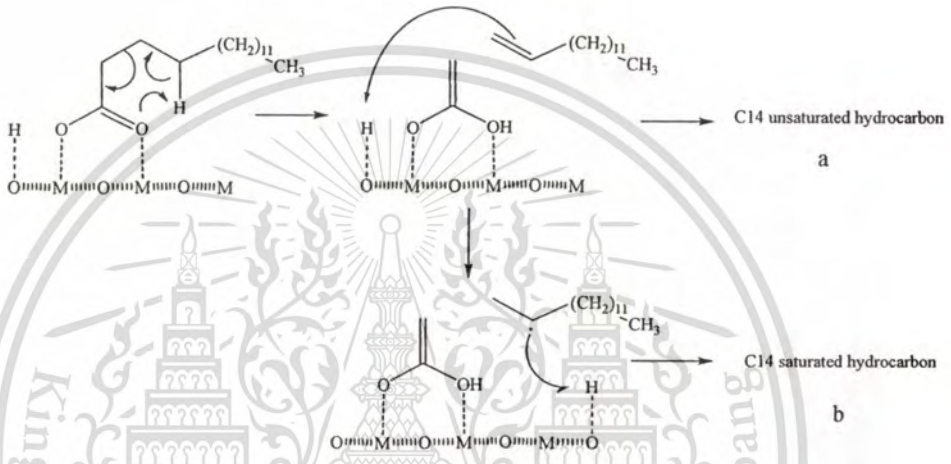

Figure 4.7 Deacetylation of alkaline earth palmitate a) C14 unsaturated hydrocarbon; b) C14 saturated hydrocarbon

After deacetylation the acetate species remained on the catalyst surface could decompose to CO and H_2O. This is evidenced by observed CO in gas phase and water condensed in the cold trap. Beside, gas products were consisted hydrogen, and LPG gas as shown in Figure 4.8.

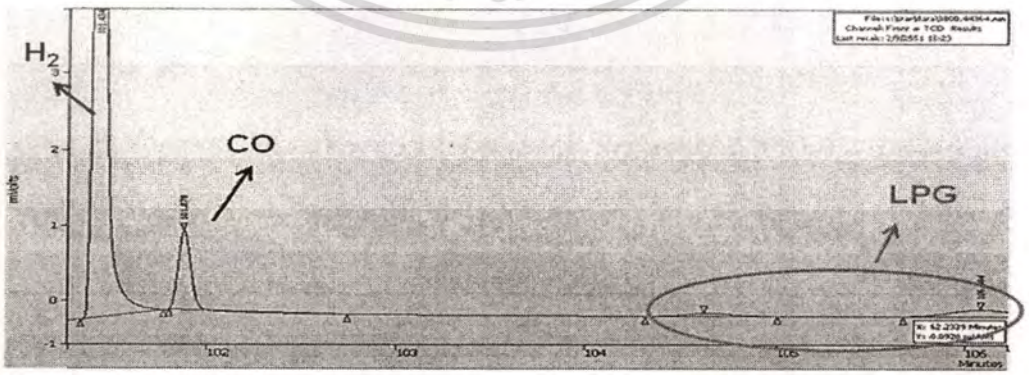

Figure 4.8 Chromatogram of gas product from deoxygenation of palmitic acid and CaO

However, the methyl group may survive from the decomposition and retain on the catalyst surface as methoxy species. This was concluded from the observed yield of 2-heptadecanone as co-product. It was suggested that alkaline earth palmitate was ketonized with methoxy group on surface catalyst that retained on the surface from the deacetylation, forming 2-heptadecanone, a ketone with one methyl group (Figure 4.9).

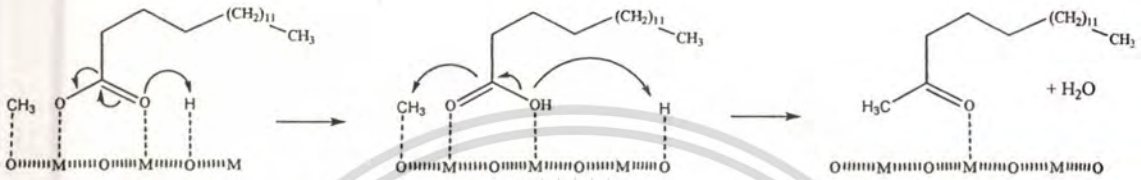

Figure 4.9 Ketonisation of alkaline earth palmitate with methoxy group

Another main product was C15 hydrocarbon (>13%yield), it would be obtained from direct decomposition of carboxylic group of alkaline earth palmitate to form C15 radical and CO_2, (decarboxylation). The C15 radical could abstract hydrogen atom on surface to form C15 saturated hydrocarbon (>8% yield) or hydrogen elimination to formed C15 unsaturated hydrocarbon (>5% yield) as shown in Figure 4.10.

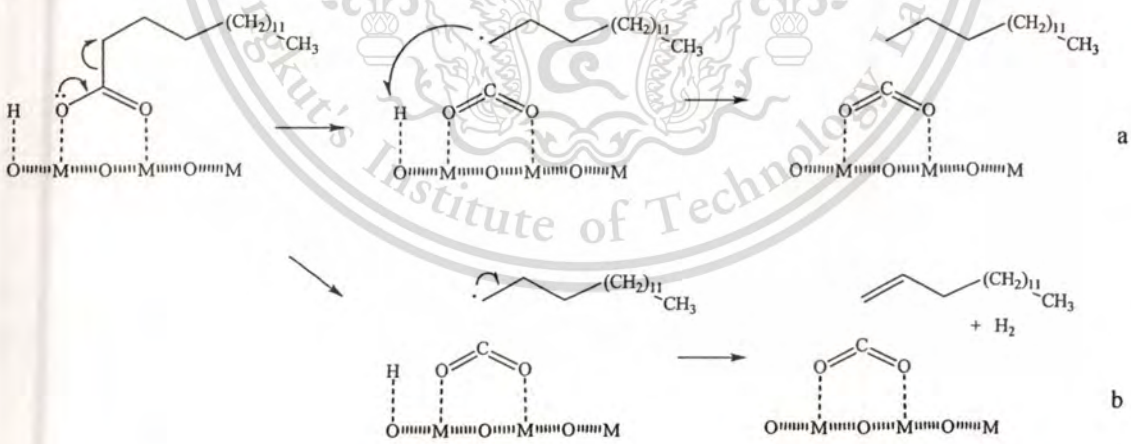

Figure 4.10 Decarboxylation of alkaline earth palmitate a) C15 saturated hydrocarbon; b) C15 unsaturated hydrocarbon

Moreover, thermal cracking of alkaline earth palmitates, and other hydrocarbons product could be expected at high temperature. For example, C14 radical would be abstract hydrogen atom within its own hydrocarbon chain, forming a new hydrocarbon radical (most likely at C8 position) that would crack at β position to form C10 unsaturated hydrocarbon and C4 radical. This inner radical (C8 position) can also either crack at C9-C10 position to form C7 hydrocarbons. The C7 hydrocarbon could also obtain from other inner radical (C11 position) in a manner similar to that discussed earlier. Hence, a number of C7 hydrocarbons were largely produced from cracking of these inner radical (C8 and C11 position) as shown in Figure 4.11

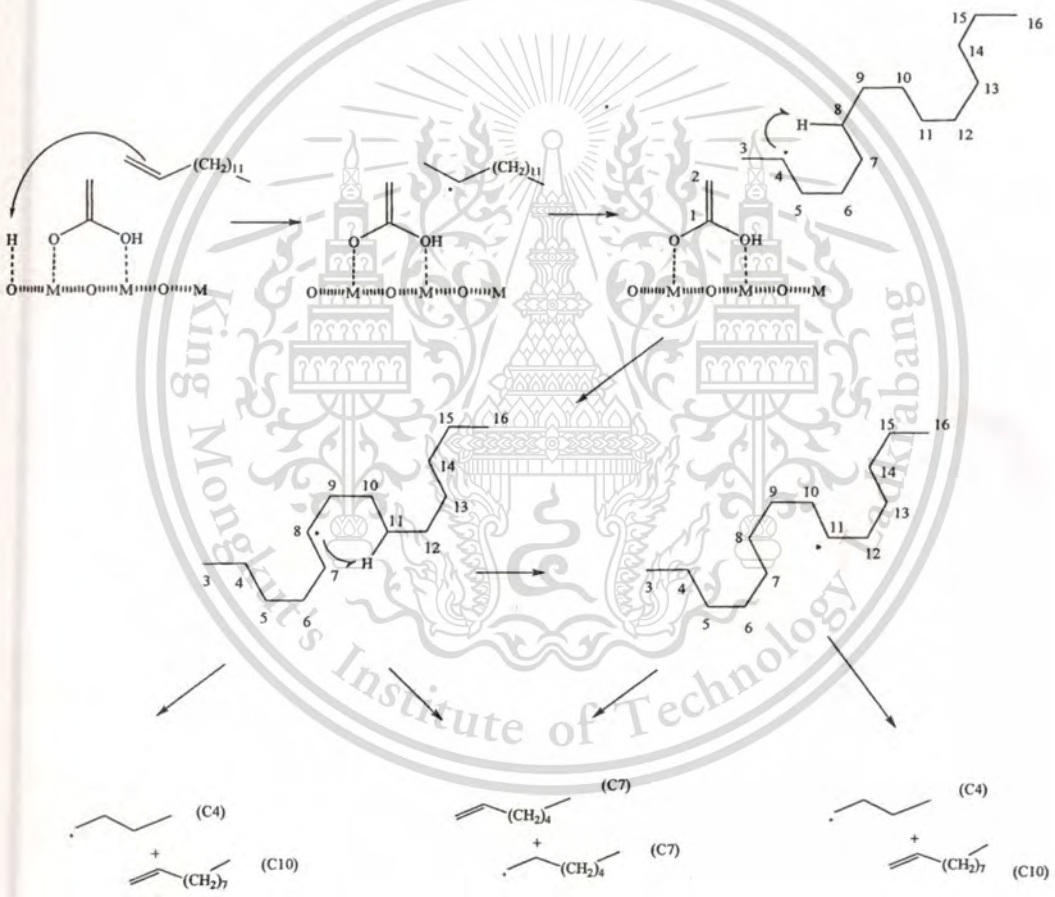

Figure 4.11 Product from cracking reaction of C14 radical; a) C10 unsaturated hydrocarbon and C4 radical; b) C7 unsaturated hydrocarbon and C7 radical c); C10 unsaturated hydrocarbon and C4 radical

From the product distribution, it could be concluded that the C15 hydrocarbons derive from decarboxylation. While the C14, C10 and C7 hydrocarbons results form of deacetylation. It could be seen from Table 4.4 that the catalysis with basic sites promoted predominantly deacetylation and cracking, and partly decarboxylation. Generally, an increase in liquid hydrocarbon yield was obtained when high amount of catalyst was employed. Liquid hydrocarbon yield from CaO catalyst was increased when CaO: palmitic acid was 1:1 mol, as compared to that 0.5:1 mol (79-84%). In particular, the C7 saturated hydrocarbon was increasingly obtained as the catalyst was increased. It could be considered that C14 radical could be readily cracked to form C7 saturated hydrocarbon in the presence of CaO.

From Table 4.4, activity of catalyst should follow basic strength order of alkaline earth metal oxide [29, 52]. In contract, SrO sample show lower activity than CaO (MgO< SrO < CaO < BaO). This is because SrO shows only hydroxide phase (XRD). Hence, basicity of SrO sample was lower than that of CaO. In other words, basic strength of alkaline earth metal oxide would be responsible for the formation of hydrocarbon products. The result shows that CaO gave higher liquid yield from decarboxylation (C15 hydrocarbon), as compared to other catalysts.

4.4.1 Study on metal oxide-carbonate interconversion

In deoxygenation of alkaline earth metal oxide, carboxylic group of metal palmitate was adsorbed on the catalyst surface and converted to metal carbonate as shown in Figure 4.12.

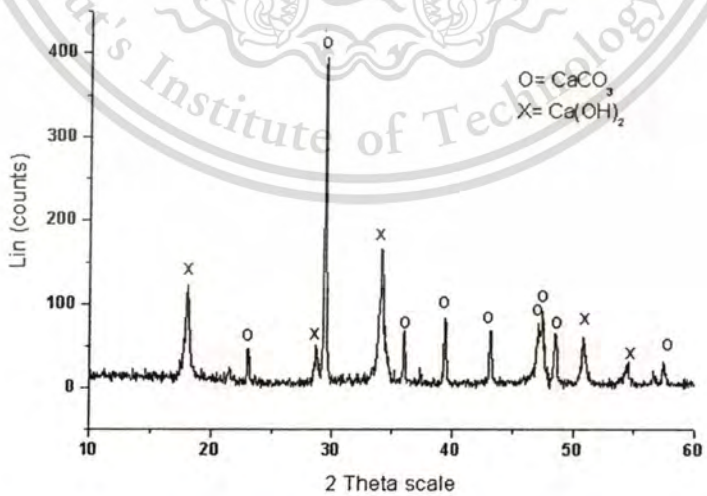

Figure 4.12 XRD pattern of residue from deoxygenation over CaO

It can be seen that use catalyst shown pattern of calcium carbonate at 2θ = 23, 29, 36, 39, 43, 47, 49 and 57. However, XRD pattern also shows pattern of calcium hydroxide at 2θ = 18, 28, 34, 47, 51 and 55. It was suggeted that $Ca(OH)_2$ was derived from the interaction of water with CaO that remain from reaction.

In order to complete the catalytic cycle (Figure1.1), the metal carbonate should be regenerated to metal oxide at temperature closely approximate to that of reaction temperature. Hence, regeneration temperature of catalyst after reaction was investigated using Thermogravimetric Analyzer (TGA).

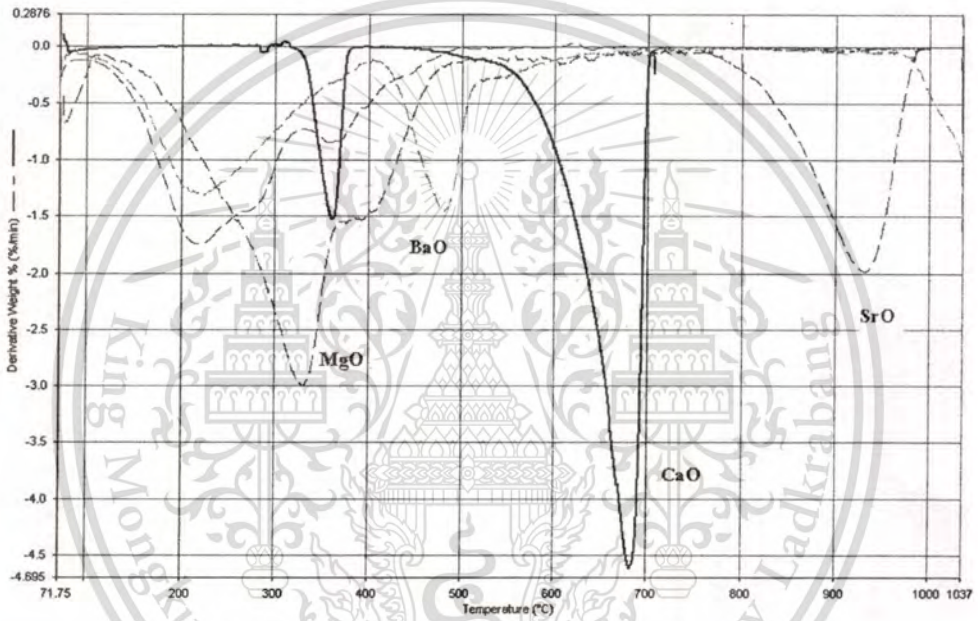

Figure 4.13 DTG of residue from deoxygenation over alkaline earth metal oxide at 6 hour

The decomposition temperature of residue after reaction was shown in Figure 4.13. It can be seen that palmitic acid is decomposed at 200-330°C and hydrocarbon is decomposed at 360-470°C. It is possible that some of palmitic acid may not react with alkaline earth metal oxide and remain in the residue, together with high molecular weight hydrocarbon. However, residue from calcium oxide shows decomposition temperature only hydrocarbon. It was expected that palmitic acid reacts completely with calcium oxide.

Table 4.6 TGA of residue from deoxygenation over alkaline earth metal oxide at 6 hour

Metal oxide	TGA of catalyst					
	T1 (palmitic acid)		T2 (residue)		T3 (CO_2)	
	Decompose	% wt. loss	Decompose	% wt. loss	Decompose	% wt loss
Calcium oxide	-	-	361°C	3.9	683°C	32.6
Magnesium oxide	330°C	33.3	406°C	13.7	-	-
Strontium oxide	217°C	21.5	362°C	9.1	933°C	19.8
Barium oxide	217°C	19.3	479°C	12.9	-	-

From DTG/TGA, decomposition of $CaCO_3$ to CO_2 takes place temperature at higher than 500 °C. Magnesium carbonate was not formed after decarboxylation and it was suggested that carbondioxide was release during the reaction [4]. However, the activity of magnesium oxide is relatively low due to a weaker basic strenght, as compared to other alkaline metal oxide [52]. Decomposition temperature of alkaline earth metal carbonate was in the order CaO<SrO<BaO. The calcium oxide shows a relatively lower decomposition temperature (700 °C), as compared to that of SrO (930°C), BaO (> 1000°C) respectively. Accordingly, calcium oxide appears to be an appropriate catalyst for deoxygenation of palmitic acid. This is because calcium oxide does not only give higher C15 hydrocarbon yield, but also give lower decomposition temperature for the carbonate-oxide interconversion. From this, it is possible to deoxygenate palmitic acid at ~500°C and regenerate the catalyst ~700°C using a swing bed reactor.

4.5 Deoxygenation of palmitic acid over cerium oxide

The deoxygenation of palmitic acid was also performed with cerium oxide (CeO_2) reduced at various temperature as shown in Table 4.7. The reaction was investigated using 1/1 by mol of catalysts/palmitic acid at 460 °C, 6 hours was 27 ml/min of nitrogen gas as carrier gas.

Table 4.7 Liquid products from reaction of palmitic acid over cerium oxide

Liquid products	Catalyst: Palmitic acid (1mol:1mol)							
	CeO_2		CeO_2 reduced 200°C		CeO_2 reduced 300°C		CeO_2 reduced 460°C	
% Yield	23.3		48.9		76.2		77.7	
Product distribution	Sat.	Uns.	Sat.	Uns.	Sat.	Uns.	Sat.	Uns.
C15	3.3	1.2	4.1	2.6	15.9	8.6	13.3	7.1
C14	1.3	4.3	2.4	8.6	5.2	14.2	5.1	13.2
C13	1.7	1.4	4.8	3.5	5.8	5.2	6.8	6.1
C12	0.7	0.4	2.4	2.5	2.9	1.8	4	2.5
C11	0.3	0.4	2	2.4	1.6	1.6	2.4	2.4
C10	0.6	0	1.9	1.9	1.3	1.1	2	1.7
C9	0.3	0.2	1.5	1.4	0.9	0.6	1.5	1
C8	0	0.1	1.2	0.8	0	0	0.7	0.3
C7	0	0	3.7	0	5.8	1.4	4.4	1.2
C6	6.3	0	0	0	0	1.1	0	1.2
C5	0	0	0.7	0	1	0	0.9	0
2-heptadecanone	0.8		0.7		0		0	

Liquid yield of CeO_2 was increased, when CeO_2 was reduced at evaluate temperature. This is because reduction at higher temperature would generate more defects of cerium oxide lattice that become active sites for deoxygenation. Such active sites can be refered to as "oxygen vacancies", which are generated upon reduction of cerium oxide. The reduction of cerium oxide can be evidenced by TPR as shown in Figure 4.14.

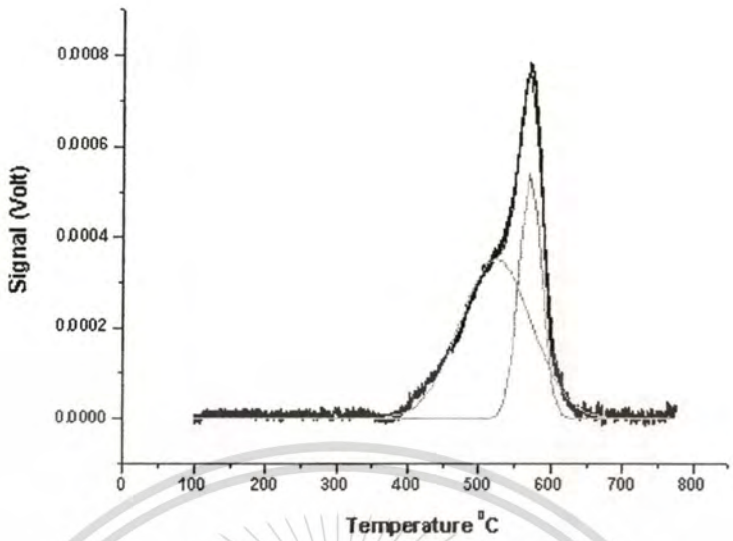

Figure 4.14 Hydrogen temperature programmed reduction of CeO_2 catalyst

From Figure 4.14 it can be seen that the cerium oxide can be reduced from 350-600°C. The result shows two reduction bands superimposed at 523°C and 570°C. Both reduction temperatures were previously observed and assigned for the reduction of cerium oxide at the surface [55, 56]. The reduction of bulk cerium oxide cannot be obtained at this temperature range. It is believed that the number of reduced surface sites (Ce^{3+}) and oxygen vacancies can be generated depending on the reduction temperature. Accordingly, it is expected that the cerium oxide reduced at higher temperature would provide more active sites and liquid hydrocarbon yield, as observed.

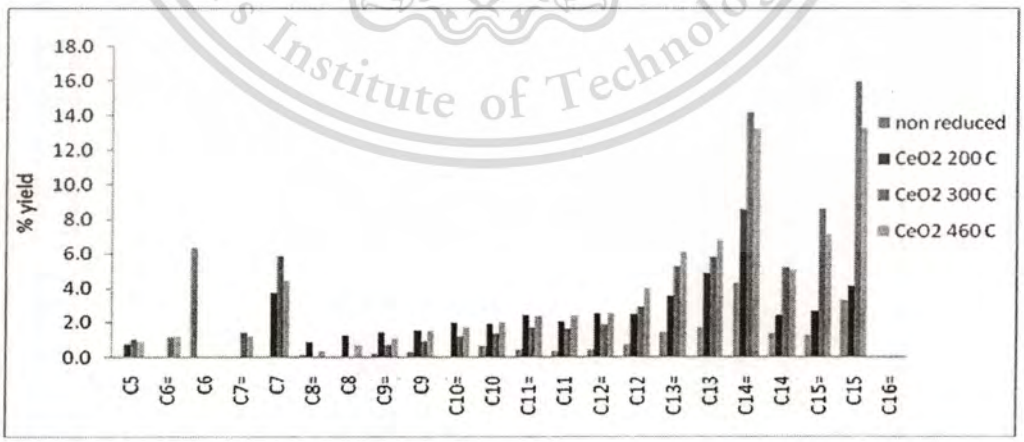

Figure 4.15 % Yield of liquid hydrocarbon form deoxygenation (palmitic acid/CeO_2 =1/1 by mol)

From Figure 4.15, the major liquid product from deoxygenation of palmitic acid over cerium oxide was C15 saturated hydrocarbon and C14 unsaturated hydrocarbon, similar to that observed with alkaline earth metal oxide. However, gas product from deoxygenation over cerium oxide was increased, especially carbondioxide. Unlike alkaline earth metal oxide, it was shown by XRD that cerium oxide cannot form cerium carbonate. After reaction, only cerium oxide phase can be observed (Figure 4.16). According to the above observation, liquid and gas products from deoxygenation over cerium oxide were not decomposed from the palmitate salt.

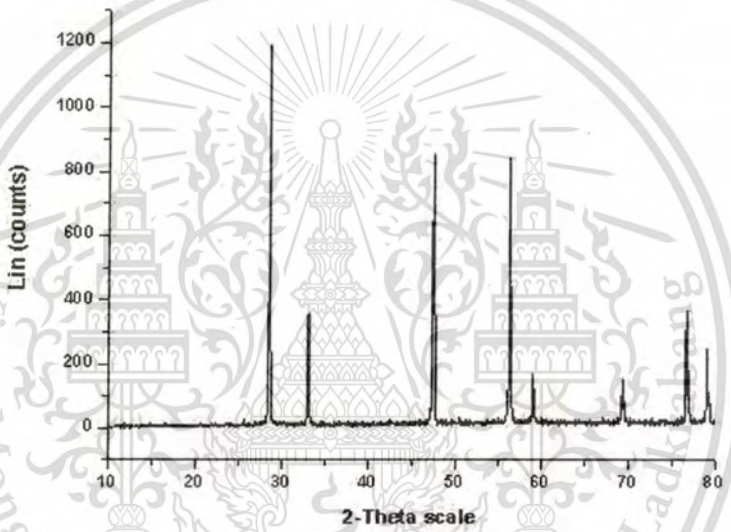

Figure 4.16 XRD pattern of cerium oxide after deoxygenation with palmitic acid

Together with an observed high carbon dioxide yield, it is likely that the reaction pathway for the decomposition over cerium oxide was different from that over alkaline earth metal oxide.

Over cerium oxide, the carboxylic group of palmitic acid would strongly interact with two oxygen vacancies upon heating [57-58]. This leads to the competition between desorption and decomposition of the adsorb palmitic acid on the surface of cerium oxide, forming C15 hydrocarbon radical and carbon dioxide as observed in the gas product. The C15 radical could abstract hydrogen atom on surface to form C15 saturated hydrocarbon or hydrogen elimination to form C15 unsaturated hydrocarbon as shown in Figure 4.17.

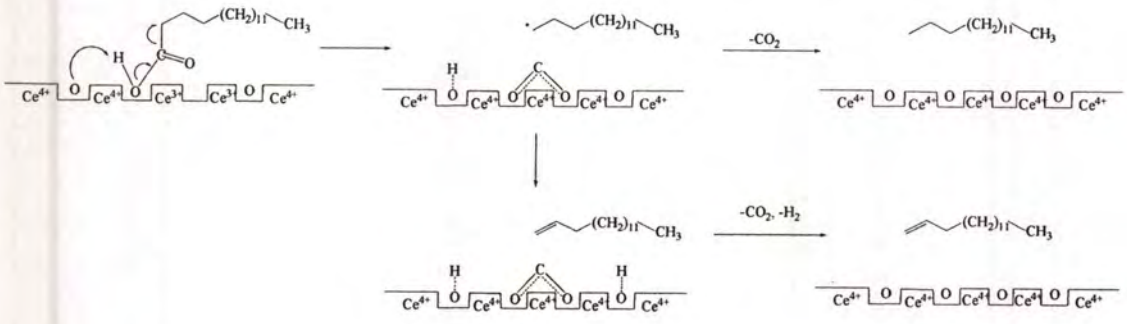

Figure 4.17 Decarboxylation of reduced cerium oxide a) C15 saturated hydrocarbon; b) C15 unsaturated hydrocarbon

For C14 hydrocarbons, it was belived that the carboxylic group of palmitic acid may also adsorb on single oxygen vacancies site. Unlike those adsorb on two-approximate site this species would decompose to C14 unsaturated hydrocarbon and acetate on the surface. The C14 unsaturated hydrocarbon can also abstract hydrogen atom on the surface of the catalyst to form C14 saturated hydrocarbon as shown in Figure 4.18.

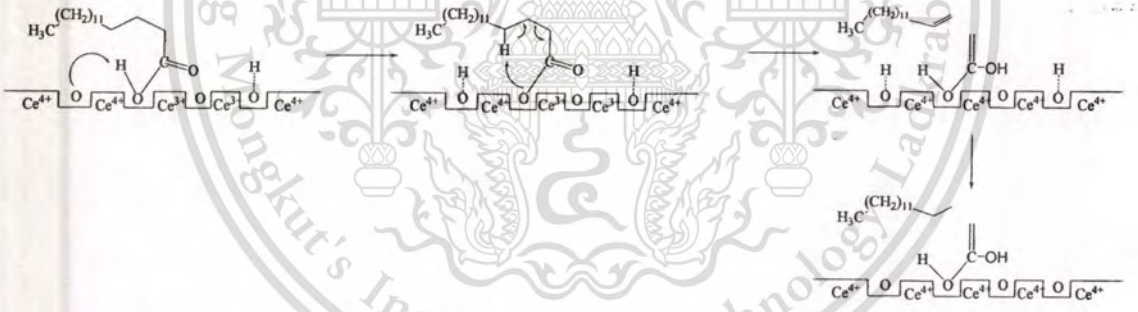

Figure 4.18 Deacetylation of reduced cerium oxide a) C14 unsaturated hydrocarbon; b) C14 saturated hydrocarbon

The adsorb acetate species may decompose to water and carbon dioxide or remain on the surface. It is observed that gas products from deoxygenation of palmitic acid over reduced cerium oxide were consist of CO, CO_2, H_2 and LPG (Figure 4.19). This is because cerium oxide does not form carbonate. Hence, carbon dioxide can be obtained in the gas phase. While LPG was decomposed from cracking of intermediate and H_2 was released from surface.

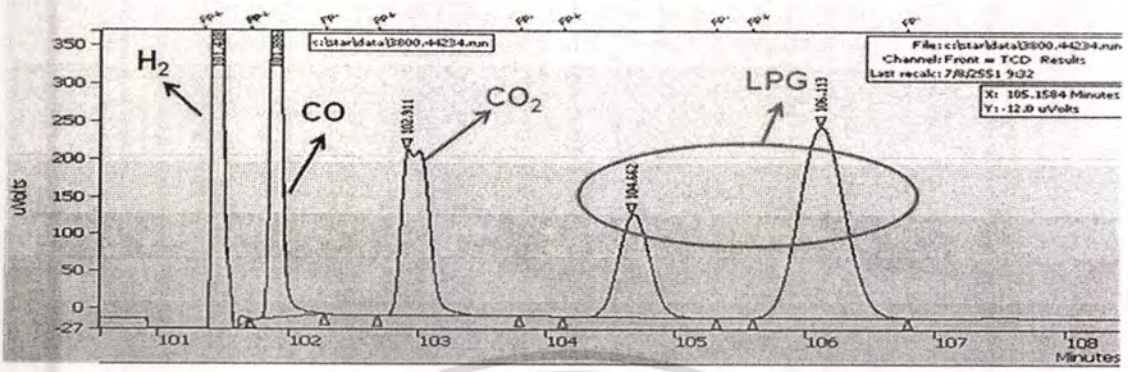

Figure 4.19 Chromatogram of gas product from deoxygenation of palmitic acid over CeO_2 reduced 300°C

For cerium oxide reduced at 460°C, the catalyst also possessd excess Lewis acid site [59-60]. Such Lewis acid site can also promote cracking of palmitic acid and its corresponded deoxygenated intermediates leading to a higher yield of cracking product and coke formation. It can be clearly seen from Figure 4.15 that cracking product was increase when reduction temperature was increased.

4.6 Catalytic deoxygenation of different fatty acids

Deoxygenation of most common fatty acids in palm oil, namely palmitic acid, oleic acid and linoleic acid were investigated over CaO, at 460°C under flow of N_2. The result is shown in Figure 4.20

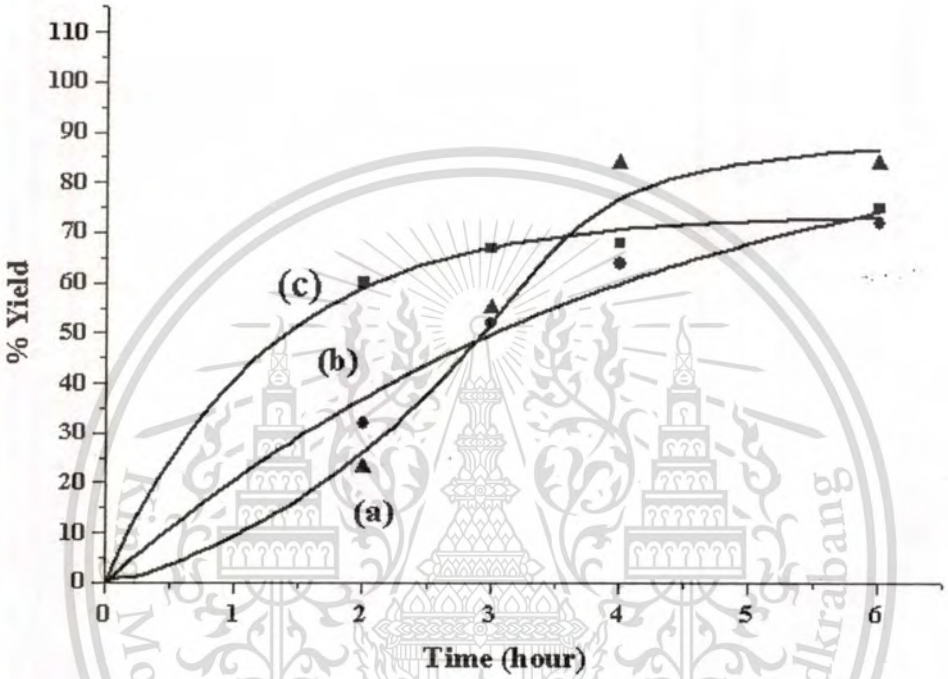

Figure 4.20 Liquid hydrocarbon yield from the reaction of fatty acids with CaO at various reaction times; (a) palmitic acid, (b) linoleic acid and (c) oleic acid

It can be seen that, at the beginning of the reaction, liquid hydrocarbon yield up to (60%) from oleic acid and linoleic acid are relatively higher than that from palmitic acid. This is because oleic acid (monounsaturated C18 fatty acid) and linoleic acid (diunsaturated C18 fatty acid) do not only contain higher carbon number, as compared to palmitic acid (saturated C16 fatty acid), but also possess reactive double bond in the hydrocarbon chain. These make oleic acid and linoleic acid relatively more reactive for the formation of free radical or carbanion intermediate when contact with CaO. Hence, deoxygenation and thermal cracking of C18 fatty acids can be readily facilitated at the beginning of the reaction. However, when the reaction is completed, liquid yield form linoleic acid

was relatively low, as compared to oleic acid and palmitic acid. This is because linoleic acid contains two double bonds that essentially stabilize radical intermediate. Such radicals can undergo crosslinking to form high weight molecules deposit on catalyst surface, as shown in Figure 4.21.

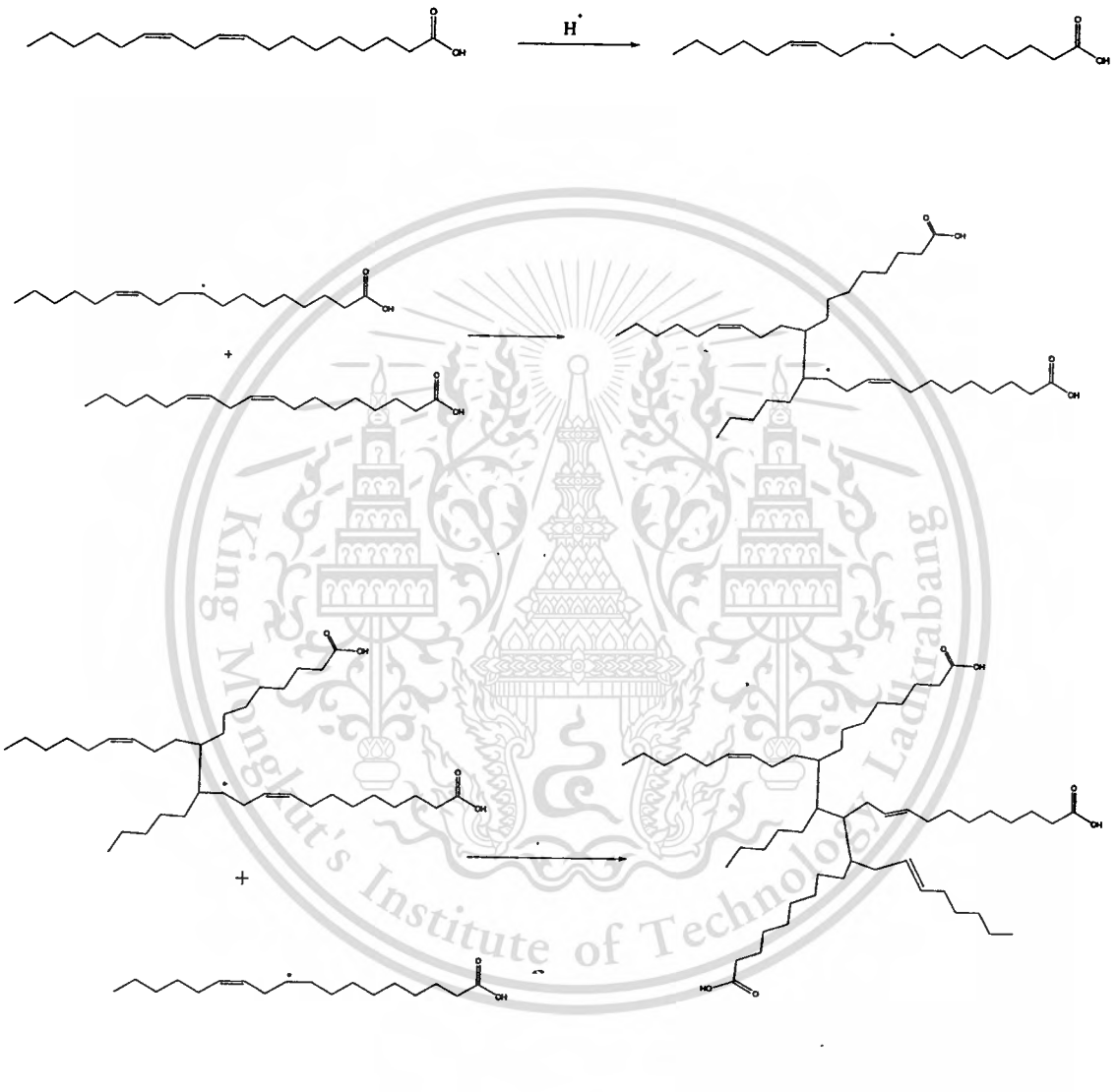

Figure 4.21 Crosslink reaction of unsaturated fatty acid

Table 4.8 DTG/TGA of residue from deoxygenation of linoleic acid with CaO

Reaction of fatty acid over CaO		DTG/TGA of residue							
		T1 (palmitic acid)		T2 (Crosslink product)		T3 (residue)		T4 (CO_2)	
		Decompose	% wt. loss	Decompose	% wt. loss	Decompose	% wt loss	Decompose	% wt loss
Linoleic acid	2 hr	299°C	20.95	-	-	457°C	45.19	751°C	13.44
	3hr	288°C	24.50	420°C	14.29	462°C	17.64	770°C	18.11
	4hr	254°C	29.72	400°C	8.67	469°C	13.59	722°C	19.04
	6hr	276°C	26.99	417°C	16.59	473°C	8.77	752°C	21.81
Palmitic acid	2 hr	309°C	28.21	-	-	471°C	17.61	752°C	19.38
	3hr	201°C	20.01	-	-	449°C	9.95	751°C	22.34
	4hr	201°C	12.31	-	-	382°C	3.83	638°C	26.86
	6hr	-	-	-	-	370°C	3.92	683°C	28.74

From Table 4.8 it can be seen that the residue of linoleic acid shows higher weight loss at 400-420°C, as compared to palmitic acid. This suggests the higher number of high molecular weight

deposit, presumably by crosslinking. The residue at 6 hr shows higher decomposition temperature of crosslink product, as compared with that at lower reaction times.

In contrast, palmitic acid contains no double bond and possess only 16 carbon atom. Hence, the initial rate was lower than those of oleic acid and linoleic acid. Nevertheless crack product from palmitic acid would be relatively stable and readily leave the catalyst surface. Accordingly, small weight loss at 420 °C can be observed and high liquid hydrocarbon can be obtained at high resident time.

4.7 Effect of catalyst/ fatty acid ratio

The effect of catalyst/ fatty acid ratio was studied at 460°C, reaction time at 6 hours. Mole ratio of catalyst/palmitic acid acid was varied from 0.5/1 by mol to 2/1 by mol over calcium oxide and cerium oxide reduced 300°C. Yield of liquid product are shown in Table 4.9

Table 4.9 Yield of liquid hydrocarbons using various amount of catalysts

catalyst	Yield from catalyst:palmitic acid			
	0.5 mol	1 mol	1.5 mol	2.0 mol
CaO	79%	84%	67%	26%
CeO_2 reduced 300°C	46%	76%	56%	42%

It can be seen that, for both catalysts, yield of hydrocarbons were increased as the catalyst/palmitic acid ratio increased from 0.5:1 to 1:1 mol. This is because number of active sites of the catalyst is increased However, when of catalyst: palmitic acid ratio increase up to 2:1mol, the yield of liquid was decreased. This is because, in the access of basic sites (i.e. catalyst: palmitic acid 2:1), ketonization of palmitic acid can be facilitated over CaO [61]. As the number of basic site increased, absorb fatty acid on CaO active sites would be closely proximate. The fatty acid on the adjacent site can undergo dehydration to form acid anhydride. At high temperature, such acid anhydride can be readily decarboxylated to form symmetrical ketone, as shown

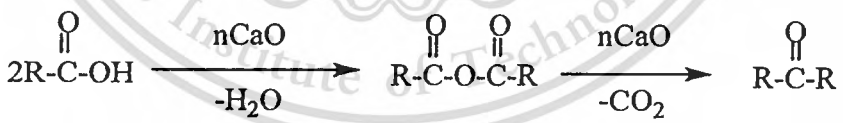

For the case of CeO_2 reduced at 300°C, the ketone is also observed and it was suggested to arise from coupling of palmitic acid at the oxygen vacancies site on CeO_2 surface [62-63]. When the amount of CeO_2 was increased, the number of Lewis acid site in reaction was increased leading to an increase in coupling products, i.e. dipalmitone. Accordingly, liquid product from decarboxylation at high catalyst/palmitic acid ratio is decreased. The structure of coupling products obtained from both CaO and CeO_2 can be confirmed by FT-IR and H-NMR, as shown in Figure 4.22 and 4.23.

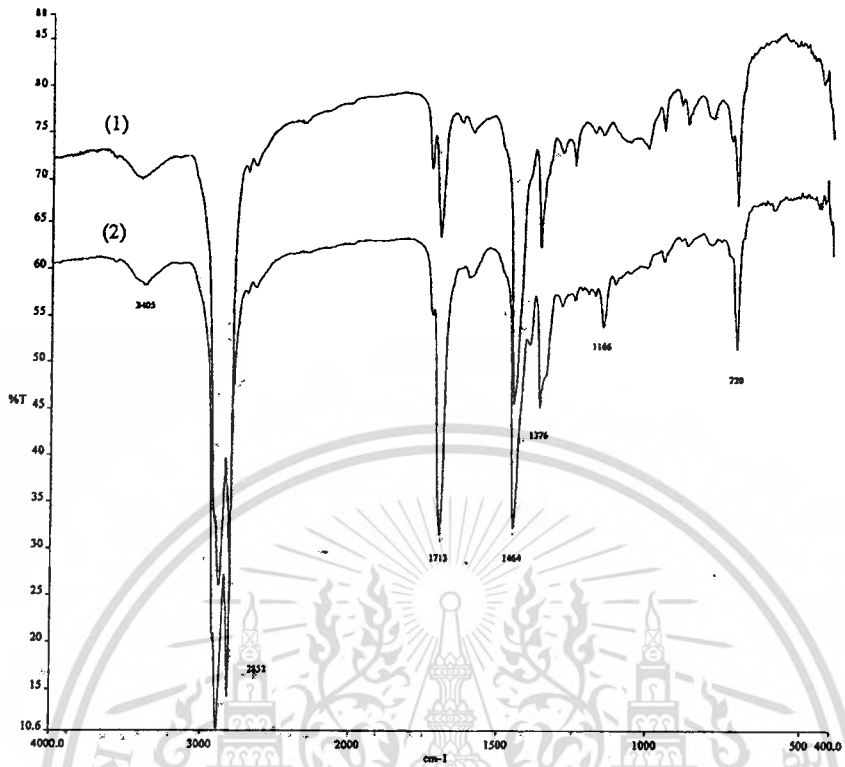

Figure 4.22 FT-IR spectra of product from ketonization; (1) CaO/palmitic acid (2:1mol), (2) CeO_2 reduced 300 °C /palmitic acid (2:1mol)

FT-IR spectra shows mainly C=O stretching vibration of ketone at 1716 cm^{-1} (C=O), 2853 cm^{-1} (C-H stretching) and 1465 cm^{-1} (C-H bending). As palmitone contain 31 carbon atoms, FT-IR spectra show strong band of C-H stretching and bending. However, FT- IR spectra show that small amount of palmitic acid is retaining in the samples. This can be evident by a shoulder peak at 1755 cm^{-1} of C=O carboxylic and at 1100-1200 cm^{-1}(C-O-C). Intensity of C=O ketone from the coupling products of CeO_2 is relatively higher than that over CaO suggesting the coupling product from CeO_2 possess relatively shorter chain length as compared to that from CaO. It is likely that coupling products from CeO_2 are mainly consist of 2-heptadecanone that was previously observed in small amount from the liquid product.

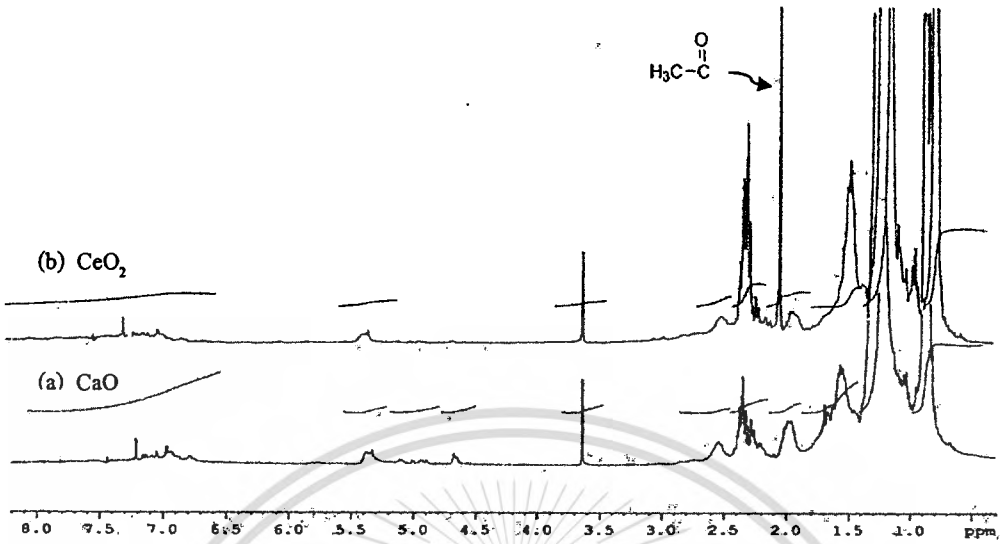

Figure 4.23 H-NMR of product from ketonization; (a) CaO/palmitic acid (2:1mol), (b) CeO_2 reduced 300 °C /palmitic acid (2:1mol)

In consistent with FT-IR, ^{1}H NMR spectrum of the coupling product from CeO_2 shows characteristic signal of the methyl proton of the ketone (2.2 ppm). While coupling product from CaO does not show the signal at 2.2 ppm, indicating that this product consists mainly of palmitone as discussed previously. The difference in coupling products from ketonization over CaO and CeO_2 was also confirmed by thermogravimetric analysis (TGA)

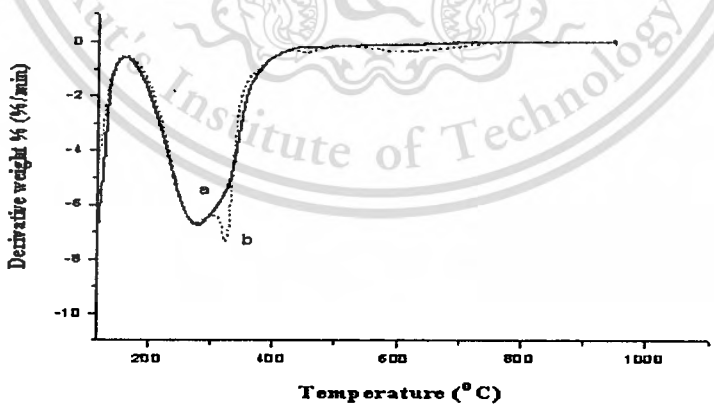

Figure 4.24 DTG of residue form palmitic acid over catalyst; (a) CaO:palmitic acid (2:1mol), (b) CeO_2:palmitic acid (2:1mol)

It can be seen that, coupling product from CeO_2 shows additional higher decomposition temperature at 325 °C, presumably for decomposition of 2-heptadecanone. While coupling product from CaO shows only decomposition temperature of palmitone at 280°C. This is again in line with FT-IR and ^{1}H-NMR results showing that CeO_2 give mainly 2-heptadecanone as coupling product, while coupling product over CaO is palmitone. In addtion, signal of aromatic at 6.5-7.5 ppm (^{1}H-NMR) can be observed for the residue. It was suggested that thermal degradation of palmitic acid lead to the formation of hydrocarbon radical that become precursor for aromatics [64].

4.8 Regeneration of catalyst

4.8.1 Regeneration temperature of reused CaO

The used calcium oxide was collected from the reaction using 1/1 by mol of catalyst/fatty acid at 460°C for 6 hours. The used calcium oxide was filtered and was recalcined in air at various temperatures for 5 hours. The regenerated catalysts were reused under the same reaction condition as above and yield of liquid hydrocarbon was shown in Figure 4.25.

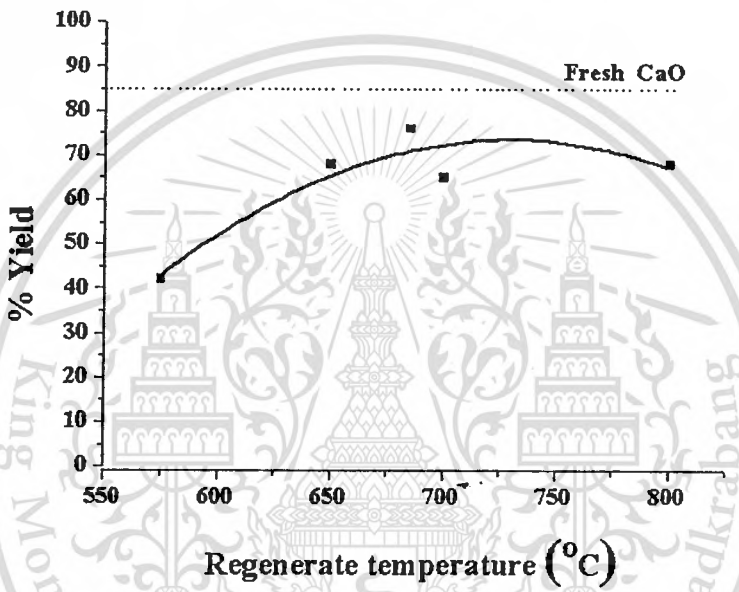

Figure 4.25 Liquid hydrocarbon from deoxygenation of CaO regenerate

It can be seen that yield from the regenerated CaO catalyst was increased, when regeneration temperature was increased from 575°C-685°C. This is because $CaCO_3$, formed during decarboxylation, can readily decompose to reactive CaO and CO_2. The CaO regenerated at 685 °C give higher liquid yield up to (76%), as compared to others. This is because $CaCO_3$ can be decomposed to CaO at > 685 °C, as confirmed with XRD pattern of CaO.

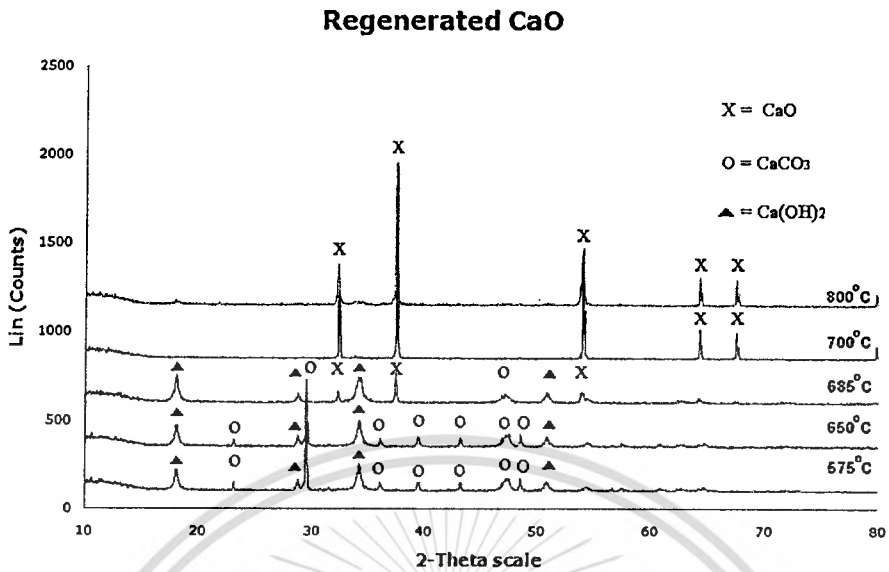

Figure 4.26 XRD pattern of CaO regenerated at various temperature

From XRD patterns, it can be seen that $CaCO_3$ phase is remained on the catalyst regenerated at 575 °C and 650 °C. While for CaO regenerated at 685 °C, patterns of CaO can be observed. Although XRD patterns show an increased CaO phase when the catalyst is regenerated at evaluated temperature especially at 700°C-800°C, the liquid yield is decreased (65-68%). This is because surface area of catalyst regenerated at 700°C-800°C is markedly reduced. It was expected that CaO regenerated at 700°C and 800°C was sintered, as seen by the increased in crystallinity (XRD) and a decreased in surface area in Table 4.10

Table 4.10 Surface area of regenerated calcium oxide

Regeneration temperature	Surface area (m^2/g)
685 °C	17
700 °C	13
800 °C	13

This suggested that not only active species but also high surface area of the catalyst is required for decarbonylation. Accordingly, the catalyst regenerated at 685°C which contains active sites and relatively high surface area shows the optimum yield of liquid hydrocarbons.

4.8.2 Regeneration of CeO_2

As cerium carbonate is not formed during decarbonylation as in CaO, the deactivation of CeO_2 is believed to result from the loss of oxygen vacancies and coke deposited on surface. This can be recovered by reducing the catalyst with H_2 as shown in Figure 4.27.

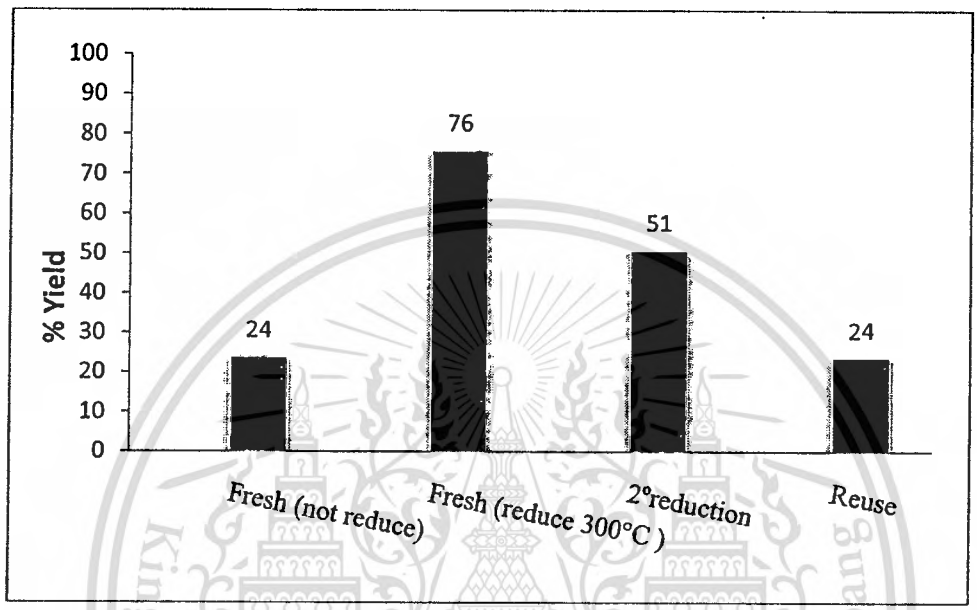

Figure 4.27 Liquid hydrocarbon from deoxygenation of CeO_2 regenerated

It can be seen that when CeO_2 was reused without 2°-reduction, liquid yield is extremely low. This is because an oxygen vacancy of reused CeO_2 was lost during the reaction. Hence, yield of liquid hydrocarbon from reused CeO_2 is similar to that yield of liquid hydrocarbon from fresh CeO_2 without reduction. However, while the used CeO_2 catalyst was reduced again with H_2 at 300°C, liquid hydrocarbon was increased up to 51%. This is because oxygen vacancies site can be recovered and activity can be enhanced. However, regenerated CeO_2 with H_2 at 300°C gives lower yield of liquid hydrocarbon as compared to the fresh CeO_2 reduced at 300 °C. It was suggested that surface area of regenerated CeO_2 with H_2 at 300°C was partly covered with coke deposited. Hence, sum of oxygen vacancies cannot be regenerated leading to the lower liquid hydrocarbon yield.

CHAPTER 5

CONCLUSION AND SUGGESTION

5.1 Conclusion

The alkaline earth metal oxide and lanthanide metal oxides are active catalyst for deoxygenation of palmitic acid to produce linear long chain hydrocarbons in a batch reactor. The appropriate reaction condition of deoxygenation of palmitic acid was as follows; reaction time 6 hr; reaction temperature 460 °C; 1/1 by mol of catalyst/palmitic acid.

The alkaline earth metal oxide is a basic catalyst. The catalyst primarily react with palmitic acid to form metal palmitate salt. After that, metal palmitate can be decarboxylated, deacethylated and cracked into mainly C_{14}-C_{15} and lower hydrocarbons. After reaction, the alkaline earth metal carbonate can be observed. Gas product was consist of carbon monoxide hydrogen and LPG gas. Barium oxide gives highest yield of liquid hydrocarbon, but barium oxide required high temperature for regeneration (>1000 °C). While calcium oxide can be regenerated at 685 °C and shows activity up to 84% liquid hydrocarbons. The regenerated calcium oxide gives 76% liquid hydrocarbon yield due to loss in surface area during regeneration. When catalyst content was increased up to >1:1 by mol, yield of liquid hydrocarbon was decreased. This is because calcium palmitate undergoes ketonisation to form high molecular weight ketone.

A cerium oxide shows high activity for deoxygenation when reduced at 300 °C. This is because an oxygen vacancy of cerium oxide was increased when the reduction temperature was increased. Cerium oxide gives up to 76% of liquid hydrocarbons. However, cerium oxide does not form cerium carbonate and carbon dioxide can be observed in the gas phase. Beside, gas products were consisted carbon monoxide, hydrogen, and LPG gas. However, cerium oxide reduced at 460 °C; give lower hydrocarbons due to cracking reaction. This is because the reduction temperature at 460 °C leads to defect of cerium oxide that may possess some acidity. Yield of liquid hydrocarbon is decreased when the amount of cerium oxide was increased. This is because cerium oxide can also promote ketonisation of palmitic acid to form high molecular weight ketone. When the used catalyst was reduced with hydrogen at 300 °C, an improved activity can be observed with activity of 51 % liquid

hydrocarbons. This is because coke deposit cannot decompose during secondary reduction with H_2. It was believed to remain on surface of cerium oxide causing a lower activity.

5.2 Suggestion for future studies

5.2.1 Magnesium oxide catalyst gives lower activity (73% of liquid hydrocarbon). However, magnesium oxide can be regenerated at lower temperature (<600 °C). Therefore, magnesium oxide should be appropriated catalyst and could be obtained the higher activity, if the basic site of magnesium oxide can be applied.

5.2.2 Saturated hydrocarbon products from deoxygenation of palmitic acid with metal oxides are raw materials for gasoline production. The unsaturated hydrocarbon products could be hydrogenated to saturated hydrocarbons. However, properties of saturated hydrocarbon products such as flash point, pour point, viscosity and octane number should be investigated.

5.2.3 A cerium oxide was reduced on fixed bed reactor before react with palmitic acid in batch reactor. However, a suitable process could be single bed reactor, which could be switched hydrogen-nitrogen gas for cerium oxide reduction and reaction with palmitic acid in same reactor.

5.2.4 The structure and constituents of the coupling product from effect of amount catalyst should be examined for synthetic lubricant oil production. However, properties of coupling product should be investigated compared to conventional lubricant oil.

REFERENCES

[1] K. Ayato, M. Koh and H. Katsuhisa. "Development of heterogeneous base catalysts for biodiesel production" **Bioresource Technology**, vol. 99, 2008. pp. 3439–3443.

[2] EMA (Engine manufacturers association). **Use of Raw Vegetable Oil or Animal Fats in Diesel Engines.** 2006.

[3] K. Iva, S. Mathias, E. Kari, A. M. Paivi and M. Y. Dmitry. "Hydrocarbons for diesel fuel via decarboxylation of vegetable oils" **Catalysis Today**, vol. 106, 2005. pp. 197–200.

[4] Z. Aihua, M. Qisheng, W. Kangshi, L. Xicai, S. Patrick and T. Yongchun. "Naphthenic acid removal from crude oil through catalytic decarboxylation on magnesium oxide" **Applied Catalysis A: General,** vol. 303, 2006. pp. 103–109.

[5] A. Igarashi, N. Ichikawa, S. Sato, R.i Takahashi, and T. Sodesawa. "Dehydration of butanediols over CeO_2 catalysts with different particle sizes" **Applied Catalysis A: General,** vol. 300, 2006. pp. 50–57.

[6] F. B. Noronha, E. C. Fendley, R. R. Soares, W. E. Alvarez and D. E. Resasco. "Correlation between catalytic activity and support reducibility in the CO_2 reforming of methane over $Pt/Ce_xZr_{1-x}O_2$ catalysts" **Chemical Engineering Journal,** vol. 82, 2001. pp. 21–31.

[7] R. J. Maria, F. M. Carmen, C. Abraham, R. Lourdes and P. Angel. "Influence of fatty acid composition of raw materials on biodiesel properties" **Bioresource Technology**, vol. 100, 2009. pp. 261–268.

[8] Andi baca. "Animal fat as fuel alternative " [Online] : http://www.polimerieuropa.com/200Page.lasso.html.2001

[9] Enginemanufacturers.org . "Use of Raw Vegetable Oil or Animal Fats in Diesel Engines" 2006.

[10] R. Alton, S. Cetinkaya and H. S. Yucesu. "The potential of using vegetable oil fuels as fuel for diesel engine" **Energy Conversion and Management**, vol. 42, 2001. pp. 529-538.

[11] E. Fischer. " esterification" [Online] : http://en.wikipedia.org/wiki/Esterification

[12] S. Chongkhong, C. Tongurai, P. Chetpattananondh and C. Bunyakan. "Biodiesel production by esterification of palm fatty acid distillat" **Biomass and Bioenergy**, vol.31, 2007. pp. 563–568.

[13] C.W. William. **Preparation of ester derivatives of fatty acids for chromatographic**. 1993.

[14] G.C. Bruce. **Catalytic Chemistry,** New York : John Wiley & Sons, Inc. 1992.

[15] M.J. Mendes, O.A.A. Santos, E. Jordao, and A.M. Silva." Hydrogenation of oleic acid over ruthenium catalysts" **Applied Catalysis A: General,** vol. 217, 2001. pp. 253–262.

[16] K. Amoa. "Catalytic Hydrogenation of Maleic Acid at Moderate Pressures A Laboratory Demonstration" **Chemical Education**, vol. 84, 2007.

[17] S. Mathias, K. Iva, A. M. Paivi, E. Kari and M. Y. Dmitry. " Heterogeneous catalytic deoxygenation of stearic acid for production of biodiesel" **Industrial Engineer Chemistry Research,** vol. 45, 2006. pp. 5706-5715.

[18] P. Mki-Arvela, M. Snre, K. Ernen, J. Myllyoja and D. Yu. Murzin. "Continuous decarboxylation of lauric acid over Pd/C catalyst" **Fuel**, vol. 87, 2008. pp. 3543–3549.

[19] A. Saadi, Z. Rassoul and M.M. Bettahar. "Reduction of benzaldehyde on alkaline earth metal oxides" **Journal of Molecular Catalysis A: Chemical,** vol, 258, 2006. pp. 59–67.

[20] **Studies Surface Science and Catalysis,** vol. 51, Amsterdam, Elsevier, 1989.

[21] L. Xuejun, H. Huayang, W. Yujin and Z. Shenlin. "Transesterification of soybean oil to biodiesel using SrO as a solid base catalyst" **Catalysis Communications,** vol. 8, 2007. pp. 1107-1111.

[22] C.G. David, J.G.Lisa, L.F.Adam and K. Wilson. "Structure-reactivity correlations in MgAl hydrotalcite catalysts for biodiesel synthesis" **Applied Catalysis A: General** , vol. 287, 2005. pp. 183–190.

[23] X. Liu, H. He, Y. Wang, S. Zhu and X. Piao. "Transesterification of soybean oil to biodiesel using CaO as a solid base catalyst" **Fuel,** vol. 87,2008 pp. 216–221.

[24] I.T. Horvath. **Encyclopedia of catalysis**, John wiley & sons, USA, 2003.

[25] H. Hattori. "Solid Base Catalysis: Generation of Basic Sites and Application to Organic Synthesis" **Applied catalysis A: General,** vol. 222, 2001. pp. 247-259.

[26] T. Seki, H. Kabashima, K. Akutsu,.H. Tachikawa and H. Hattori . "Mixed Tishchenko Reaction over Solid Base Catalysts" **Journal of Catalysis**, vol. 204, 2001. pp. 393–401.

[27] A. Saadi, Z. Rassoul and M.M. Bettahar. "Reduction of benzaldehyde on alkaline earth metal oxides"**Journal of Molecular Catalysis A: Chemical,** vol. 258, 2006. pp. 59–67.

[28] P. Broqvist, H. Gronbeck and I. Panas. "Surface properties of alkaline earth metal oxides" **Surface Science**, vol. 554, 2004. pp. 262–271.

[29] K. Tanabe and Y. Fulmda. "Basic properties of alkaline earth metal oxides and their catalytic activity in the decomposition of diacetone alcohol" **Reaction Kinetics and Catalysis Letters**, vol. 1, No. 1, 1974 pp. 21-14.

[30] K. Masato, K. Takekazu, T. Masahiko, S. Yoshikazu, Y. Shinya and H. Jusuke. "Calcium oxide as a solid base catalyst for transesterification of soybean oil and its application to biodiesel production" **Fuel**, vol. 87, 2008. pp. 2798–2806.

[31] T. C. Charles and P. H. F. Charles. "Oxygen Vacancies and Catalysis on Ceria Surface" **Science**, vol. 309, 2005. pp. 713-714.

[32] Istadi and A. S. Nor Aishah. "Screening of MgO- and CeO_2-Based Catalysts for Carbon Dioxide Oxidative Coupling of Methane to C2+ Hydrocarbon" **Journal of Natural Gas Chemistry**, vol. 13, 2004. pp. 23-35.

[33] N. Laosiripojana , D. Chadwick and S. Assabumrungrat. "Effect of high surface area CeO_2 and Ce-ZrO_2 supports over Ni catalyst on CH_4 reforming with H_2O in the presence of O_2, H_2, and CO" **Chemical Engineering Journal**, vol. 138, 2008. pp. 264–273.

[34] G. J. Speight. **The Chemistry and Technology of Petroleum**, 3rd Ed., New York : Marcel Dekker.

[35] A. G. Olah and A. Molnar. **Hydrocarbon Chemistry**. New York : John Wiley & Son, Inc. 1995.

[36] L. W. Nelson. **Petroleum Refinery Engineering.** 4th Ed., New York : Megraw-Hill book company. 1985.

[37] J. J. Sheehan, J. A. Dufield, R. B. Codon and V. J. Camobreco. " Life –cycle assessment of biodieel versus petroleum diesel fuel" 1996.

[38] George Lappin (ed.) (1989). "Alpha Olefins Applications Handbook" [Online] http://en.wikipedia.org/wiki/Linear_alpha_olefin

[39] Ineosoligomers "Polyalpha Olefin (PAO)" [Online] http://www.ineosoligomers.com/126-Products.htm

[40] **Chevron Phillips Chemical Company.** "Normal Alpha Olefins" [Online] http://www.cpchem.com/enu/nao_a_applications.asp

[41] S.M. Sadrameli and Alex E.S. Green. "Systematics of renewable olefins from thermal cracking of canola oil" **J. Anal. Appl. Pyrolysis**, vol.78, 2007. pp. 445–451.

[42] M.A. Paivi, K. Iva, S. Mathias, E. Kari and D.Y. Murzin. "Catalytic Deoxygenation of Fatty Acids and Their Derivatives" **Energy & Fuels**, vol. 21, 2007. pp. 30-41.

[43] M. Snare, I. Kubickova, P. Maki-Arvela, D. Chichova, K. Eranen and D.Yu. Murzin. "Catalytic deoxygenation of unsaturated renewable feedstocks for production of diesel fuel hydrocarbons" **Fuel**, vol. 87, 2008. pp. 933–945.

[44] W.Masaru, I.Toru and I.Hiroshi. "Decomposition of a long chain saturated fatty acid with some additives in hot compressed water" **Energy Conversion and Management,** vol. 47, 2006. pp. 3344–3350.

[45] Y, Sakata and V. Ponec. "Reduction of benzoic acid on CeO_2 and the effect of additives" **Applied Catalysis A: General**, vol. 166, 1998. pp. 173-184.

[46] M. Watanabe, H. Inomata, R. L. Smith Jr. and K. Arai. "Catalytic decarboxylation of acetic acid with zirconia catalyst in supercritical water" **Applied Catalysis A: General**, vol. 219, 2001. pp. 149–156.

[47] I. Simakova, O. Simakova, P. Maki-Arvela, A. Simakov, M. Estrada and D. Yu. Murzin. "Deoxygenation of palmitic and stearic acid over supported Pd catalysts:Effect of metal dispersion" **Applied Catalysis A: General,** vol. 355, 2009. pp. 100–108.

[48] H. Tian, , C.Y. Li, C.H. Yang and H.H. Shan. "Alternative Processing Technology for Converting Vegetable Oils and Animal Fats to Clean Fuels and Light Olefins" **Chinese Journal of Chemical Engineering**, vol. 16(3), 2008. pp. 394-400.

[49] B. Renard, J. Barbier Jr., D. Duprez and S. Dure´cu. "Catalytic wet air oxidation of stearic acid on cerium oxide supported noble metal catalysts" **Applied Catalysis B: Environmental**, vol. 55, 2005. pp. 1–10.

[50] C. Li, K. Domen, K.I. Maruya and T. Onishi. "Spectroscopic Identification of Adsorbed Species Derived from Adsorption and Decomposition of Formic Acid, Methanol, and Formaldehyde on Cerium Oxide" **Journal of Catalysis,** vol. 125, 1990. pp. 445-455.

[51] J. P. Holgado, R. Alvarez and G. Munuera. "Study of CeO_2 XPS spectra by factor analysis: reduction of CeO_2" **Applied Surface Science**, vol. 161, 2000. pp. 301–315.

[52] H. Hattori. "Heterogeneous Basic Catalysis" **Chemical Review**, vol.95, 1995. pp. 537-550.

[53] S. Sugiyama, K. Sato, S. Yamasaki, K. Kawashiro and Hiromu Hayashi. "Ketones from carboxylic acids over supported magnesium oxide and related catalysts" **Catalysis Letters,** vol. 14, 1992. pp. 127-133.

[54]A. Sen. "Catalytic Functionalization of Carbon-Hydrogen and Carbon-Carbon Bonds in Protic Media" **Accounts of Chemical Research,** vol. 31, 1998. NO. 9.

[55] E.N. Ndifor, T. Garcia, B. Solsona and S. H. Taylor. "Influence of preparation conditions of nano-crystalline ceria catalysts on the total oxidation of naphthalene, a model polycyclic aromatic hydrocarbon" **Applied Catalysis B: Environmental**, vol.76, 2007. pp. 248–256.

[56] Y. Zhang, Z. Wang, J. Zhou and K. Cen. "Ceria as a catalyst for hydrogen iodide decomposition in sulfur–iodine cycle for hydrogen production" **International Journal of Hydrogen Energy,** vol.34, 2009. pp. 1688-1695.

[57] F. Dury, E.M. Gaigneaux. "The deoxygenation of benzoic acid as a probe reaction to determine the impact of superficial oxygen vacancies (isolated or twin) on the oxidation performances of Mo-based oxide catalysts" **Catalysis Today,** vol. 117, 2006. pp. 46–52.

[58] F. Dury, S. Meixner, D. Cl´ement and E.M. Gaigneaux. "Coupling the deoxygenation of benzoic acid with the oxidation of propylene on a Co molybdate catalyst" **Journal of Molecular Catalysis A: Chemical,** vol. 237, 2005. pp. 9–16.

[59] H. Idriss. "Ethanol reactions over the surfaces of noble metal/cerium oxide catalysts" **Platinum Metals Rev,** vol. 48, 2004. pp. 105-115.

[60] G. R. Rao and H. R. Sahu. "XRD and UV-Vis diffuse reflectance analysis of CeO_2–ZrO_2 solid solutions synthesized by combustion method" **Chem. Sci,** vol. 113, 2001. pp. 651–658.

[61] A. Corma, M.Renz and C. Schaverien. "Coupling fatty acids by ketonic decarboxylation using solid catalysts for the direct production of diesel, lubricants, and chemicals" **ChemSusChem,** vol.1, 2008. pp. 739 – 741.

[62] S. D. Randery, J. S. Warren and K. M. Dooley. "Cerium oxide-based catalysts for production of ketones by acid condensation" **Applied Catalysis A: General**, vol.226, 2002. pp.265–280.

[63] K. M. Dooley, A. K. Bhat, C. P. Plaisance and A. D. Roy. "Ketones from acid condensation using supported CeO_2 catalysts: Effect of additives" **Applied Catalysis A: General,** vol. 320, 2007. pp.122–133.

[64] M. Julia. "Free radical cyclizations" University of Paris, Paris, France.

APPENDIX A

CALCULATION

Calculations of catalytic parameters

Yield

Yield of each product is defined as percentage of molar ratio of particular product obtained and the reactant fed during a certain period of time.

EX . *Reaction time 2 hr.*

Sample CaO + Palmitic acid (1:1 mol)

Calcium oxide	1.68 g
Palmitic acid	7.69 g
Total	9.37 g.

Results

Residue in reactor	6.87 g	
Trap condenser 1	1.09 g	} Total oil = 1.2 g
Trap condenser 2	0.11 g	
Total	8.07 g	

Calculate % Yield

Palmitic acid	6.26 g
MW Palmitic acid	256.42 g/mol
MW Oil ($-CO_2$)	=256.42-44
	=212.42 g/mol

$$\text{Theories oil } \frac{6.26\ \text{g}}{256.42\text{g/mol}} \times 212.42\ \text{g/mol} = 5.18\ \text{g}$$

$$\% \text{ Yield} = \frac{1.2\text{g}}{5.18\text{g}} \times 100 = 23\%$$

Selectivity

Selectivity of the products was defined as the ratio of mole of particular product and the total mole of the reactant converted. High selectivity of a desired product was preferred. %Selectivity can be obtained from the following equation.

$$\% \text{ Selectivity} = \frac{yield\ oil}{Total\ Yield} \times 100$$

Ex. Yield of C15 saturated hydrocarbon 10.4

Total yield 84.2

$$\underline{\% \text{ Selectivity}} = \frac{10.4}{84.2} \times 100 = 12.35\ \%$$

APPENDIX B

REACTION DATA

Table B1 Result of temperature from reaction of fatty acid using calcium oxide

Reaction with CaO												
	2 hr			3 hr			4 hr			6 hr		
	Palmitic acid	Oleic acid	Linolei c acid	Palmitic acid	Oleic acid	Linoleic acid	Palmitic acid	Oleic acid	Linoleic acid	Palmitic acid	Oleic acid	Linoleic acid
% yield	23%	60%	32%	55%	67%	52%	84%	68%	64%	84%	75%	72%
Weigh product (g)	1.20	4.29	2.26	3.46	4.81	3.70	5.39	4.83	4.54	5.08	5.36	5.11
Weight residue(g)	6.87	5.36	6.82	5.20	4.54	5.04	3.17	4.68	4.90	2.47	4.17	4.40

Table B2 The Amount of palmitic acid and alkaline earth metal oxide in deoxygenation

Time	Palmitic acid + MgO		Palmitic acid + CaO		Palmitic acid + SrO		Palmitic acid + BaO	
(hr)	Palmitic acid (g)	MgO (g)	Palmitic acid (g)	CaO (g)	Palmitic acid (g)	SrO (g)	Palmitic acid (g)	BaO(g)
6 hr	7.693	1.206	7.692	1.682	7.692	4.788	7.707	4.598

Table B3 The result of alkaline earth metal oxide in deoxygenation with palmitic acid

	Reaction with alkaline earth metal oxide			
	MgO	**CaO**	**SrO**	**BaO**
% yield	73 %	84 %	74 %	83 %
Weigh product (g)	4.709 g	5.511 g	4.716 g	5.278 g
Weight residue(g)	2.763 g	2.472 g	4.045 g	3.858 g

Table B4 The Amount fatty acid and calcium oxide in deoxygenation

Time (hr)	Palmitic + CaO		Linoleic acid + CaO		Oleic acid + CaO	
	Palmitic acid (g)	CaO (g)	Linoleic acid (g)	CaO (g)	Oleic acid (g)	CaO (g)
2 hr	7.693	1.682	8.413	1.682	8.471	1.684
3 hr	7.696	1.683	8.418	1.684	8.470	1.683
4 hr	7.697	1.684	8.417	1.683	8.471	1.688
6 hr	7.691	1.681	8.418	1.687	8.475	1.681

Table B5 Result of reduction temperature in deoxygenation of palmitic acid using cerium oxide

Reaction with CeO_2				
	Non-reduced	Reduced 200°C	Reduced 300°C	Reduced 460°C
% yield	23 %	49%	76%	78%
Weigh product (g)	1.483 g	3.121 g	4.862 g	4.991 g
Weight residue(g)	10.698 g	7.034 g	7.063 g	7.878 g

Table B6 The Amount fatty acid and cerium oxide in deoxygenation

Reaction with CeO_2								
Time (hr)	**Non reduced**		**Reduced 200°C**		**Reduced 300°C**		**Reduced 460°C**	
	Palmitic acid (g)	CeO_2 (g)	Palmitic acid (g)	CeO_2 (g)	Palmitic acid (g)	CeO_2 (g)	Palmitic acid (g)	CeO_2 (g)
6 hr	7.101	5.173	7.696	5.185	7.703	5.194	7.673	5.174

Table B7 The amount fatty acid, reused cerium oxide and 2° reduction cerium oxide in deoxygenation for 6 hr

Regeneration				
Time (hr)	2-Reduced 300°C		Reuse	
	Palmitic acid (g)	CeO_2 (g)	Palmitic acid (g)	CeO_2 (g)
6 hr	6.689	4.497	7.703	5.172

Table B8 The amount fatty acid and calcium oxide regenerated at various temperature in deoxygenation for 6 hr

CaO	Regeneration of calcium oxide	
	Palmitic acid (g)	CaO (g)
575	7.692	1.683
650	7.703	1.697
685	7.698	1.684
700	7.708	1.695
800	7.699	1.682

APPENDIX C

GAS CHROMATOGRAM

Analysis liquid product from gas chromatography

The liquid products from trap 1 and trap 2 were analysed by GC-FID. The chromatogram of liquid products were identified using reference standard for comparison in table c1

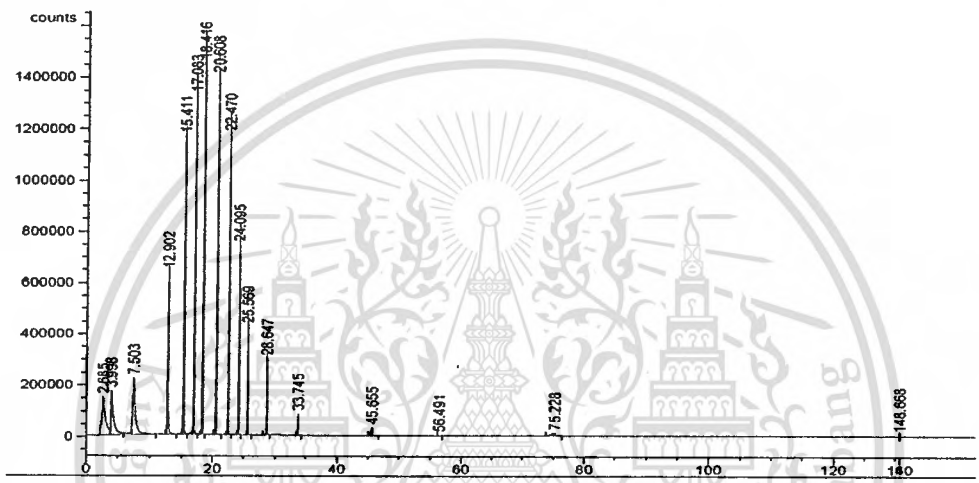

Figure C1 Chromatogram of standard hydrocarbon C6-C44

Table c1 Chromatogram of saturated standard hydrocarbon

Hydrocarbon (Alkane)	Retention time of standard (min)	Hydrocarbon (Alkane)	Retention time of standard (min)
C6	2.685	C18	24.095
C7	3.998	C20	25.569
C8	7.503	C24	28.647
C9	12.902	C28	33.745
C10	15.411	C32	45.655
C11	17.083	C36	56.491
C12	18.416	C40	75.228
C14	20.608	C44	148.668
C16	22.470		

The GC-FID of oil from reaction fatty acid with CaO

Product from Palmitic acid

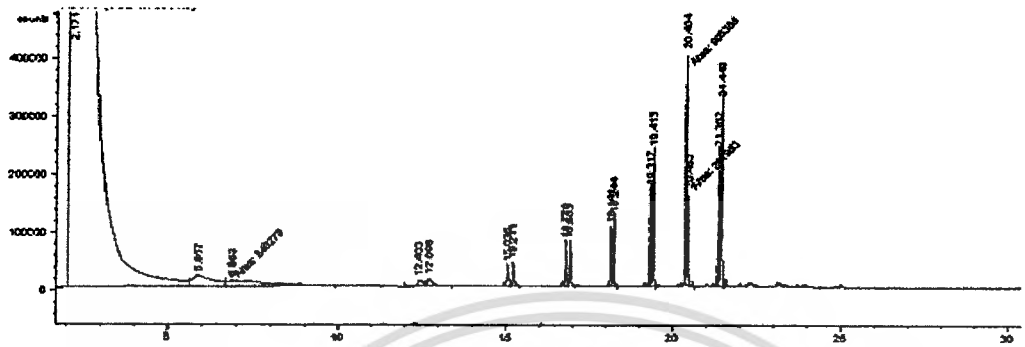

Figure C2 Chromatogram of product trap 1 from palmitic acid using calcium oxide (1:1mol, 460°C, 6 h.)

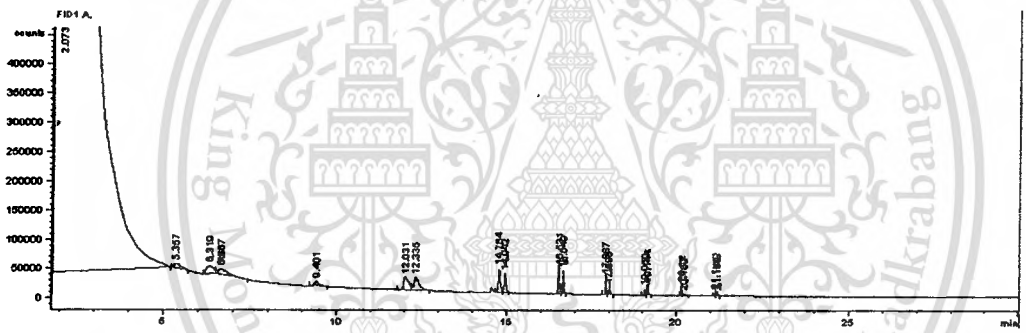

Figure C3 Chromatogram of product trap 2 from palmitic acid using calcium oxide (1:1mol, 460°C, 6 h.)

Table C2 Chromatogram of liquid product from palmitic acid using calcium oxide

Retention time (min)	Hydrocarbon	Retention time (min)	Hydrocarbon
2.079	Acetone	12.657	Nonane
2.531	Hexene	15.027	Decene
3.857	Heptene	15.215	Decane
5.533	Heptane	16.790	Undecene
6.649	Octene	16.924	Undecane
7.423	Octane	18.169	Dodecene
12.344	Nonene	18.280	Dodecane

Retention time (min)	Hydrocarbon	Retention time (min)	Hydrocarbon
19.317	Tridecene	20.463	Tetradecane
19.413	Tridecane	21.302	Pentadecene
20.404	Tetradecene	21.440	Pentadecane

Product from Linoleic acid

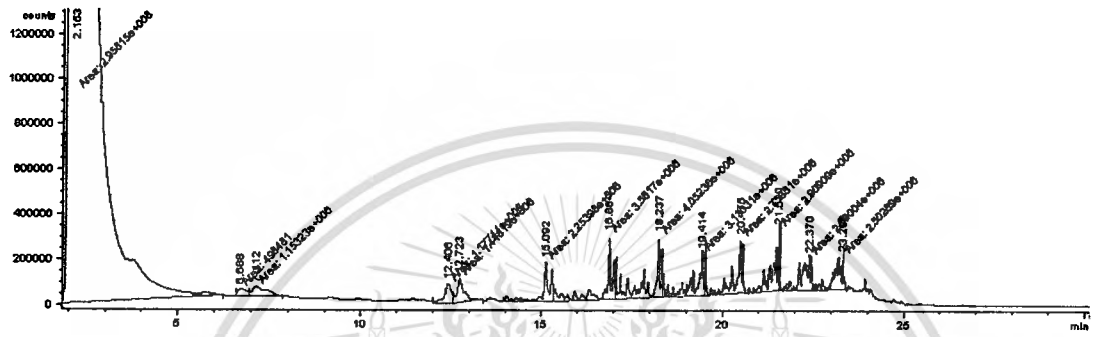

Figure C4 Chromatogram of product trap 1 from linoleic acid using calcium oxide (1:1mol, 460°C, 6 h.)

Figure C5 Chromatogram of product trap 2 from linoleic acid using calcium oxide (1:1mol, 460°C, 6 h.)

Product from oleic acid

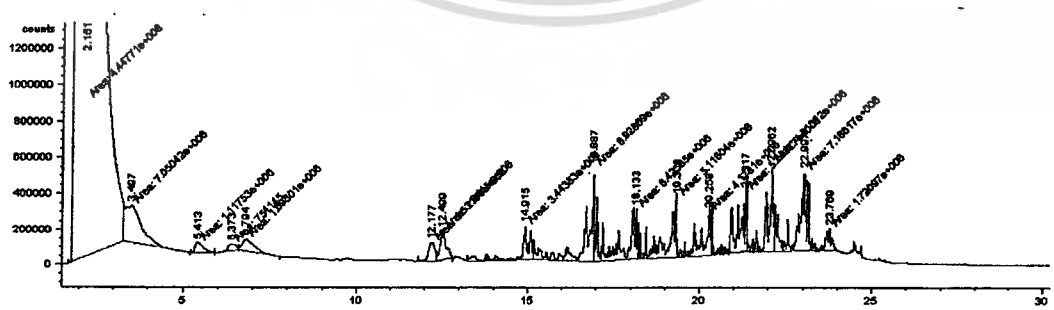

Figure C6 Chromatogram of product trap 1 from oleic acid using calcium oxide (1:1mol, 460°C, 6 h.)

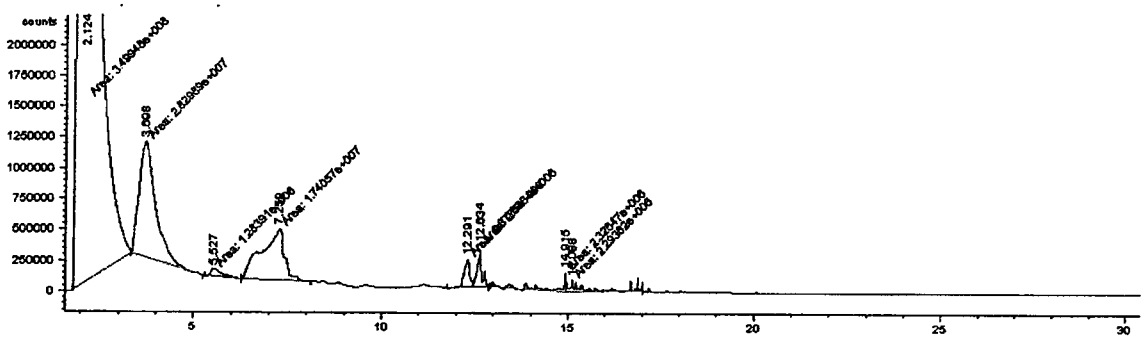

Figure C7 Chromatogram of product trap 2 from oleic acid using calcium oxide (1:1mol, 460°C, 6 h.)

Table c3. The retention time and product from linoleic acid and oleic acid using calcium oxide

Retention time (min)	Hydrocarbon	Retention time (min)	Hydrocarbon
1.59	Acetone	17.91	2-Undecanone
2.00	Hexene	17.96	Tridecane
2.96	Heptene	18.43	Heptylcyclohexane
3.09	Heptane	18.82	Tetradecene
5.37	Octene	18.90	Tetradecane
5.70	Octane	19.37	Cyclopentane
11.01	Nonene	19.42	Cyclopentene
11.40	Nonane	19.55	Cyclohexene
13.93	Decene	19.66	Cyclopentadecane
14.09	Decane	19.70	Pentadecene
15.58	Undecene	19.76	Pentadecane

Retention time (min)	Hydrocarbon	Retention time (min)	Hydrocarbon
15.69	Undecane	20.04	1-Hexadecyne
15.77	2-Undecene	20.25	n-Nonylcyclohexane
15.88	5-Undecene	20.41	Benzocyclodecaene
16.03	Cyclodecene	20.47	Cyclohexadecane
16.47	2,4-Undadiene	20.52	Hexadecene
16.82	Dodecene	20.58	Hexadecane
16.91	Dodecane	20.83	2-Cyclohexen-1-one
16.97	2-Dodecane	21.19	8-Heptadecene
17.20	Cycloheptane	21.34	Heptadecane
17.88	Tridecene		

Analysis gas product from gas chromatography

The chromatogram of gas products were identified using standard gas. The gas product were analyzed by online GC-TCD

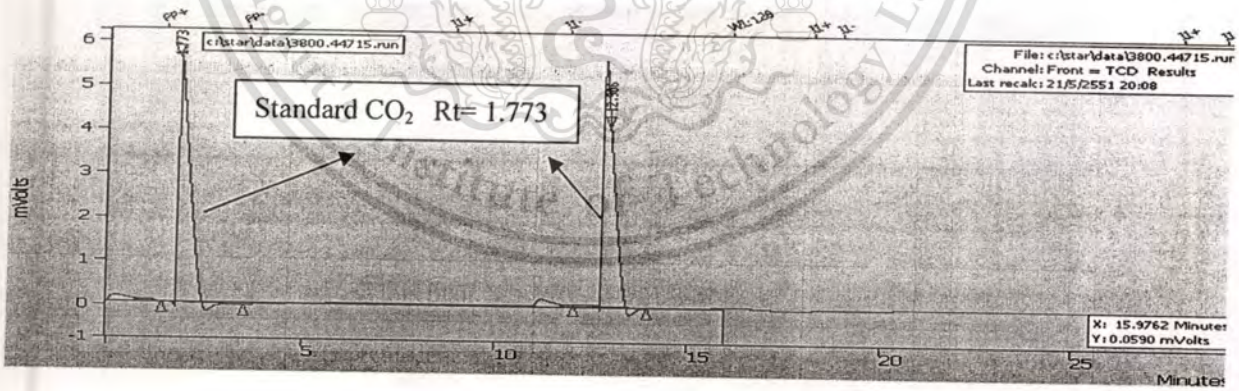

Figure C8 Retention time of carbon dioxide standard gas

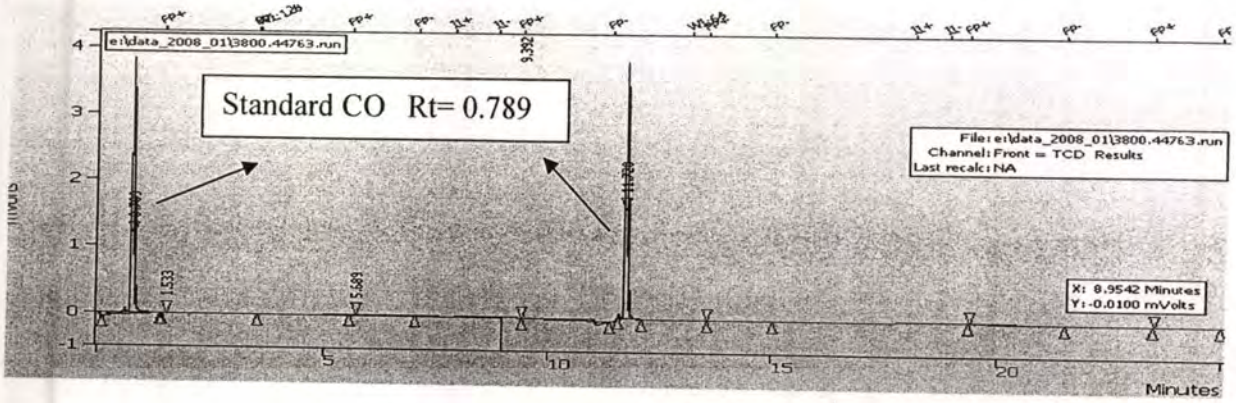

Figure C9 Retention time of carbon monoxide standard gas

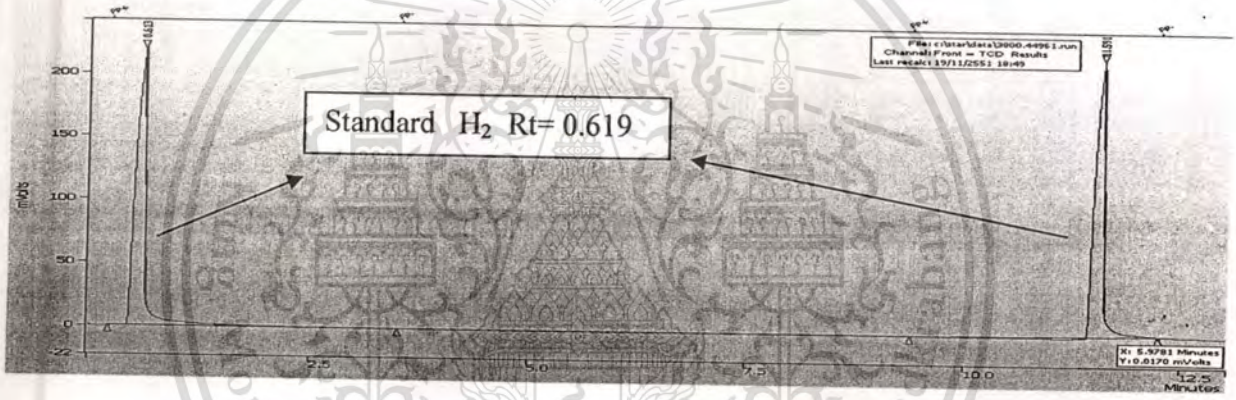

Figure C10 Retention time of hydrogen standard gas

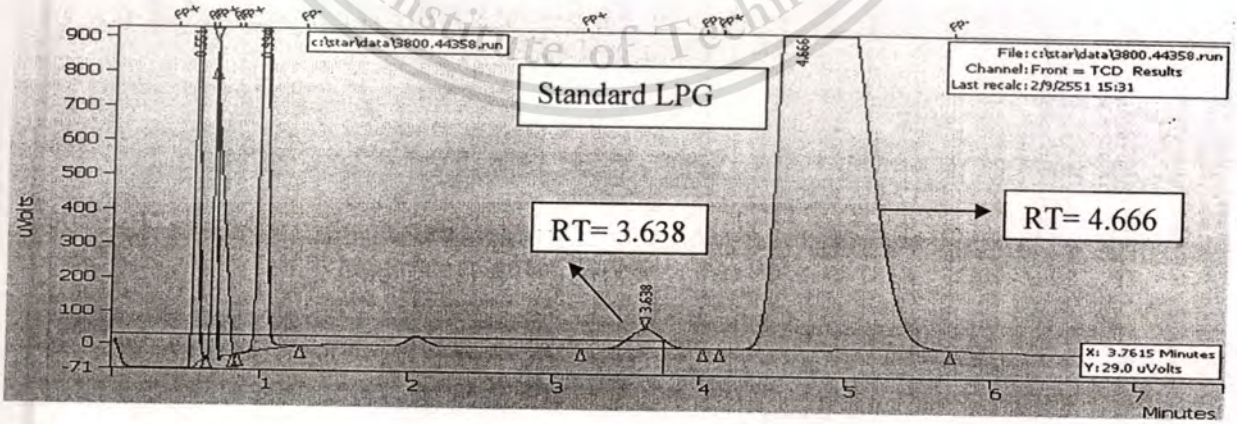

Figure C11 Retention time of LPG standard gas

APPENDIX D

CHARACTERIZATION DATA

The X-ray diffraction patterns of metal oxide

Calcium oxide

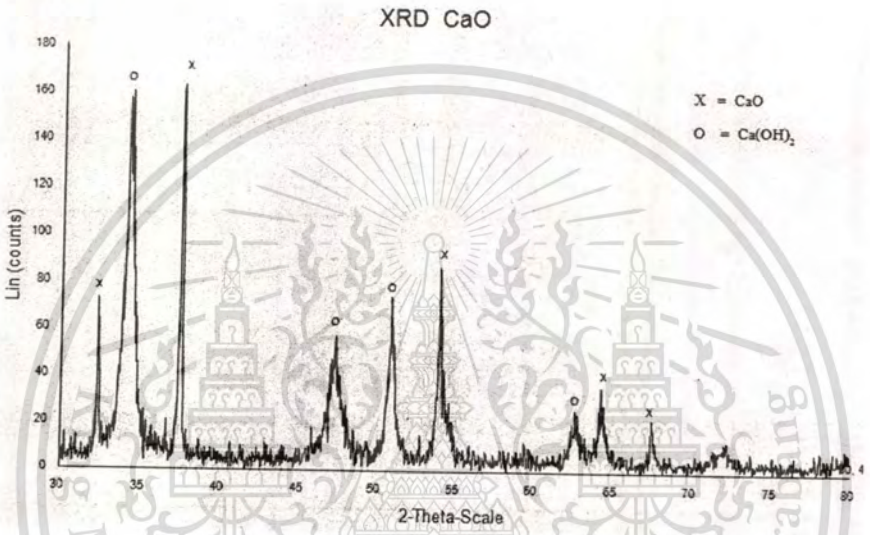

Figure D1 X-ray diffraction pattern of calcium oxide

Magnesium oxide

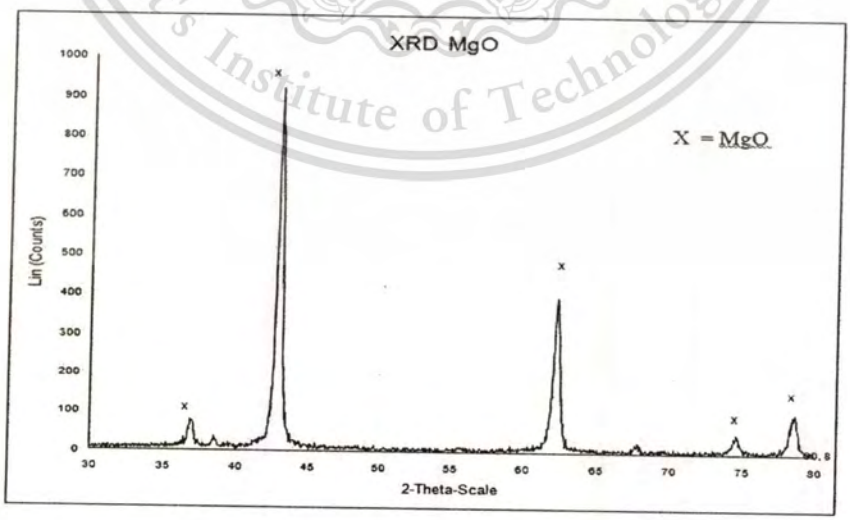

Figure D2 X-ray diffraction pattern of magnesium oxide

Cerium oxide

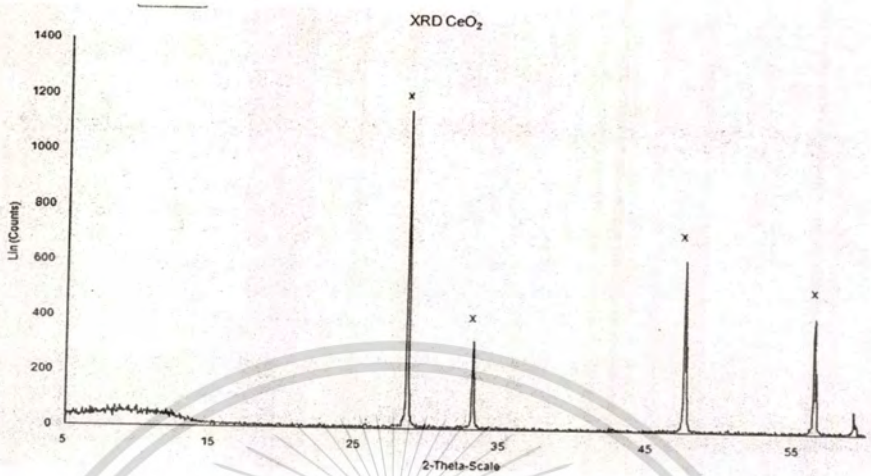

Figure D3 X-ray diffraction pattern of cerium oxide

Strontium oxide

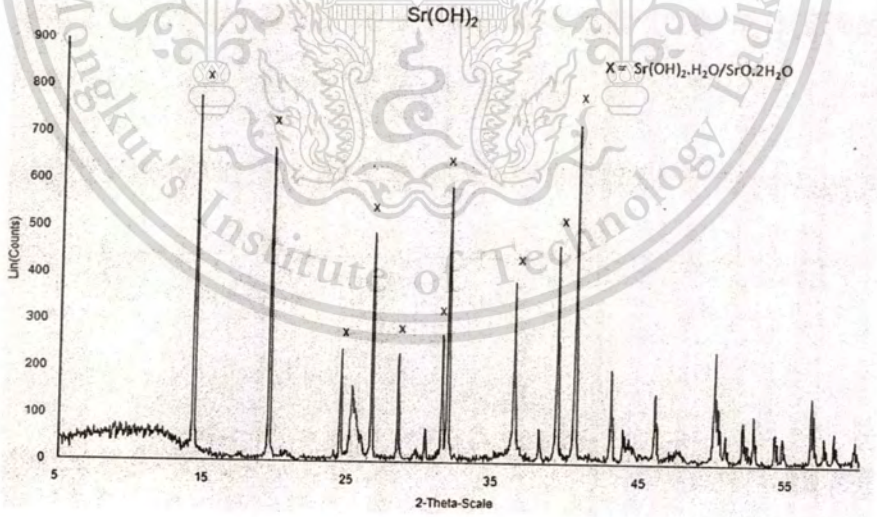

Figure D4 X-ray diffraction pattern of strontium oxide

Barium oxide

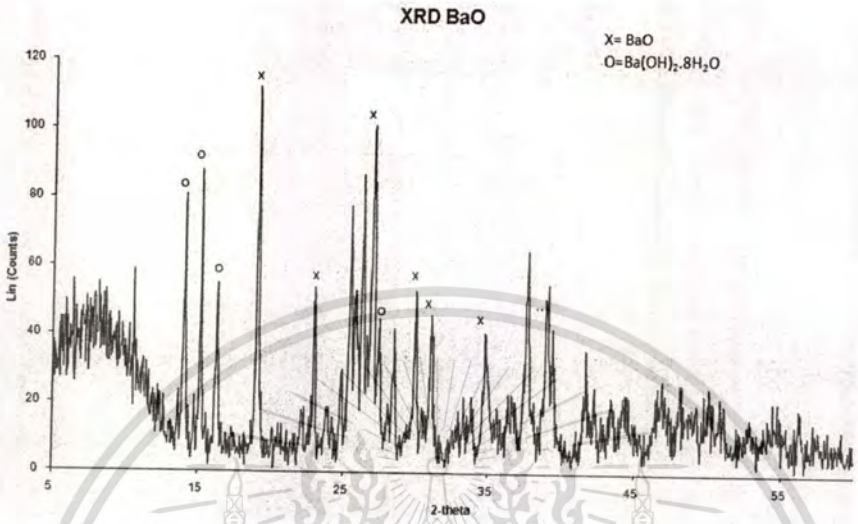

Figure D5 X-ray diffraction pattern of barium oxide

Surface Area of Metal oxide

Calcium oxide

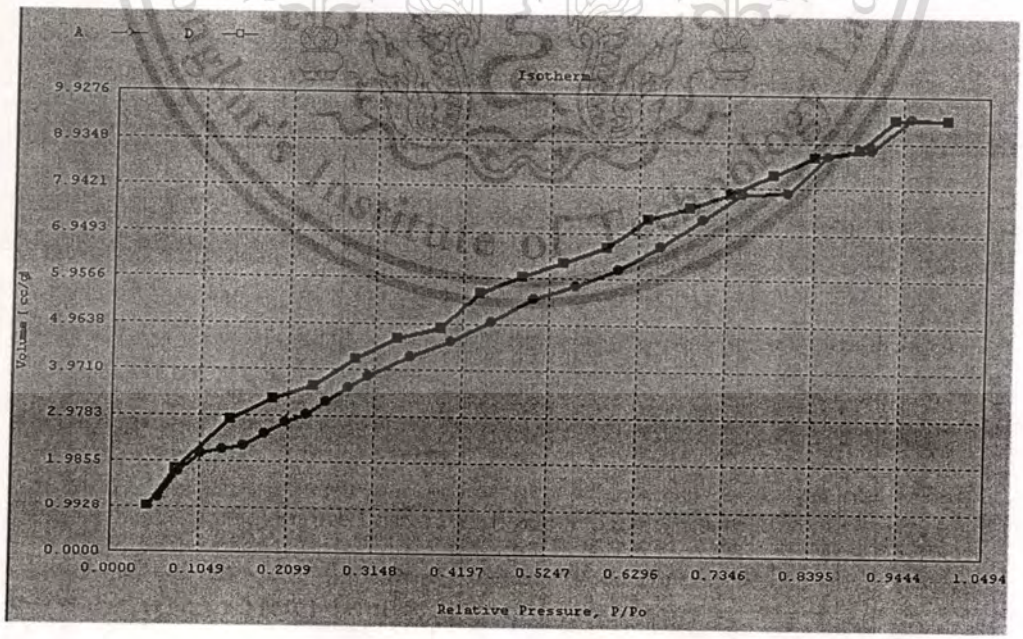

Figure D6 Isotherm of calcium oxide

Sample ID	CaO				
Description	Adsorption 20 pts, Desorption 20 pts, BET				
Comments					
Sample Weight	0.0460 g				
Adsorbate	NITROGEN	Outgas Temp	350 °C	Operator	Off
Cross-Sec Area	16.2 Å²/molec	Outgas Time	20.0 hrs	Analysis Time	453.6 min
NonIdeality	6.580E-05	P/Po Toler	0	End of Run	07/12/2007 23:3
Molecular Wt	28.0134 g/mol	Equil Time	3	File Name	500712_1.RAW
Station #	1	Bath Temp.	77.40		

Isotherm

P/Po	Volume [cc/g] STP	P/Po	Volume [cc/g] STP	P/Po	Volume [cc/g] STP
5.8178e-02	1.2173	5.5777e-01	5.8008	6.9238e-01	7.5223
8.1441e-02	1.7738	6.0815e-01	6.1787	6.4131e-01	7.2548
1.0749e-01	2.1570	6.5807e-01	6.6599	5.9252e-01	6.6404
1.3256e-01	2.2584	7.0749e-01	7.2521	5.4197e-01	6.3200
1.5902e-01	2.3323	7.5537e-01	7.8284	4.9180e-01	5.9945
1.8350e-01	2.5875	8.0982e-01	7.8368	4.4207e-01	5.6339
2.0836e-01	2.8350	8.5581e-01	8.6512	3.9413e-01	4.8915
2.3377e-01	3.0199	9.0896e-01	8.7837	3.4203e-01	4.6595
2.5749e-01	3.2965	9.5529e-01	9.4548	2.9219e-01	4.2167
2.8471e-01	3.6070	9.9940e-01	9.4370	2.4134e-01	3.6281
3.0842e-01	3.8575	9.3698e-01	9.4385	1.9265e-01	3.3337
3.5784e-01	4.2556	8.9382e-01	8.7967	1.4328e-01	2.8807
4.0688e-01	4.6083	8.4139e-01	8.6274	7.7327e-02	1.8240
4.5610e-01	5.0202	7.9168e-01	8.2260	4.4349e-02	1.0263
5.0608e-01	5.5281	7.4210e-01	7.8140		

Figure D7 Data isotherm of calcium oxide

Magnesium oxide

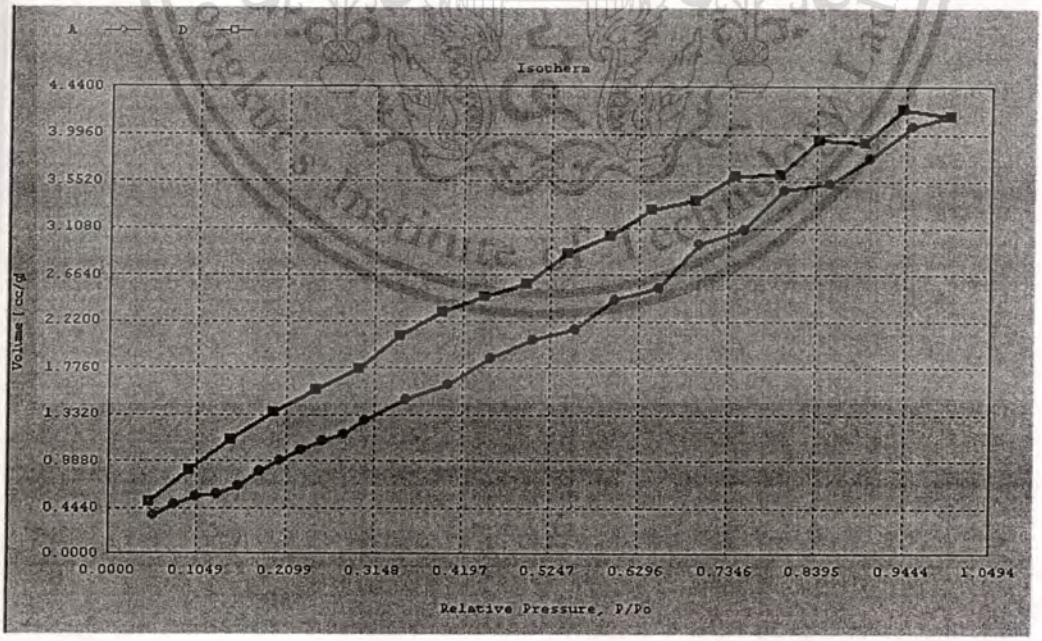

Figure D8 Isotherm of magnesium oxide

Sample ID	MgO				
Description	Adsorption 20 pts, Desorption 20 pts, BET				
Comments					
Sample Weight	0.0481 g				
Adsorbate	NITROGEN	Outgas Temp	350 °C	Operator	Off
Cross-Sec Area	16.2 Å²/molec	Outgas Time	20.0 hrs	Analysis Time	478.3 min
NonIdeality	6.580E-05	P/Po Toler	0	End of Run	07/09/2007 01:10
Molecular Wt	28.0134 g/mol	Equil Time	3	File Name	500708_1.RAW
Station #	1	Bath Temp.	77.40		

Isotherm

P/Po	Volume [cc/g] STP	P/Po	Volume [cc/g] STP	P/Po	Volume [cc/g] STP
5.2004e-02	17.1100	5.5588e-01	33.7690	6.9377e-01	36.8958
7.7205e-02	20.5370	6.0411e-01	34.8171	6.4620e-01	36.3349
1.0547e-01	23.0200	6.5289e-01	35.7441	5.9526e-01	35.3031
1.2696e-01	24.2526	7.0416e-01	36.7495	5.4428e-01	34.4944
1.5335e-01	25.3690	7.5686e-01	36.8981	4.9443e-01	33.6353
1.7874e-01	26.1917	8.0447e-01	38.3345	4.4323e-01	32.7349
2.0566e-01	26.9690	8.5274e-01	39.3320	3.9686e-01	31.5299
2.3227e-01	27.2765	9.0532e-01	39.7832	3.4619e-01	30.6356
2.5680e-01	27.8364	9.5398e-01	41.2306	2.9617e-01	29.5480
2.8231e-01	28.3385	9.9677e-01	42.3241	2.4471e-01	28.4031
3.0814e-01	28.8254	9.4701e-01	41.0728	1.9780e-01	27.1543
3.5401e-01	29.9809	8.9323e-01	40.5133	1.5049e-01	25.2617
4.0395e-01	30.9356	8.4422e-01	39.4129	9.6060e-02	22.4967
4.5486e-01	31.9674	7.9369e-01	38.5917	4.0892e-02	15.7172
5.0401e-01	33.0457	7.4462e-01	37.7391		

Figure D9 Data isotherm of magnesium oxide

Strontium oxide

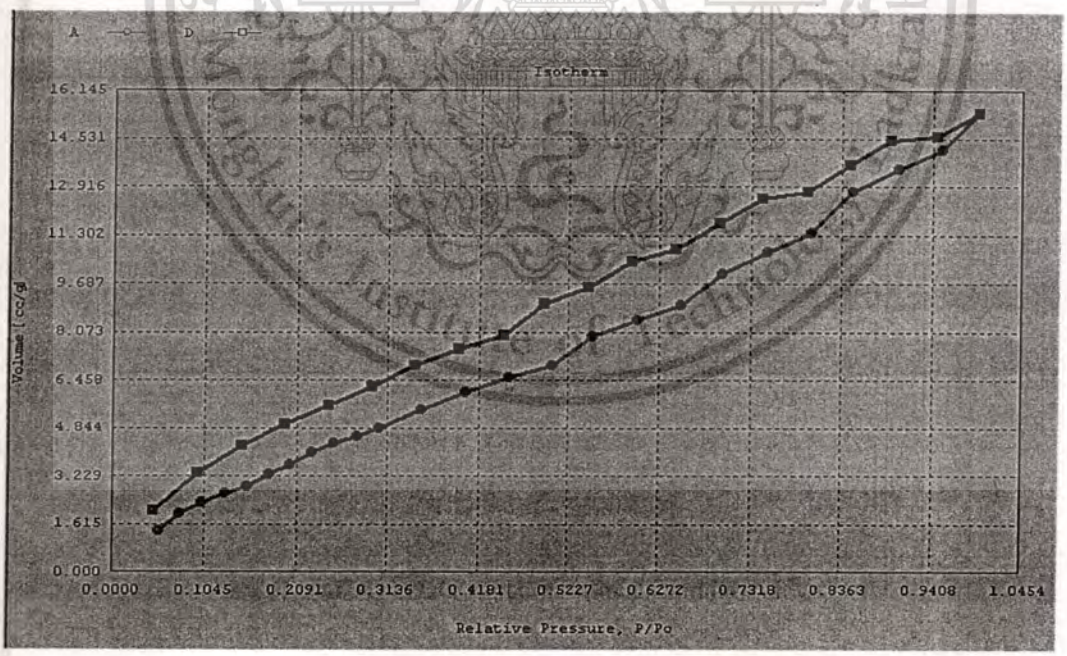

Figure D10 Isotherm of strontium oxide

Sample ID	Sr(OH)2				
Description	Adsorp 20 pts,Desorp 20 pts,BET 11 pts				
Comments					
Sample Weight	0.0597 g				
Adsorbate	NITROGEN	Outgas Temp	350 °C	Operator	golf
Cross-Sec Area	16.2 Å²/molec	Outgas Time	10.0 hrs	Analysis Time	372.4 min
NonIdeality	6.580E-05	P/Po Toler	0	End of Run	05/07/2008 23:20
Molecular Wt	28.0134 g/mol	Equil Time	3	File Name	510506_1.RAW
Station #	1	Bath Temp.	77.40		

Isotherm

P/Po	Volume [cc/g] STP	P/Po	Volume [cc/g] STP	P/Po	Volume [cc/g] STP
5.3614e-02	1.3692	5.5219e-01	7.9319	6.9757e-01	11.7011
7.7476e-02	1.9609	6.0359e-01	8.4808	6.4767e-01	10.8428
1.0345e-01	2.3351	6.5391e-01	8.9949	5.9674e-01	10.4441
1.2910e-01	2.6756	7.0128e-01	10.0058	5.4778e-01	9.5783
1.5493e-01	2.8833	7.5256e-01	10.7490	4.9599e-01	9.0118
1.7900e-01	3.2970	8.0311e-01	11.4112	4.4738e-01	7.9983
2.0359e-01	3.6332	8.4995e-01	12.7675	3.9664e-01	7.5382
2.2897e-01	4.0100	9.0254e-01	13.5463	3.4628e-01	7.0016
2.5395e-01	4.3239	9.5305e-01	14.1876	2.9690e-01	6.2361
2.7953e-01	4.5704	9.9559e-01	15.3766	2.4693e-01	5.5949
3.0496e-01	4.8582	9.4731e-01	14.6075	1.9643e-01	4.9845
3.5340e-01	5.4775	8.9432e-01	14.4787	1.4774e-01	4.2423
4.0374e-01	6.0595	8.4735e-01	13.6620	9.8652e-02	3.3629
4.5398e-01	6.5526	7.9769e-01	12.7741	4.7649e-02	2.0784
5.0436e-01	6.9920	7.4602e-01	12.5330		

Figure D11 Data isotherm of strontium oxide

Cerium oxide

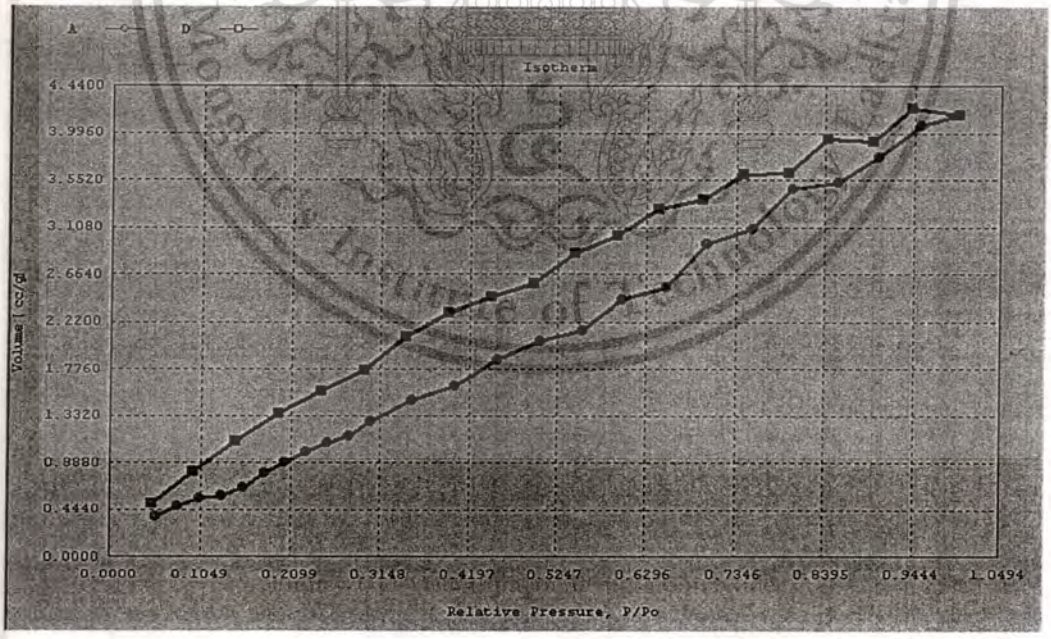

Figure D12 Isotherm of cerium oxide

Sample ID	CeO2uncal				
Description	Adsorption 20 ,Desorption 20 ,Bet 11				
Comments					
Sample Weight	0.1140 g				
Adsorbate	NITROGEN	Outgas Temp	350 °C	Operator	golf
Cross-Sec Area	16.2 Å²/molec	Outgas Time	10.0 hrs	Analysis Time	347.2 min
NonIdeality	6.580E-05	P/Po Toler	0	End of Run	01/17/2008 01:37
Molecular Wt	28.0134 g/mol	Equil Time	3	File Name	510116_1.RAW
Station #	1	Bath Temp.	77.40		

Isotherm

P/Po	Volume [cc/g] STP	P/Po	Volume [cc/g] STP	P/Po	Volume [cc/g] STP
5.5000e-02	0.3828	5.5533e-01	2.1510	6.9683e-01	3.3653
7.9602e-02	0.4758	6.0346e-01	2.4357	6.4498e-01	3.2777
1.0474e-01	0.5529	6.5542e-01	2.5420	5.9667e-01	3.0390
1.3034e-01	0.5824	7.0212e-01	2.9568	5.4593e-01	2.8645
1.5483e-01	0.6626	7.5509e-01	3.1013	4.9672e-01	2.5834
1.7983e-01	0.7961	8.0259e-01	3.4667	4.4592e-01	2.4611
2.0448e-01	0.8904	8.5563e-01	3.5306	3.9552e-01	2.3081
2.2932e-01	0.9902	9.0419e-01	3.7668	3.4528e-01	2.0885
2.5464e-01	1.0855	9.5396e-01	4.0765	2.9655e-01	1.7711
2.8017e-01	1.1486	9.9940e-01	4.1708	2.4604e-01	1.5733
3.0469e-01	1.2870	9.4376e-01	4.2285	1.9610e-01	1.3554
3.5442e-01	1.4839	8.9724e-01	3.9266	1.4544e-01	1.0882
4.0490e-01	1.6216	8.4393e-01	3.9450	9.6781e-02	0.8084
4.5403e-01	1.8644	7.9746e-01	3.6249	5.0275e-02	0.5006
5.0491e-01	2.0471	7.4443e-01	3.6071		

Figure D13 Data isotherm of cerium oxide

Cerium oxide reduced H_2 at 200°C 4hr

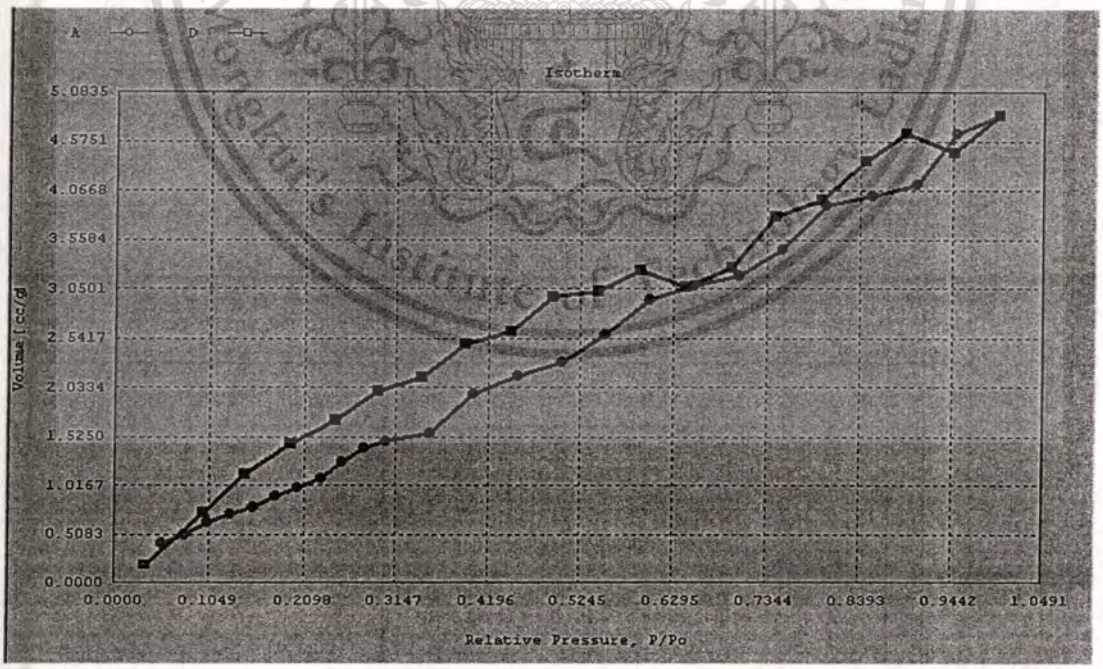

Figure D14 Isotherm of cerium oxide reduced H_2 at 200°C 4hr

Sample ID	CeO2 reduced 460C				
Description	Adsorp 20 pts,Desorp 20 pts,BET 11 pts				
Comments					
Sample Weight	0.1141 g				
Adsorbate	NITROGEN	Outgas Temp	350 °C	Operator	golf
Cross-Sec Area	16.2 Å²/molec	Outgas Time	10.0 hrs	Analysis Time	360.1 min
NonIdeality	6.580E-05	P/Po Toler	0	End of Run	05/13/2008 15:52
Molecular Wt	28.0134 g/mol	Equil Time	3	File Name	510513_1.RAW
Station #	1	Bath Temp.	77.40		

Isotherm

P/Po	Volume [cc/g] STP	P/Po	Volume [cc/g] STP	P/Po	Volume [cc/g] STP
5.4489e-02	0.4236	5.5314e-01	2.5893	6.9780e-01	3.2755
7.9207e-02	0.5074	6.0347e-01	2.9475	6.4567e-01	3.0770
1.0401e-01	0.6331	6.5471e-01	3.0788	5.9254e-01	3.2377
1.2917e-01	0.7281	7.0480e-01	3.1841	5.4561e-01	3.0245
1.5493e-01	0.8002	7.5322e-01	3.4611	4.9344e-01	2.9704
1.7989e-01	0.9150	8.0269e-01	3.9204	4.4616e-01	2.6190
2.0466e-01	1.0022	8.5476e-01	4.0232	3.9533e-01	2.4888
2.3005e-01	1.0977	9.0452e-01	4.1288	3.4629e-01	2.1376
2.5478e-01	1.2703	9.5088e-01	4.6591	2.9543e-01	1.9959
2.7903e-01	1.4156	9.9914e-01	4.8414	2.4584e-01	1.6992
3.0514e-01	1.4753	9.4722e-01	4.4566	1.9620e-01	1.4599
3.5495e-01	1.5661	8.9206e-01	4.6555	1.4646e-01	1.1418
4.0347e-01	1.9624	8.4632e-01	4.3732	9.9524e-02	0.7307
4.5447e-01	2.1483	7.9712e-01	3.9782	3.5403e-02	0.1992
5.0459e-01	2.2953	7.4519e-01	3.7950		

Figure D15 Data isotherm of cerium oxide reduced H_2 at 200°C 4hr

Cerium oxide reduced H_2 at 300°C 4hr

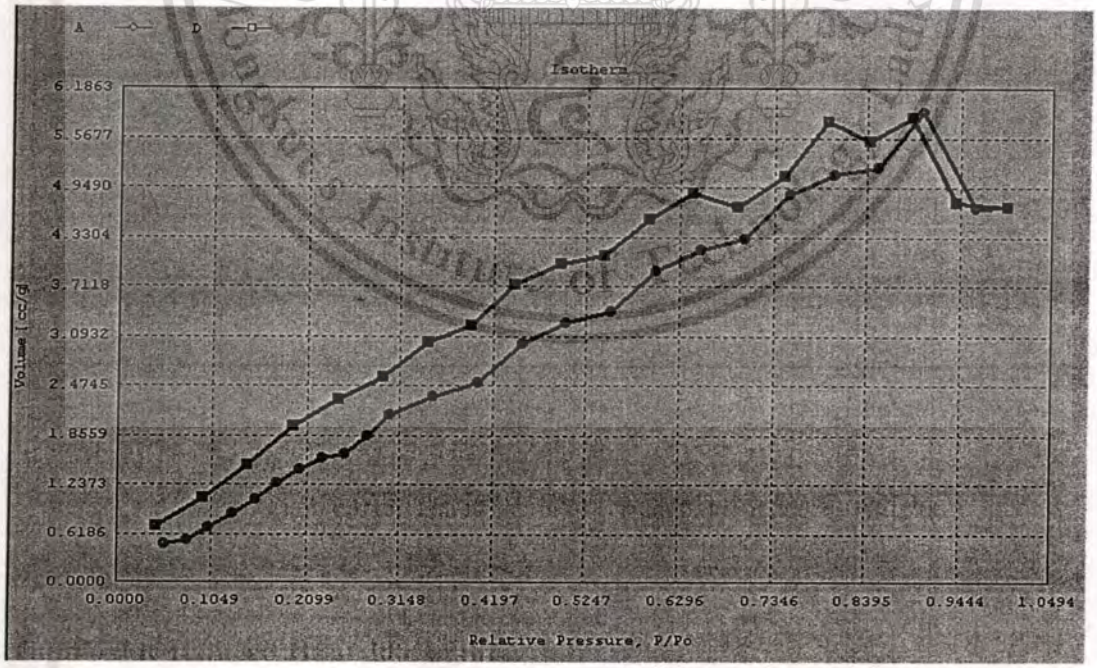

Figure D16 Isotherm of cerium oxide reduced H_2 at 300°C 4hr

Sample ID	Ce02 reduced 200C				
Description	Adsorb 20 pts,Desorb 20 pts,BET 11 pts				
Comments					
Sample Weight	0.0783 g				
Adsorbate	NITROGEN	Outgas Temp	350 °C	Operator	Off
Cross-Sec Area	16.2 Å²/molec	Outgas Time	10.0 hrs	Analysis Time	367.6 min
NonIdeality	6.580E-05	P/Po Toler	0	End of Run	05/17/2008 03:18
Molecular Wt	28.0134 g/mol	Equil Time	3	File Name	510516_2.RAW
Station #	1	Bath Temp.	77.40		

Isotherm

P/Po	Volume [cc/g] STP	P/Po	Volume [cc/g] STP	P/Po	Volume [cc/g] STP
5.4561e-02	0.5025	5.5355e-01	3.4061	6.9517e-01	4.7171
7.9410e-02	0.5507	6.0380e-01	3.9088	6.4578e-01	4.8963
1.0385e-01	0.7103	6.5392e-01	4.1743	5.9646e-01	4.5621
1.2953e-01	0.8820	7.0279e-01	4.3126	5.4554e-01	4.0992
1.5470e-01	1.0500	7.5373e-01	4.8749	4.9724e-01	3.9967
1.7962e-01	1.2559	8.0408e-01	5.1215	4.4505e-01	3.7345
2.0398e-01	1.4294	8.5295e-01	5.2094	3.9564e-01	3.2402
2.2931e-01	1.5752	9.0365e-01	5.8917	3.4694e-01	3.0205
2.5457e-01	1.6362	9.6297e-01	4.6895	2.9643e-01	2.5813
2.8016e-01	1.8645	9.9940e-01	4.7164	2.4603e-01	2.3008
3.0444e-01	2.1142	9.4171e-01	4.7627	1.9582e-01	1.9695
3.5436e-01	2.3370	8.9083e-01	5.8260	1.4631e-01	1.4843
4.0390e-01	2.5103	8.4414e-01	5.5335	9.7435e-02	1.0803
4.5383e-01	3.0139	7.9625e-01	5.7837	4.5370e-02	0.7268
5.0399e-01	3.2597	7.4735e-01	5.1028		

Figure D17 Data isotherm of cerium oxide reduced H_2 at 300°C 4hr

Cerium oxide reduced H_2 at 460°C 4hr

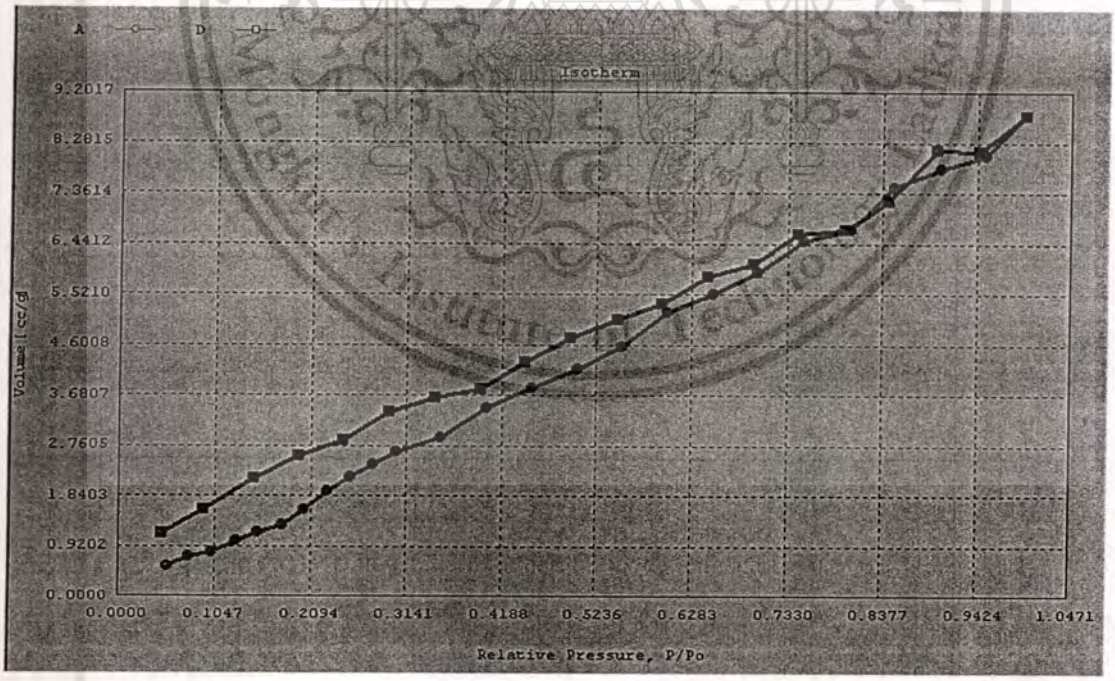

Figure D18 Isotherm of cerium oxide reduced H_2 at 460°C 4hr

Sample ID	CeO2 reduced 300C				
Description	Adsorp 20 pts,Desorp 20 pts,BET 11 pts				
Comments					
Sample Weight	0.1141 g				
Adsorbate	NITROGEN	Outgas Temp	350 °C	Operator	golf
Cross-Sec Area	16.2 Å²/molec	Outgas Time	10.0 hrs	Analysis Time	391.0 min
NonIdeality	6.580E-05	P/Po Toler	0	End of Run	05/08/2008 21:03
Molecular Wt	28.0134 g/mol	Equil Time	3	File Name	510508_1.RAW
Station #	1	Bath Temp.	77.40		

Isotherm

P/Po	Volume [cc/g] STP	P/Po	Volume [cc/g] STP	P/Po	Volume [cc/g] STP
5.4557e-02	0.5621	5.5188e-01	4.5730	6.9675e-01	6.0819
7.7790e-02	0.7374	6.0225e-01	5.2002	6.4741e-01	5.8519
1.0369e-01	0.8272	6.5343e-01	5.5270	5.9699e-01	5.3444
1.2911e-01	1.0267	7.0270e-01	5.9173	5.4715e-01	5.0778
1.5378e-01	1.1889	7.5248e-01	6.4885	4.9578e-01	4.7307
1.7930e-01	1.3120	8.0391e-01	6.6885	4.4612e-01	4.2845
2.0291e-01	1.5878	8.5180e-01	7.4684	3.9637e-01	3.8014
2.2865e-01	1.9249	9.0351e-01	7.8058	3.4704e-01	3.6485
2.5392e-01	2.1805	9.5341e-01	8.0566	2.9577e-01	3.3873
2.7915e-01	2.4154	9.9726e-01	8.7635	2.4679e-01	2.8523
3.0460e-01	2.6681	9.4508e-01	8.1153	1.9757e-01	2.5815
3.5279e-01	2.9214	8.9875e-01	8.1535	1.4794e-01	2.1769
4.0364e-01	3.4670	8.4523e-01	7.2217	9.3992e-02	1.5983
4.5362e-01	3.8139	7.9790e-01	6.6963	4.7552e-02	1.1430
5.0373e-01	4.1702	7.4656e-01	6.6204		

Figure D19 Data isotherm of cerium oxide reduced H_2 at 460°C 4hr

Thermal gravimetric analysis data

Calcium oxide

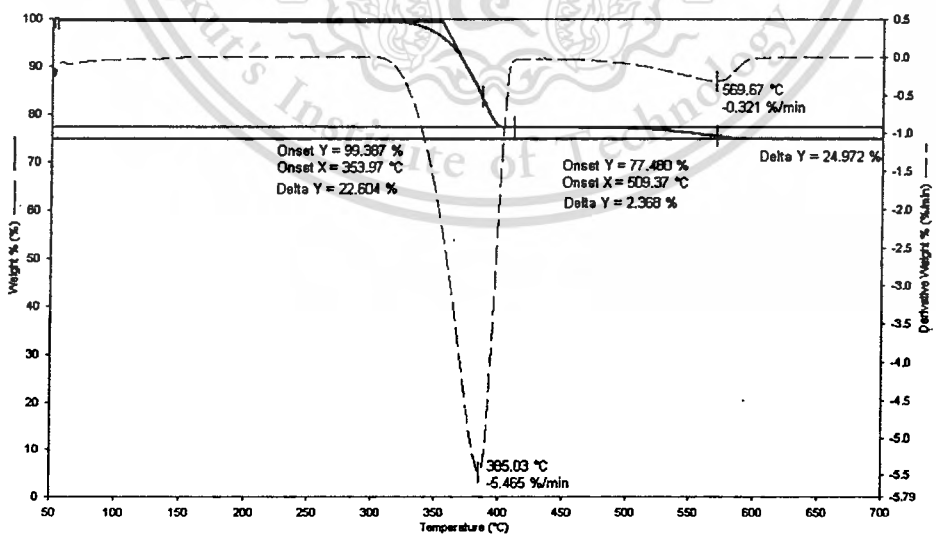

Figure D20 Thermogravimetric Analyzer of Calcium oxide

Magnesium oxide

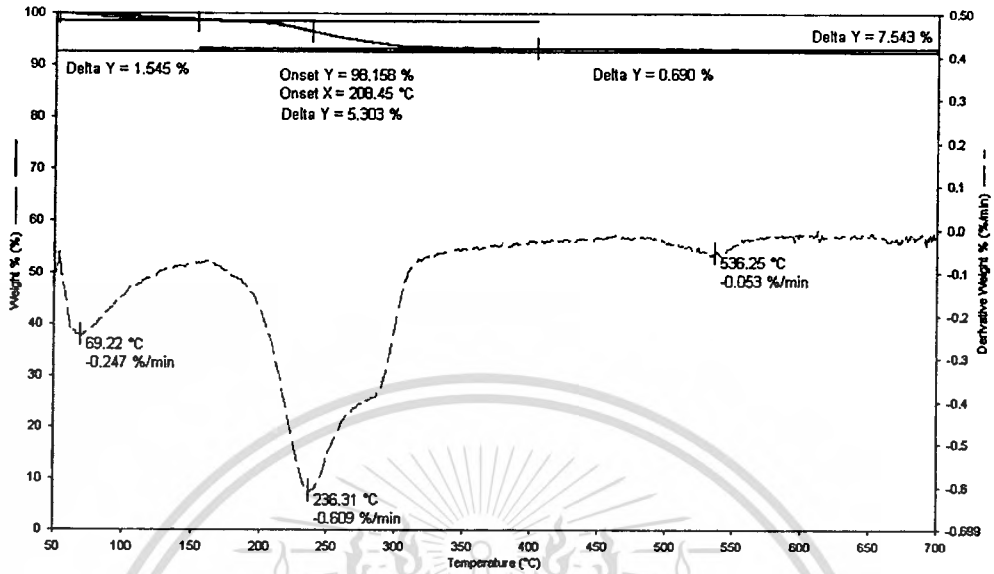

Figure D21 Thermogravimetric Analyzer of Magnesium oxide

Strontium oxide

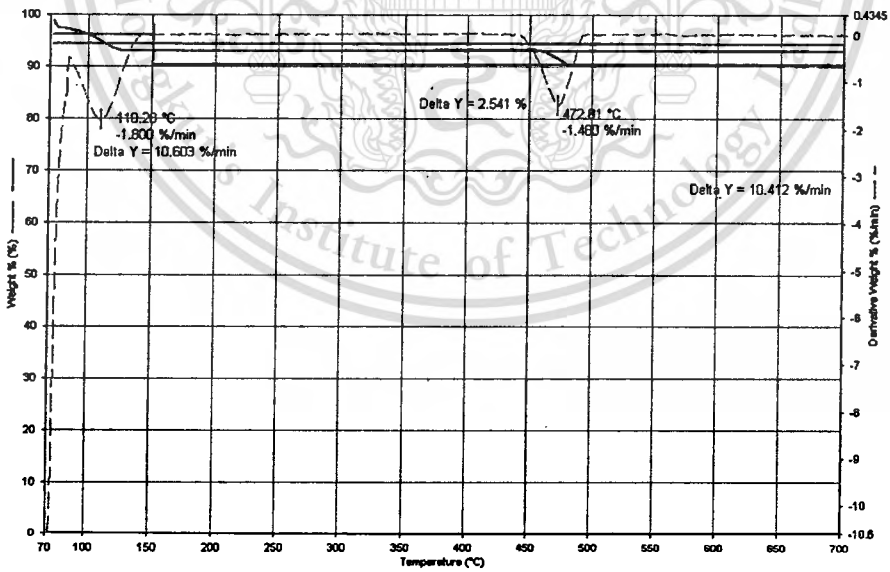

Figure D22 Thermogravimetric Analyzer of Strontium oxide

Barium oxide

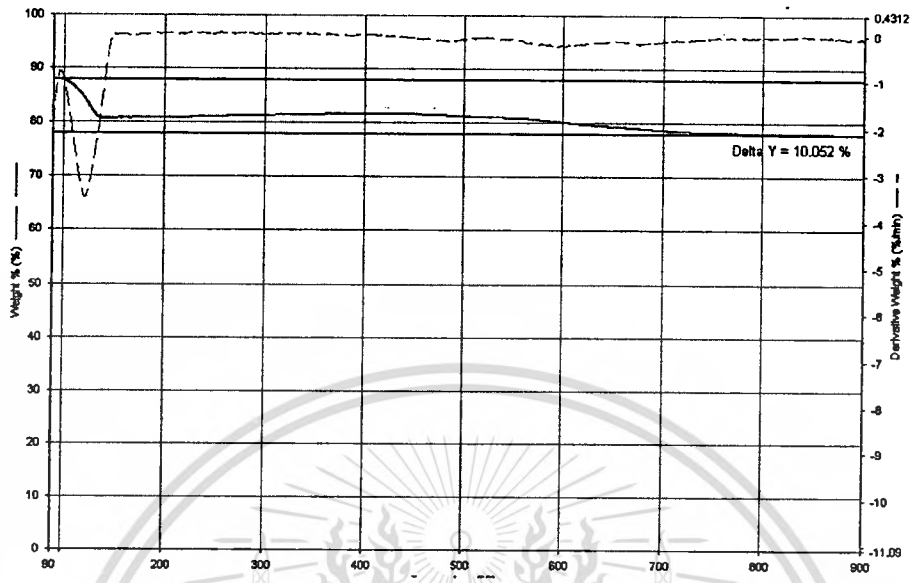

Figure D23 Thermogravimetric Analyzer of Barium oxide

Cerium oxide

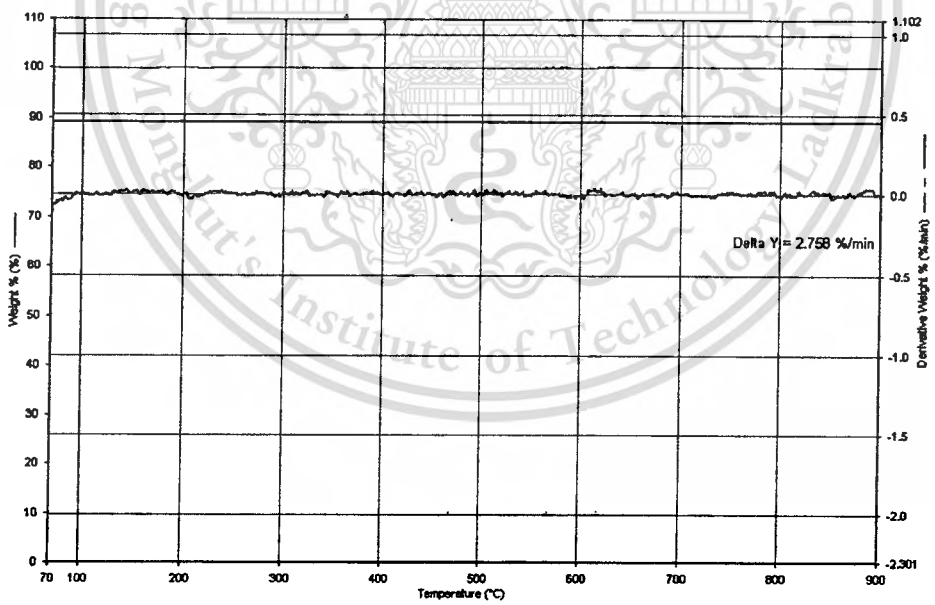

Figure D24 Thermogravimetric Analyzer of Cerium oxide

Residue from deoxygenation of palmitic acid with cerium oxide

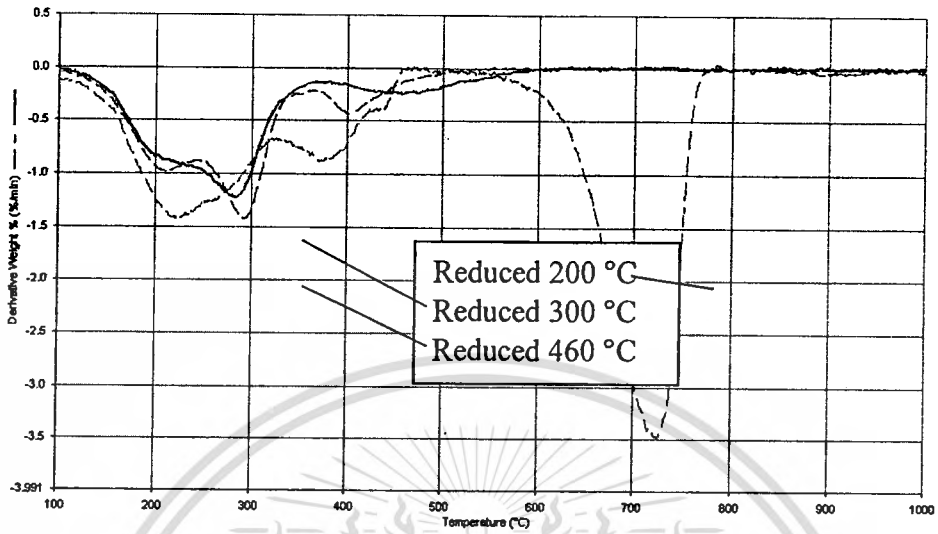

Figure D25 Thermogravimetric Analyzer of palmitic acid with reduced cerium oxide at 200°C, 300°C and 460 °C

AUTHOR BIOGRAPHY

Mr. Suppawat Taweesin was born on December 26, 1983 in Bangkok. He received a Bachelor degree of Chemistry Science from Prince of Songkla University in 2006. He has been a graduate student of the Program of Petrochemicals and Hydrocarbon Chemistry, Graduate School, King Mongkut's Institute of Technology Ladkrabang, since 2006.

Work experiences:

2008 –2009	Teacher Assistant, King Mongkut's Institute of Technology Ladkrabang.
2007 - 2008	Researcher Assistant (Part-time), Project: Renewable Diesel: Decarboxylation of Fatty Acids with Moderate Condition, PTT public company limited.

Conferences

Suppawat Taweesin, and Tawan Sooknoi, Linear long chain hydrocarbon from decarboxylation of palmitic acid over metal oxide, Oral presentation, Pure and Applied Chemistry International Conference 2009 (PACCON 2009), January 14-16, 2009, Naresuan University, Phitsanulok, Thailand.